minerals

MDPI

Review

Advances in Analytical Techniques and Applications in Exploration, Mining, Extraction, and Metallurgical Studies of Rare Earth Elements

V. Balaram

CSIR-National Geophysical Research Institute (NGRI), Hyderabad 500 007, India; balaram1951@yahoo.com

Abstract: The use of analytical techniques is important and critical in all areas related to REE, such as basic fundamental research, exploration, mining, extraction, and metallurgical activities at different stages by different industries. At every stage of these activities, rock, ore, minerals, and other related materials have to be analyzed for their REE contents in terms of elemental, isotopic, and mineralogical concentrations using different analytical techniques. Spectacular developments have taken place in the area of analytical instrumentation during the last four decades, with some of them having shrunk in size and become handheld. Among laboratory-based techniques, F-AAS, GF-AAS, ICP-OES, and MP-AES have become very popular. Because of high sensitivity, fewer interference effects, and ease of use, ICP-MS techniques, such as quadrupole ICP-MS, ICP-MS/MS, ICP-TOF-MS, MH-ICP-MS, HR-ICP-MS, and MC-ICP-MS, with both solution nebulization as well as direct solid analysis using laser ablation sample introduction methods, have become more popular for REE analysis. For direct analysis of solids, INAA, XRF, and LIBS techniques, as well as LA-based ICP-MS techniques, are being extensively utilized. The LIBS technique in particular requires little to no sample preparation. TIMS, SIMS, and SHRIMP techniques are being used for isotopic as well as dating REE depots. Portable analytical techniques, such as pXRF, pLIBS, and Raman spectrometers are able to perform in situ analysis even in the field, helping to make fast decisions during exploration studies. At present, hyperspectral remote sensing techniques including handheld, drone, and satellite-based techniques have become very popular in REE exploration studies because of their ability to cover larger areas in a limited time and, thus, became very cost-effective. Deployment of microanalytical devices/sensors mounted in remotely operated vehicles (ROV) is being successfully utilized in detecting REE-rich deposits in the deep oceans. Providing updated in-depth information on all these important aspects with suitable examples, especially from the point of view of REE research studies is the focal point of this review article.

Keywords: rare earth elements; ICP-MS; SHRIMP dating; LIBS analysis of REE; INAA; REE in coal; hyperspectral imaging; laser ablation; mineral analysis

Citation: Balaram, V. Advances in Analytical Techniques and Applications in Exploration, Mining, Extraction, and Metallurgical Studies of Rare Earth Elements. *Minerals* **2023**, *13*, 1031. https://doi.org/10.3390/min13081031

Academic Editors: Pierpaolo Zuddas and Shifeng Dai

Received: 6 June 2023
Revised: 13 July 2023
Accepted: 28 July 2023
Published: 31 July 2023

1. Introduction

At present there is intense exploration activity going on worldwide for critical elements, like rare earth elements (REEs), lithium, gold, platinum, palladium, copper, and cobalt, because of their wide applications in several green technologies required to transition to a low-carbon economy [1,2]. In fact, currently, these elements are fulfilling thousands of different industrial needs in our technology-powered society. The REE group of elements consists of the 15 lanthanide elements (La to Lu) plus Y and Sc. Based on atomic numbers, they are divided into two groups. The lower atomic weight elements from La to Sm, and the most abundant ones, with atomic numbers 57–62, are referred to as light REEs (LREEs); while Eu to Lu, and the least common and the most valuable, with atomic numbers 63–71, are known as heavy REEs (HREEs). Despite their low atomic weights, Y and Sc are included in the HREE subgroup because of their co-occurrence, similar ionic radii, and closer

behavioral properties to HREEs than LREEs (Figure 1). Because of their unique physical, chemical, electronic, optical, mechanical, catalytic, and magnetic properties, they are being extensively used to make different high-technology devices, such as computers, televisions, smartphones, catalysts for fuel cells, light emitting diodes, hard drives for computers, corrosion inhibitors, and magnets for wind turbines and other power generating systems. Concentrations of REEs in different earth materials (Table 1) provide critical information about the origin and evolution of the Earth. The concentrations of Ce and Eu are extremely sensitive to changes in atmospheric conditions with two different oxidation states each (Ce^{3+}/Ce^{4+} and Eu^{2+}/Eu^{3+}); hence, these two redox pairs are used to understand oxygen fugacity (fO_2) in different geological environments [3,4]. Because of these similarities, all these elements are usually studied as a group in several research and development studies. Though REEs exhibit similar properties chemically and frequently occur together in several geologic formations in many ores or minerals as major or minor constituents, they differ in some physical respects and possess different electronic and magnetic properties.

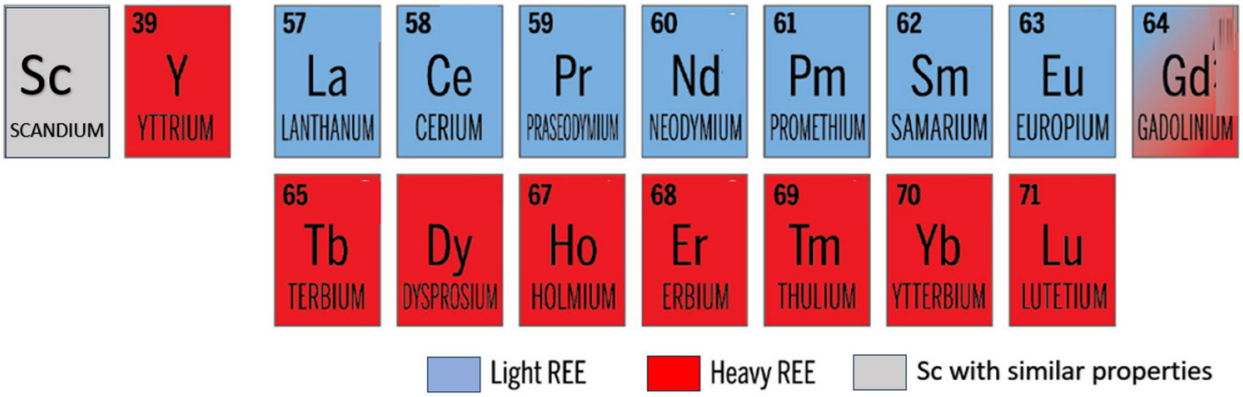

Figure 1. List of 17 and classification of REEs, modified from [5].

The demand for REEs, Y, and Sc is increasing day by day, especially because of their utility in green technology applications as mentioned above. As a result, there has been a significant surge in the exploration, mining, and extraction activities for these elements worldwide. The European Commission and the US government declared REE groups as economically critical elements [6,7] and, currently, there is intense exploration activity going on the world over for discovering new economically viable deposits. Even the mining, efficient extraction of REEs from the ore materials, and their metallurgy studies assume a lot of importance at present. Hence, there is a great need to have rapid, ecological, and cost-efficient analytical techniques during exploration, geochemical mapping, mining, and ore processing operations, and even during metallurgical works [8,9]. In all these activities, it is essential to analyze several types of geological and industrial materials for REE, Y, and Sc. Usually, it is very complicated to determine them by classical methods, such as gravimetry, titrimetric methods, and spectrophotometry, because of close similarities in their physical and chemical properties, particularly when a selected REE element among them has to be determined in the mixture of the other REEs, because of numerous interferences and coincidences. Moreover, it is extremely difficult to determine them at crustal levels of concentrations (ranging from 0.3 to 33 μg/g in crustal rocks) in various geological materials [7]. But astonishing advances have taken place during the last three decades in the analytical techniques for the detection and determination of different elements including REE not only in terrestrial materials but also in faraway bodies, such as the Moon and Mars. Recently, eight elements, including one of the REEs, Tb, were detected in an exoplanet's (KELT-9 b's) atmosphere using high-resolution spectrographs [10]. Exoplanets are planets that are in other solar systems than our own. Usually, sophisticated instrumental analytical techniques, like instrumental neutron activation analysis, (INAA) and different forms of inductively coupled plasma–mass spectrometry (ICP-MS) including tandem-ICP-MS, ICP-time-of-flight-MS (ICP-TOF-MS), high-resolution-ICP-MS

(HR-ICP-MS), multi-collector-ICP-MS (MC-ICP-MS), and Mattauch–Herzog geometry-ICP-MS (MH-ICP-MS) are commonly used for REE determination in different kinds of materials because of their multi-element capability, high sensitivity, wide linear dynamic range, fewer interferences, and ease of operation. Dai et al. [11] n a study related to the understanding of modes of occurrences of different elements including REEs, used techniques ranging from a simple AAS to the complex SHRIMP instrument. Recent developments in various instrumental analytical techniques, including the introduction of portable techniques and some new analytical techniques and their applications in the determination of REEs in various geological materials during exploration studies, mining, extraction, and metallurgical processes form the focal point of this review. In addition, advances in sample preparation/sample dissolution, and quality control protocols for obtaining accurate data are also discussed. Some of the important analytical techniques and their utility towards REE elemental, isotopic, and mineral analyses are considered and discussed in the following.

Table 1. REE concentrations in different earth materials (Data from [12–18]).

Source	∑ REE
Earth's crust	150 to 220 μg/g
REE ore	0.1%–10%
Surface and groundwater	0.1–100 pg/g
Geothermal fluids	Up to 21.76 μg/g
Acid mine drainage	1–1000 ng/g
Coal and pre-combustion by-products	10–1000 μg/g
E-waste	~600 μg/g
Coal ash	10–1000 μg/g
Ferromanganese crust from the Indian Ocean	1727 to 2511 μg/g
Laterites	0.021 to 0.099 wt%
Red mud	0.23 to 0.38 wt%
Phosphorites	up to 0.5 wt%
Bauxite mine waste ponds	1900 to 2600 μg/g

2. Instrumental Analytical Techniques

Recent advances, especially in ICP-MS technology, have led to the development of several types of ICP-MS instruments with amazing performance characteristics, such as rapid elemental as well as isotopic analyses, very high sensitivity, and fewer interference effects. Recent developments in microelectronics and computer technologies helped some of the analytical techniques, like XRF and LIBS, to shrink in size and became handheld, helping scientists to take them directly into the field to generate data rapidly. These portable techniques have, together, made the analysis of REE in different types of geological and industrial materials rapid and easy. The latest ICP-MS instruments, like ICP-MS/MS and HR-ICP-MS, provide more choices and effective solutions for separating spectral interferences in REE analysis while taking the detection limits down to sub-pg/g levels. Internal standardization only minimizes the drift effects because the drift is usually non-linear, depends on mass, and changes frequently when analyzing over large mass ranges, and many times offline data reduction procedures were helpful for the correction of drift [19]. Figure 2 is a schematic representation of different major analytical techniques used for elemental, isotopic, and mineralogical studies related to REEs in geological materials.

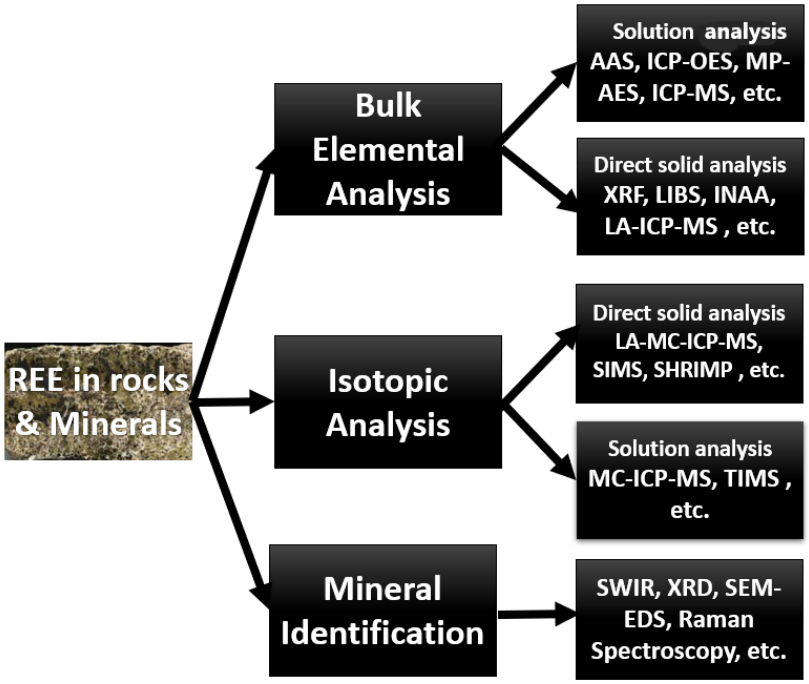

Figure 2. Schematic representation of different major analytical techniques used in REE studies related to elemental, isotopic, and mineralogical studies of geological materials.

2.1. UV/Vis Spectrophotometry

UV/Vis. spectrophotometry is one of the oldest techniques that can be used to determine extremely low concentrations of several metals including REEs. If the desired constituent is not self-colored, the addition of a selective ligand selectively binds to metal to produce a colored complex with a higher molar absorptivity to enable their sensitive determination. The intensity of the color of the given solution is directly proportional to the concentration of a desired element. By comparison with a standard, the unknown concentration of an element can be calculated. There are a number of spectrophotometric methods available in the literature for the determination of different REEs. For example, Pu et al. [20] developed a spectrophotometric method that involves microcolumn online preconcentration for the determination of ∑REE, which is highly sensitive, selective, and accurate. Saputra et al. [21] developed a fast quantitative analytical method by combining ultraviolet–visible spectroscopic and multivariate analysis for the determination of Sm, Eu, Gd, Tb, and Dy, and successfully applied it to the quantitative analysis of these REE in monazite samples. Though spectrophotometry is an established technique for the determination of several metals including REE in geological materials, most methods are complex and suffer from several interferences from the matrix components, are not very sensitive, and some procedures are lengthy, while it is often difficult to determine one REE in the presence of other because of close chemical similarities. Moreover, a lot of other instrumental multi-element analytical techniques are available currently. As a result, spectrophotometry methods seem to be not very popular, especially during exploration, mining, ore processing, and metallurgy studies.

2.2. X-ray Fluorescence Spectrometry (Both WD-XRF and ED-XRF)

X-ray fluorescence spectrometry (XRF) is one of the most frequently used non-destructive analytical techniques for determining the elemental composition of different geological materials, like rock, sediment, soil, and ore samples. The technique can be classified into wavelength-dispersive X-ray fluorescence spectrometry (WD-XRF) and energy-dispersive X-ray fluorescence spectrometry (ED-XRF) depending on the methods of excitation, dispersion, and detection [22]. Both forms of X-ray fluorescence techniques are very popular for the determination of REEs in geological and environmental materials. XRF works on the principle

that when a sample is bombarded with high-energy X-rays, the atoms in the sample become ionized by losing electrons. The resulting electron hole in the inner shell is then filled by an outer-shell electron accompanied by the release of energy in the form of a photon, which is known as fluorescence. The energy of the emitted radiation reflects the energy difference between the two shells involved, which is also characteristic to the element present in the sample, and its intensity is directly proportional to the concentration. When the instrument is calibrated with the known concentration of a particular element, it is possible to determine the exact concentration of the same element in an unknown sample. XRF is a reliable non-destructive and multi-element analytical technique for several trace element analyses at the μg/g level, although the technique is relatively insensitive to REEs. In general, XRF offers very high detection limits for REEs and is not suitable for many types of geological materials; hence, several determination procedures involve the separation and preconcentration of REEs for their accurate determination [23]. For example, Juras et al. [24] separated all REEs from other constituents by an ion-exchange procedure and determined different types of geological materials ranging from ultramafic rocks to rhyolites. De Vito et al. [23] developed a separation and preconcentration method for REE using (o-[3,6-disulfo-2-hydroxy-1-naphthylazo]—benzenearsonic acid, which is retained on a polyamide membrane by a chemo-filtration process. The membrane containing the REEs is measured by XRF and this preconcentration method allows the detection of very low concentrations of REEs. A comprehensive report on the applications of XRF spectroscopy in the Chinese REE industry was given by Wu et al. [25]. These applications involve the XRF analysis of REE in rocks, minerals, ores, soils, concentrates, raw metals, alloys, and functional materials, along with a fast and online separation and preconcentration process, such as ion-exchange and precipitation methods. De Pauw et al. [26] determined REEs in geological materials using the WD-XRF technique, which was designed to measure the L-lines of REEs between 4.5 and 7 keV with a sensitivity down to the μg/g level. The method could detect REEs in the inclusions in deep Earth diamonds with detection limits lower than 0.50 μg/g for characteristic L-lines which were 10 times lower than those of regular K-lines. Adeti et al. [27] demonstrated the limitations of the tube-based XRF for the determination of REE in geological materials. The major reason was found to be the interference between the K-series X-ray emission from-the transition metals and the relatively low intensities of the L-series lines of the REEs. Carbonatite tailings from an Australian mine were analyzed by XRF and ICP-MS for assessing the REE recovery potential. The carbonatite-related tailings were found to contain about 9% REEs [28]. ED-XRF is capable of measuring from Na through U, including elements, like sulfur, in a variety of geological matrices for a wide range of applications, including mineral exploration and quality control [29]. Table 2 presents selected REEs determined in an in-house monazite CRM by ED-XRF. High error and a high average lower limit of detection (1–10 μg/g) are the disadvantages of XRF for the determination of REEs in geological materials. In general, XRF techniques are not sensitive enough to detect and determine low concentrations of REEs in rocks in the range of μg/g and below, and, usually, separation and preconcentration methods are employed to make these trace elements detectable. Table 3 presents a few more applications in REE research studies. Figure 3 presents a schematic diagram showing REE analysis by ED-XRF.

Table 2. REE concentrations determined by ED-XRF In the in-house monazite sand CRM [30].

Element	ED-XRF Value (μg/g)	Certified Value
La	10.78	11.23
Ce	26.44	25.65
Nd	9.59	9.45
Sm	1.72	1.69
Y	3.14	3.10

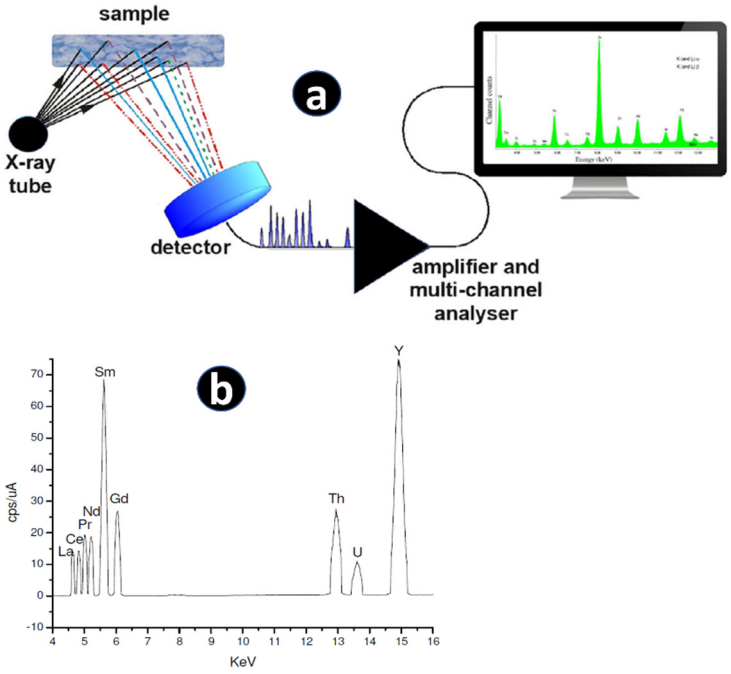

Figure 3. REE analysis by ED-XRF: (**a**) schematic diagram of ED-XRF depicting the sample excitation to the measurement of different elements; (**b**) ED-XRF scan of a mixture of standards, modified from [31,32].

Table 3. Some more applications of different analytical techniques in REE research studies.

Nature of Material	Analytes	Sample Preparation/Decomposition Method	Analytical Technique	Remarks	Reference
REE-bearing rock and soil samples	La, Ce, Nd and Y	Pressed pellets of homogenized soil samples	LIBS	Portable LIB spectrometers are useful in the exploration of new REE deposits	[33]
Lunar meteorites	REE	Directly ablating the sample	LIBS	Information on the constituents in sample drawn from spectral details	[34]
Waste Sm–Co magnets	REE and several other major, minor, and trace elements	Microwave digestion procedure using HNO_3, H_2SO_4, HCl, and HF	ICP-MS and ICP-OES	Recoveries were between 99%–100% and RSD was <5%	[35]
Rocks	REE	Low dilution glass beads made with a sample to lithium borate ratio (1:1), heated twice at 1200 °C with agitation	XRF	Using this method, Y, La, Ce, Pr, Nd, Sm, Gd, Dy, and several other elements were determined in rhyolitic and granitic rocks	[36]
Surface waters and sediments of the Mgoua watershed, Cameroon	REE	Acidified water samples analyzed directly. Sediments were dissolved using a mixture of acids before analysis	ICP-MS	REE concentrations in waters of 0.11 to 6.60 ng/mL and 282.12 to 727.67 µg/g in sediments	[37]

Table 3. *Cont.*

Nature of Material	Analytes	Sample Preparation/Decomposition Method	Analytical Technique	Remarks	Reference
JCp-1 (coral) and JCt-1 (giant clam) CRMs	REE	Two methods: (i) simple dissolution by HCl, and (ii) HF + HNO_3 + $HClO_4$ digestion and a further fusion process with Na_2CO_3 and H_3BO_3 in a Pt-crucible	ID-ICP-MS	No significant differences in REE results were found between the two decomposition methods	[38]
Sedimentary cores from Laguna Mar Chiquita, Argentina	La, Ce, Nd, Sm, Eu, Tb, Yb & Lu	200 mg of sediment samples in polyethylene bags were irradiated	INAA	Global REE averages show higher REE contents in clastic than in chemical sediments	[39]
Phosphate rocks from Egypt and Saudi Arabia	REE	30 g aliquots encapsulated in a polyethylene vial and irradiated	INAA	Choice of the nuclear reaction, irradiation and decay times, and of the proper gamma radiation are important	[40]
Brazilian geological CRMs	REE	For each sample, one CRM was simultaneously processed in exactly the same way	INAA	Geological CRMs GB-1 and BB-1 provided new trace element data	[41]
Sediments of Bouregreg river, Morocco	REE	100 mg sample of CRMs were irradiated for about 7 h	INAA	INAA offers good sensitivity and selectivity for the analysis of sediments	[42]
Apatite mineral	La, Ce, Pr, Nd, Sm, Eu, Gd, and Dy	About 25 mg digested in 25 mL HNO_3 and 6 mL HCl. Then, 1 mL of the solution was pipetted onto a Millipore membrane filter (1.2 mm pore size) and dried under an IR heater at 50 °C	WD-XRF	Determination in emission–transmission method. Precisions are ~3% RSD with comparable accuracies	[43]
Uranium oxide	Eu, Nd, and Yb	Sample powders were encapsulated in clear tape and analyzed directly	pLIBS	REE constituents in sub-percent levels detected	[44]
Alabaster rocks (crystalline $CaCO_3$)	Sc, Lu, Ce, Sm, La, Yb, and Eu	100 mg powder in polyethylene capsules irradiated	INAA	Technique is useful for geochemical and mineral exploration studies	[45]
Fluids from deep-sea hydrothermal vents	REE	REE are isolated from other elements on miniature cation-exchange columns	ICP-MS	ID-TIMS results compare favorably with ICP-MS results and are accurate at the 6% (2a) level	[46]
Natural carbonates	REE	Samples dissolved in HNO_3	ICP-MS	The carbonate REE-related studies are useful in climate change, paleoceanography, and environmental research	[47]
		Drilling subsamples of 50–100 mg analyzed directly	LA-ICP-MS and LA-HR-ICP-MS		

2.3. Instrumental Neutron Activation Analysis (INAA)

INAA is a highly sensitive and versatile multi-element analytical technique for the accurate determination of the concentration of major, minor, and trace elements, including REEs, in a variety of geological materials. Usually, small amounts of samples (~5 to 100 mg) in polythene bags along with standards are subjected to a neutron flux in a nuclear reactor. The stable nuclei absorb neutrons during irradiation and become radioactive, and the resultant radioactive nuclides decay with the emission of particles or, more importantly, gamma rays, which are characteristic of the elements from which they are emitted. The nuclide is identified by its gamma-ray energy, and the intensity of the gamma-ray is directly proportional to its concentration; by comparing it to that of the known standard, the concentration of a particular nuclide/element can be calculated. Both scintillation and semiconductor-type detectors are normally used for quantitative measurement. As nuclear reactions and decay processes are virtually unaffected by the chemical and physical structure of the material during and after irradiation and the composition of the matrix has little influence on the induced activity, matrix effects are minimal, with several types of geological materials and the results are very accurate. These methods are very popular in places where nuclear reactors are available for sample irradiation. Although INAA is a nondestructive method and detects all REE at ng/g levels (Table 3) in several rock types, it is difficult to make accurate measurements when the matrix radionuclides with higher radioactivity led to a high background in the gamma-ray spectrum. Sometimes after sample irradiation, the matrix is separated by certain methods, such as coprecipitation, ion-exchange, and solvent extraction, and the measurement is performed by radiochemical NAA (RNAA). However, several studies ranging from pure geochemical studies to REE exploration studies employed INAA techniques for the determination of REEs in different earth materials [42,48,49]. Table 4 presents REE concentrations determined by INAA in zircon concentrate CRM OREAS 100a together with certified values. Depending upon the background intensity and half-life, different elements were determined by two different techniques, namely INAA and ED-XRF. More details on the methodology followed are provided by Silachyov [50]. Ravisankar et al. [51] used INAA to measure REE in beach rock samples using a single comparator method. Samples along with SRM 1646a (estuarine sediment) were irradiated using a thermal neutron flux of ~10^{11} n cm^{-2} s^{-1} at 20 kW power using the Kalpakkam mini reactor, IGCAR, Kalpakkam, Tamil Nadu, India. REEs were determined in 15 samples using high-resolution gamma spectrometry. Figure 4 depicts the INAA analysis set up for geoanalysis.

Table 4. REE concentrations determined by INAA in zircon concentrate CRM OREAS 100a together with reference values [50].

REE	Concentration (µg/g)	
	INAA Value	**Certified Value**
La	264 ± 25	260 ± 9
Ce	460 ± 45	463 ± 20
Pr	47.6 ± 5.7	47.1 ± 2.4
Nd	145 ± 14	152 ± 8
Sm	24.0 ± 2.3	23.6 ± 0.4
Eu	3.64 ± 0.43	3.71 ± 0.23
Gd	23.6 ± 3.0	23.6 ± 1.4
Tb	3.71 ± 0.32	3.80 ± 0.23
Dy	23.7 ± 2.8	23.2 ± 0.4
Ho	4.89 ± 0.45	4.81 ± 0.14

Table 4. *Cont.*

REE	Concentration (µg/g)	
	INAA Value	Certified Value
Er	15.4 ± 1.9	14.9 ± 0.5
Tm	2.33 ± 0.21	2.31 ± 0.11
Yb	15.7 ± 1.3	14.9 ± 0.4
Lu	2.30 ± 0.20	2.26 ± 0.11
Sc	6.68 ± 0.50	6.10
Y (ED-XRF)	132 ± 23	142 ± 3

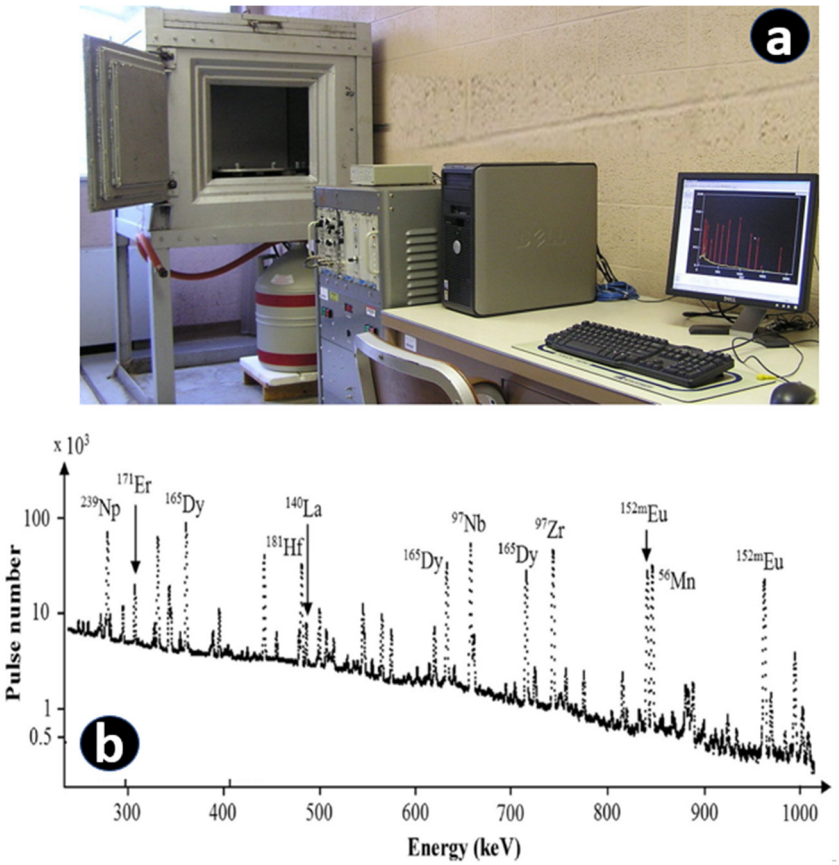

Figure 4. INAA analysis set up: (**a**) gamma-ray spectroscopy system (modified from https://serc.carleton.edu/details/images/8971.html (accessed on 27 July 2023)); (**b**) an example of gamma-ray spectrum of zircon-concentrate CRM sample, GSO4087, containing REEs and other elements. Some REE peaks can be seen in the in the range between 300–1000 keV, modified from [50].

In order to understand the distributions of REEs and their source in surface mangrove sediments of the Juru River, West Coast of Peninsular Malaysia, Krishnan and Saion [52] used INAA. Samples, along with CRM, SL-1, and blank samples, were irradiated together before measurements. Ahmed et al. [53] analyzed REE in soil samples collected from gold-mining sites by INAA to understand REE concentrations in gold-mining areas in Sudan. The accuracy of REE data was checked using SRM–NIST 2586. Kin et al. [54] made a comparative study on the determination of REEs by INAA and ICP-MS and found that INAA is more powerful with very good precision and accuracy, though some REEs, like Pr, Gd, Dy, Ho, Er, and Tm, cannot be determined accurately by INAA due their short half-lives [55]. However, they can also be determined by using radiochemical neutron activation analysis (RNAA) methods. El-Taher et al. [56] presented an overview of the

capabilities of different nuclear techniques, such as INAA, radiochemical NAA (RNAA), WD-XRF, ED-XRF, and total reflection XRF (TXRF) for the determination of REE in different kinds of materials, including geological samples, such as rocks, minerals, sediments, and soils, along with some case studies. According to the author, the INAA appears to be an attractive technique for determining REEs in geological materials, as this technique provides good results within a reasonable timescale. However, the accuracy of the determination depends strongly on the type of material analyzed (matrix) and the concentration levels of the element of interest. Adeti et al. [27] used four nuclear analytical techniques for the determination of Sc, La, Ce, Nd, Sm, Eu, Tb, and Lu in volcanic rock specimens along with an IAEA-Soil-7 CRM. These techniques are as follows: (i) Am-241 excitation-based XRF, (ii) Ag-anode X-ray tube XRF, (iii) INAA, and (iv) regular XRF. Except for the Ag-anode X-ray tube XRF method, all other methods gave comparable results, with the best results coming from Am-241 excitation-based XRF. The measurement is faster, as the sample preparation is minimal, and the overall analysis time is shorter than with other techniques. Although INAA is popular for highly sensitive multi-element analysis, it certainly has some limitations. INAA needs matrix-matching reference materials for calibration to allow for the emitted X-rays, which are subjected to self-attenuation in the sample under the same counting conditions. Hence, synthetic standards prepared by mixtures of REEs are not suitable. It is also time-consuming, not independent, and involves longer cooling times for certain elements. On the other hand, some nuclides are very short-lived and cannot be determined with reasonable accuracy. Moreover, the method is not independent, and requires a reactor nearby.

2.4. Indirect Measurement of REEs by the Radiometric Method

Ghannadpour et al. [57] used methods based on radioactivity and radiation measurement for the exploration studies of REE in the Central Sangan iron ore mine, in northeastern Iran. These authors found a direct correlation between the concentration of radioactive elements (U, Th, and K) and REE mineralization, and, thus, this is a useful exploration tool for REE and presents a novel viewpoint to decision makers in the exploration industry. Drill core samples in the field were directly analyzed for radioactive elements, testing for U, Th, and K separately with the handheld gamma-ray spectrometer, which is highly specialized and has widespread use. Individual REEs were determined by ICP-MS, and it was observed that radioactivity in the study area was entirely affected by uranium and ∑REE showed acceptable correlation with radioactivity and consequently uranium. This is some kind of indirect determination of ∑REE using a handheld gamma-ray spectrometer [58]. In order to understand the radioactivity levels of radionuclides of ^{238}U, ^{232}Th, ^{226}Ra, and ^{40}K, near the REE processing plant in Guangdong, China, the natural radioactivity of these radionuclides in the surrounding soil samples was determined using a high-purity Germanium energy spectrometer. Mohanty et al. [59] used radiometry to study beach and alluvial placers along the eastern coast of India for the exploration of REEs and radionuclides and found out that the total REEs were −90 times higher in the Podampata Beach sediments and −20 times higher in the Paradeep Beach sediments compared to the average crustal abundance levels, respectively. The concentration of radionuclides as well as REEs exhibited a marked enrichment in beach sediments at particular locations along the east coast of India.

2.5. Atomic Absorption Spectrometry (Both Flame-AAS and GF-AAS)

Flame atomic absorption spectrometry (F-AAS) is based on the principle that the amount of light absorbed by the atoms in the flame is a measure of the concentration of a particular analyte at a particular wavelength [60]. By comparing the absorption of a known standard with that of an unknown, the concentration of a particular element can be computed in an unknown sample. On the other hand, graphite furnace AAS (GF-AAS) is a technique that offers better sensitivity and involves the injection of a small amount of sample solution to be analyzed into a small graphite tube [61] and, thus, is suitable for the analysis of metals at ultra-trace levels (ng/mL) [62]. F-AAS methods are well-

suited for single-element analysis and useful only when very high concentrations are being analyzed, particularly from the REE analysis point of view. Because of the low cost of the equipment and low running cost, F-AAS instruments are being used even now by many industries. Determination of REEs in geological samples by flame-AAS is complicated by the low sensitivity of the technique for this group of elements, coupled with severe spectral interferences by other REEs, Si, Na, Fe, Al, hydrofluoric acid, phosphates, etc., even after using a high-temperature acetylene–nitrous oxide flame. Individual REEs were successfully determined using flame-AAS after adding excess potassium to the sample solution to suppress ionization interference. Currently, because of the availability of other powerful techniques, such as ICP-MS, the use of AAS techniques for the determination of REE is very limited, particularly at low concentration levels.

2.6. Microwave Plasma Atomic Emission Spectrometry (MP-AES)

Microwave atomic emission spectrometry (MP-AES) is a relatively new analytical technique that was introduced in 2011 and is an attractive alternative to flame-AAS and ICP-OES [63,64]. Figure 5 presents a schematic diagram that explains the principle of MP-AES, as well as REE analysis. This technique utilizes a relatively new design of plasma torch, utilizing nitrogen gas for generating high-temperature microwave plasma, and proved to be attractive for the analysis of different types of geological samples, including industrial effluents, water, sediments, soils, rocks, and ores [65–67]. The sample solution is converted to an aerosol and directed into the central channel of the plasma, where atomization takes place. Since the excitation temperature of the microwave plasma is a little lower than that of the conventional ICP, most of the excited species will be in the atomic state. The required lines of the specified elements are separated and detected using a monochromator and a detector system. Helmeczi et al. [68] developed a novel and rapid digestion procedure for the dissolution of REE ores and determined REEs using MP-AES, and the REE results obtained by MP-AES were comparable to those obtained by well-established ICP-MS, thus, demonstrating the capability of MP-AES for the analysis of REE in geological materials. A comparative study of the direct determination of REEs in water samples by ICP-OES and MP-AES showed that MP-AES is an attractive alternative to ICP-OES because of several advantages, like favorable detection limits for REEs and low running cost [69].

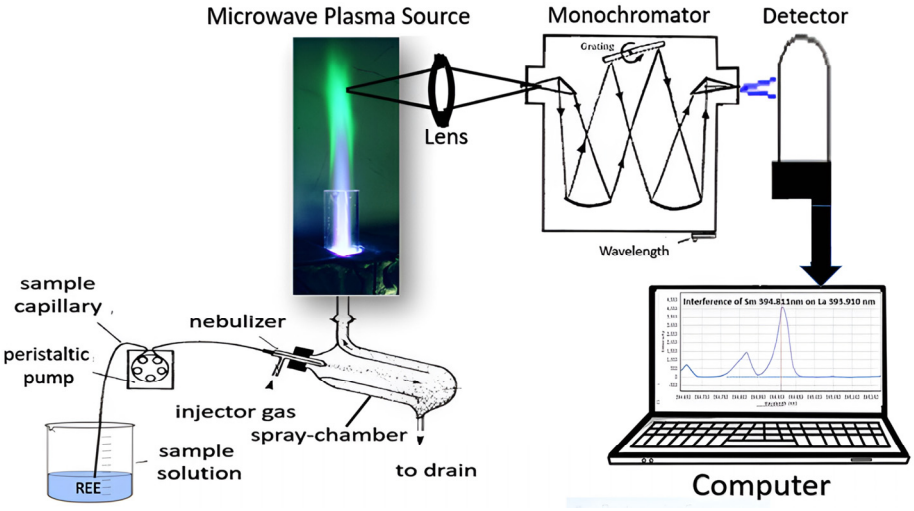

Figure 5. Schematic diagram explains the principle of MP-AES and REE analysis, modified from [60,65].

2.7. Inductively Coupled Plasma–Optical Emission Spectrometry (ICP-OES)

The ICP-OES is another very important and very popular multi-element analytical technique for the determination of not only REE but also several other elements in geological materials. When a sample solution is aspirated through the sample introduction system, the liquid sample is converted to an aerosol and transported to the high-temperature

ICP. In the plasma, the sample undergoes desolvation, vaporization, atomization, and ionization, and the electrons within the atoms, and ions absorb energy from the plasma, which causes the electrons to move from one energy level to another. When the electrons fall back to the ground state, the atoms/ions emit light of wavelengths which are specific to each element. By comparison of the measured emission intensities to the intensities of known concentrations, the respective elemental concentrations in an unknown sample are obtained [70,71]. The technique has a wide linear dynamic range with moderate sensitivity and can simultaneously measure up to 60 elements in a variety of samples, including geological materials [72,73]. Makombe et al. [74] determined REEs in sediment sample solutions dissolved by both four-acid digestion (HCl, HF, HNO_3, and $HclO_4$), and lithium metaborate fusion digestion by ICP-OES, and the results compared well with those obtained by ICP-MS. The results were also found to be within the confidence limits of the results for reference materials. The detection limits obtainable by ICP-OES presented in Table 5 are in the µg/mL range. Low sensitivity compared to some techniques, like quadrupole-ICP-MS, as well as spectral and non-spectral interferences of ICP-OES, make it difficult to detect and determine low concentrations of REEs in most rocks. However, separation and preconcentration methods can reduce detection limits as well as help in removing most interferences [75]. The complex REE spectra have long been a challenge for analysis by ICP-OES because of the hundreds of possible orbital transitions and corresponding emission wavelengths. Spectral overlaps and near-overlaps, especially in complex geological matrices, have made trace-level REE analysis nearly impossible. But the use of alternate wavelengths can help to avoid potential interferences. In addition, interference removal techniques, such as separation methods, such as solvent extraction, ion-exchange, and precipitation methods, allow the user to remove a few elements which cause spectral interferences in the rock matrices. Pradhan and Ambade [76] developed a solvent extraction method for the separation and preconcentration of REEs in geological materials, such as rock, soils, grabs (a portion of mineralized rock from an ore body), stream sediments, beneficiation products, minerals, and core samples, via determination by ICP-OES. Amaral et al. [77] determined all REEs including Sc and Y in geological samples after the samples were digested using a microwave digestion technique with ICP-OES using both a 'radial view mode' and 'dual view mode' with minimum matrix interference effects. Dual-view mode gave better detection limits than the radial view mode.

Table 5. Comparative detection limits of REE by some popular analytical techniques used in the investigations of geological research studies.

REE	ICP-MS [78] (ng/mL)	ICP-MS/MS [79] (pg/mL)	HR-ICP-MS [80] (pg/mL)	MH-ICP-MS [81] (ng/mL)	ICP-OES [74] (µg/mL)	LA-HR-ICP-MS [82] (µg/g)	INAA [54] (µg/g)	LIBS [34] (µg/g)	GD-MS [83] (ng/g)
La	910	0.12	0.15	0.005	1.1	0.002	0.3	160	5.6
Ce	260	0.15	0.33	0.007	1.6	0.01	0.9	285	1.5
Pr	3	0.16	0.09	<0.001	1.2	0.003	-	-	5.6
Nd	10	0.14	1.06	0.003	2.4	0.005	0.6	414	4.5
Sm	5	0.16	0.50	0.005	2.8	0.002	0.04	-	4.6
Eu	10	0.19	0.35	0.003	0.8	0.001	0.02	-	2.0
Gd	4	0.13	0.97	0.009	1.1	0.006	-	-	-
Tb	1	0.17	0.09	0.001	2.3	-	0.05	-	-
Dy	5	0.08	0.16	0.006	1.4	0.006	-	-	3.6
Ho	3	0.18	0.04	0.003	0.8	0.0009	-	-	0.4
Er	4	0.15	0.10	0.001	0.5	0.006	-	-	0.7
Tm	2	0.15	0.05	0.001	0.5	-	-	-	0.3

Table 5. *Cont.*

REE	ICP-MS [78] (ng/mL)	ICP-MS/MS [79] (pg/mL)	HR-ICP-MS [80] (pg/mL)	MH-ICP-MS [81] (ng/mL)	ICP-OES [74] (µg/mL)	LA-HR-ICP-MS [82] (µg/g)	INAA [54] (µg/g)	LIBS [34] (µg/g)	GD-MS [83] (ng/g)
Yb	10	0.13	0.12	0.006	0.1	0.008	0.08	-	-
Lu	1	0.15	0.05	0.002	0.1	0.001	0.03	-	1.4
Sc	60	-	17.9	0.006	-	-	-	-	0.5
Y	170	-	0.38	0.003	0.1	0.003	-	227	0.6

2.8. Laser-Induced Breakdown Spectroscopy (LIBS)

LIBS is a rapidly developing technique for the chemical characterization of different materials for element, molecule, and isotope analysis in real-time, with minimum destruction to the sample in use, and is extremely popular for the geochemical studies, monitoring of production processes in an industry, and remote analysis of materials even in a hostile environment [84,85]. Figure 6 depicts the working principle of LIBS. The technique uses an intense, highly focused laser pulse fired at a sample to be analyzed, creating a small plume of plasma consisting of electronically excited atoms and ions. The most common lasers used are excimers and Nd: YAG lasers that create a very short plasma plume—typically 5–20 nanoseconds long. An excimer laser is a form of ultraviolet laser. The emitted characteristic spectral lines are analyzed to obtain qualitative and quantitative information about different elements in a sample. This technique is an in situ analytical technique that requires little to no sample preparation. It is not easy to determine REEs by LIBS in geological samples due to higher detection limits (Table 5), significant spectral interferences, and relatively low concentrations encountered in the majority of the geological materials. However, LIBS has been widely used for the detection and quantification of elements in different materials, including geological elements irrespective of their states. Several types of samples can be directly analyzed by LIBS, as the techniques require no or minimal sample preparation. Analysis of liquid samples by LIBS is hampered by inherent drawbacks of the method, such as splashing, surface ripples, quenching of emitted intensity, and a shorter plasma lifetime. But Alamelu et al. [86] analyzed Sm, Eu, and Gd simultaneously in aqueous solutions with an accuracy of about 5%. Abedin et al. [87] identified for the first time REEs, such as Ce, La, Pr, Nd, Sm, Gd, Dy, Yb, Y, and several associated trace elements in monazite sands using LIBS. Bhatt et al. [88] used LIBS to determine La, Ce, and Nd in some geological samples, producing results which were found to be comparable to those obtained by ICP-MS analysis. The LIBS technique is used for the quantitative analysis of doped La and Nd in phosphors and the analytical performance was verified by the analysis of certified reference material [89]. Matrix effects and signal uncertainty are the two major drawbacks of LIBS for quantitative analytical applications. Long et al. [90] recently proposed a data selection method for the reduction of matrix effects and signal uncertainty and to improve repeatability during LIBS analysis. LIBS was used for the detection of REEs and associated elements including nonmetals, like Si and P in the beach sands of southern Bangladesh [91]. LIBS can be used for automatic coal-rock recognition with 97% accuracy when combined with an artificial neutral network in coal quality testing during unmanned coal mining operations [92].

LIBS is not a very highly sensitive technique for REE determination. The detection of trace amounts of REE is more difficult because weak signals are very often not detectable because of the strong interference from other major and minor elements in the rock matrix. Gaft et al. [93] detected all REEs using both atomic and ionic lines to enable effective detection. Simultaneous elemental and molecular LIBS combined with plasma-induced luminescence (PIL) is extremely sensitive for Eu, Sm, Gd, and Tb, and can be used to determine them very accurately with substantially longer acquisition times (10 to 100 times). In LIBS analysis, spectral interference and the weaker emission lines of low levels of REE

are key challenges for complex REE emission spectra. As emission intensity is dependent on laser wavelength, Afgan et al. [94] used IR (1064 nm), visible (532 nm), and UV (266 nm) irradiation and obtained higher signal intensity with even low concentrations of REE in monazite samples.

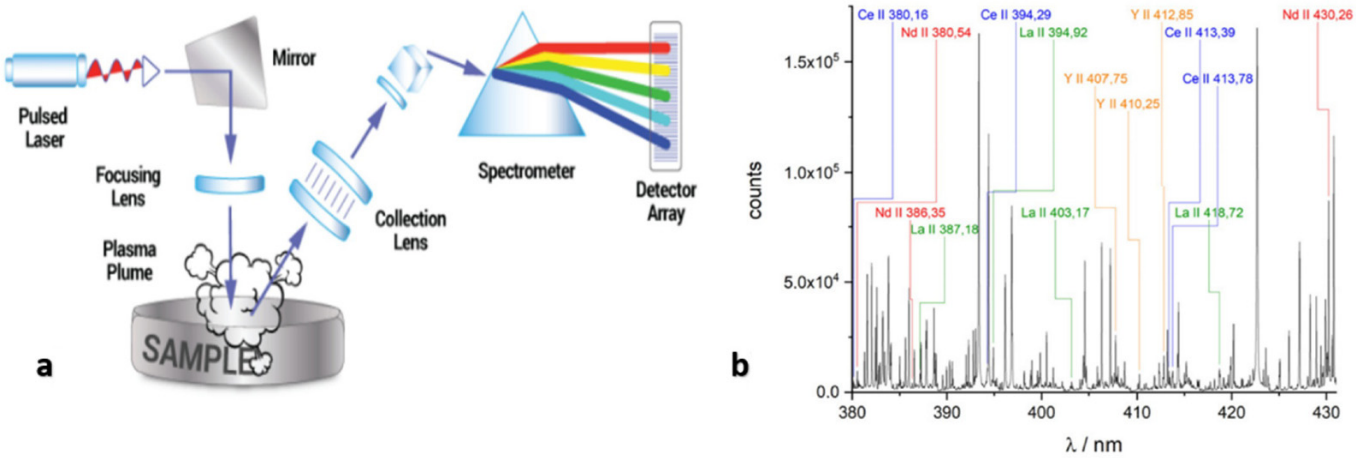

Figure 6. (**a**) Schematic diagram of LIBS, and (**b**) representative LIBS spectrum of a monazite–xenotime–apatite-bearing vein in the range 380–430 nm with important REE emission lines, modified after [34].

2.9. Inductively Coupled Plasma–Mass Spectrometry Techniques (All Forms of ICP-MS, ICP-MS/MS, ICP-TOF-MS, HR-ICP-MS, MH-ICP-MS, and MC-ICP-MS with Both Solution and Direct Solid Sampling by Laser Ablation)

Currently, ICP-MS occupies an invaluable position in the modern geochemical laboratory due to its multi-element capability, simplicity, limited interferences, excellent sensitivity, precision, and accuracy not only for REEs but also for several other groups of elements in geological samples. Several instrumental advancements have been incorporated during the last four decades into different forms of ICP-MS instruments for overcoming interferences and improving accuracy for elemental as well as isotopic determinations. The following sections present brief accounts of different types of ICP-MS instruments, like the quadrupole-ICP-MS, tandem ICP-MS (ICP-MS/MS), time-of-flight ICP-MS (ICP-TOF-MS), high-resolution ICP-MS (HR-ICP-MS), simultaneous ICP-MS or Mattauch–Herzog geometry (MH-ICP-MS), and multi-collector ICP-MS (MC-ICP-MS), and their applications in the elemental and isotopic analysis of REE in different types of geological materials.

2.9.1. Inductively Coupled Mass Spectrometry (ICP-MS)

The successful linking of ICP to a quadrupole mass spectrometer, more than four decades ago, presented a most valuable addition to the range of analytical techniques already available for elemental as well as isotopic analysis [95]. When the sample in the form of a solution as an aerosol after passing through a nebulizer and a spray chamber/desolvation is introduced into ICP, it is heated to a temperature of approximately 9000 K resulting in a series of processes involving desolvation, vaporization, dissociation, atomization, and ionization within the ICP. Thereafter, the singly charged positive ions enter the quadrupole mass spectrometer through a differentially pumped interface. At any given time, depending upon the applied RF/DC potentials, the quadrupole mass spectrometer transmits only ions of a particular mass-to-charge ratio. Any neutral species accompanying the plasma gases would be pumped away by the vacuum pumps. After mass isolation, the ions pass into the detector system, usually consisting of an electron multiplier which is used in pulse counting mode to register and generate a signal. In addition to the solution nebulization, other sample introduction systems, such as laser ablation, and different chromatography techniques, can be coupled to the instrument, allowing direct analysis of solids and speciation analysis capability, respectively. Before ICP-MS was

invented by Prof. Sam Houk of Iowa State University, USA, other analytical techniques, such as F-AAS and ICP-OES, required REEs to be separated from the rock matrix for their determination to avoid interferences from matrix elements, by using methods, such as coprecipitation, solvent extraction, or solid phase extraction. On the other hand, for REE analysis by ICP-MS, the samples can be directly nebulized without using any separation or preconcentration procedures. Over the last 40 years, ICP-MS has established itself as a powerful analytical tool that is being used for the analysis of more diverse applications, including geological materials. Even INAA methods are also very slow when compared with those of ICP-MS for the determination of REE in geological samples, because of the sample irradiation, and cooling requirements. The detection limits offered by quadrupole ICP-MS are in the ng/mL range (Table 5). Despite the fact that ICP-MS has very good performance characteristics for the determination of REE, interferences by various spectral and matrix interferences hamper the accurate determination of REE in geological materials. However, there are ways to minimize these interferences by using methods, such as internal standardization, use of matrix-matching calibrations, removing interfering matrix elements by methods, such as ion-exchange, and solvent extraction methods, and the use of collision cell/reaction chemistry, in addition to the use of other standard methods, such as standard addition, isotope dilution, and by the use of integrated sample introduction and aerosol dilution systems. Collision/reaction cells use multipoles (quadrupoles, hexapoles, or octopoles) which are placed before the analytical quadrupole and into which an inert (collision) or a reactive gas is introduced to overcome the interference by collision or reaction processes [32,96,97].

Exploration samples very often contain highly refractory phases, and such samples are effectively digested by high-temperature alkaline flux fusion, and REEs can be determined by ICP-MS which offers low detection limits, avoids sample preconcentration procedures, and is very rapid [98]. For example, beach placer deposit soils from Odisha, India were analyzed for REEs by ICP-MS [99], and Lin et al. [100] used ICP-MS to determine REEs in both organic and inorganic phases of the coal sample from the central Appalachian basin coal region, USA. The results showed that 25% of the REE concentration is associated with organic matter. Nguyen et al. [101] developed a simple and rapid HPLC-ICP-MS method for the determination of ultra-trace REE impurities in high-purity Eu_2O_3 and Yb_2O_3 due to the formation of $^{153}Eu^{16}O^+$ and $^{174}YbH^+$ which directly overlap with the monoisotopic $^{169}Tm^+$ and the most abundant isotope of Lu ($^{175}Lu^+$), respectively. The method is rapid and suitable for routine analysis of trace levels of all REE impurities, including Tm and Lu in high-purity europium and ytterbium oxides. Several studies reported the use of REE determination in a variety of rock and ore samples, such as Ni laterites by ICP-MS [78]. Barium is normally present below 2000 μg/g in several types of geological samples, except in barite-rich samples. Spectroscopic interferences caused by Ba and its oxide, and hydroxide compounds in barite-rich samples (e.g., with $BaSO_4$ ranging from 18.87 wt% to 42.41 wt%) hamper the determination of REEs in geological samples [102]. Sometimes it becomes necessary to use separation methods, such as ion-exchange chromatography for REE purification by eliminating Ba. Liu et al. [102] developed an ion-exchange separation method to eliminate Ba for the precise measurement of REE contents in Ba-rich samples by ICP-MS.

Determination of REEs in natural waters, including surface and groundwaters as well as rainwater and ice, is not easy because of the insufficient sensitivity of the technique, spectral and matrix interferences, potential contamination, and lack of water CRMs. Wysocka [103], in a review on this subject, discussed these issues comprehensively and offered solutions for obtaining the most reliable REE results in water samples. With analytical strategies, such as mathematical corrections, multi-element calibrations, and internal standardization, accurate REE results can be obtained in different types of water samples with precisions in the range of 5%–15% (RSD). In studies related to the investigation of the economic aspects of REEs in coal-by products, ICP-MS was used for the determination of REEs [104]. REEs and several other trace elements including U and Th were determined

by ICP-MS to understand the nature of the parent sediments from which these rocks were derived and to create an elemental fingerprint in phosphate rocks from the El-Sibayia and El-Hamrawein mines in Egypt [105]. ICP-MS analysis of fly ash and bottom ash generated at power stations in the Collie Basin in Western Australia revealed very high concentrations of REEs and demonstrated that Australian coal ash may represent a promising resource of REEs [103]. REEs and several other trace elements in lake bottom sediments, surface water samples in the vicinity of mines, and processing areas of rare metal ores in the Lovozero Tundra, Kola Subarctic, Russia, were determined by ICP-MS to understand the anthropogenic inputs [106]. Xin et al. [107] used ICP-MS to determine REEs in marine sediments by using ^{115}In and ^{185}Re as internal standards to overcome matrix and signal drift effects. These authors also compared two pretreatment methods: sealed acid dissolution and sodium peroxide alkali fusion, for the determination of REE by ICP-MS.

It is very difficult to accurately measure REE in seawater by ICP-MS, as their concentrations are very low and the high salt content (~3.5%) makes it difficult because of a number of spectroscopic and matrix interferences, signal drift, and frequent clogging of the sample introduction system. Li et al. [108] coupled ICP-MS with a fully automatic separation system (ELSPE-2 Precon system) which eliminates the high-salt matrix within the seawater and enables the measuring of REEs in seawater very accurately. Using a similar method, Wysocka et al. [109] determined REE concentrations in natural mineral waters from wells or mineral water bottles from the market with high elements recoveries (98% ± 4%). Li et al. [110] used crab shall particles for the separation and preconcentration of REE from seawater and determined by ICP-MS with extremely low detection limits ranging from 0.6 to 8.8 pg/mL. The concentrations of REEs in seawater were found to be in the concentration range from 0.025 ng/mL to 0.172 ng/mL. The recovery of REEs was between 95.3% and 104.4%, proving the efficiency of this proposed extraction process.

2.9.2. ICP-Tandem Mass Spectrometry (ICP-MS/MS)

Due to very close physical, chemical, and spectral properties, and associated interelemental spectral interferences, the determination of REEs is not very easy using a classical quadrupole ICP-MS instrument, though highly efficient high-temperature ICP provides nearly 100% ionization efficiency for all REEs. Figure 7 presents a schematic diagram of a typical ICP-MS/MS instrument. For example, spectral interferences from polyatomic oxide and hydroxide species, such as $^{137}Ba^{16}O^{+}$ and $^{136}Ba^{16}O^{1}H^{+}$ on $^{153}Eu^{+}$, and the interference of $^{139}La^{16}O^{+}$ on $^{155}Gd^{+}$, are a couple of examples. The spectral interference problem can be minimized by (i) procedural blank subtraction, (ii) a temperature-controlled sample introduction system, (iii) mathematical interference correction, (iv) offline and online sample pre-treatment methods, (v) internal standardization, (vi) the standard addition method, (vii) the isotope dilution method, (viii) the use of mixed plasmas, (ix) matrix-matching calibration, (x) the use of cool plasma technology, (xi) the use of high-resolution ICP-MS, and (xii) the use of collision/reaction technology [111]. However, recent studies by several authors demonstrated that the use of tandem ICP-MS or ICP-MS/MS with a collision/reaction cell (operated with gases, like NH_3, O_2, and N_2O) sandwiched by two quadrupole analyzers, and measuring all REE either on-mass mode or mass-shift mode, provided the best results with detection limits at sub-pg/mL levels (Table 5) for different REEs [111,112]. Some studies indicated that NH_3 as a cell gas was found to react with many of the polyatomic ions that interfere with the REEs and is useful in eliminating/minimizing interferences. However, NH_3 also reacts with some of the REEs leading to reduced sensitivity. On the other hand, Zhu [112] found that N_2O as a reaction gas gave more accurate values compared to the use of O_2 gas when REEs were determined by ICP-MS/MS when both N_2O and O_2 were used as reaction gases for the removal of interferences during the determination of the whole set of REEs in river water reference material. Especially the use of N_2O as the reaction gas helped to suppress Ba-related spectral interferences, and also yielded lower detection limits. Santoro et al. [113] used Na_2O_2 fusion coupled to ICP-MS/MS to rapidly screen quartz-rich geological samples for

REE contents. During the analysis, the most abundant isotopes were selected, and four different acquisition modes: no cell gas, He or H_2, and indirect mass-shift mode using O_2 gas, were used. The suitability and accuracy of the method were checked by analyzing the geological CRM, QLO-1 (USGS), and also by comparing the data with the results obtained by INAA (Table 6).

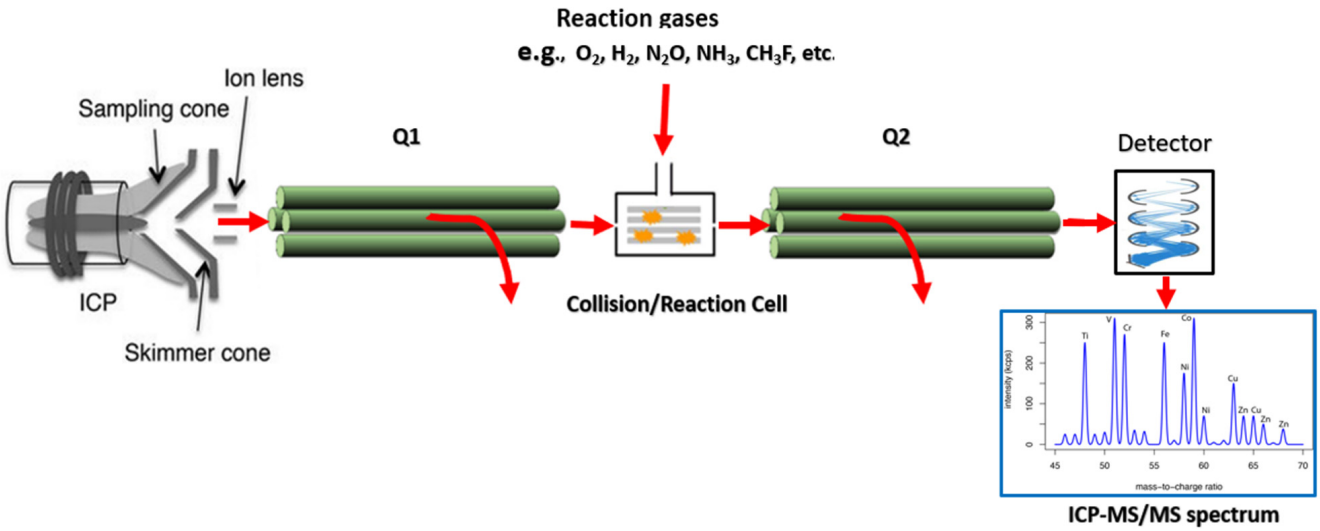

Figure 7. Schematic diagram of a typical ICP-MS/MS instrument, modified from [111].

Table 6. REE concentration values (µg/g) in quartz latite CRM, QLO-1 (USGS) determined by ICP-MS/MS in comparison with the values obtained by INAA and certified values [113].

REE	Na_2O_2 Fusion/ICP-MS/MS	INAA	Certified Value
La	26 ± 4	29.4 ± 0.8	27 ± 2
Ce	50 ± 8	58 ± 3	54 ± 6
Pr	5.7 ± 0.9	-	-
Nd	21 ± 3	28 ± 2	26
Sm	3.9 ± 0.5	4.9 ± 0.3	4.9 ± 0.2
Eu	1.2 ± 0.2	1.38 ± 0.06	1.43 ± 0.12
Gd	3.7 ± 0.5	-	-
Tb	0.7 ± 0.1	0.67 ± 0.05	0.71 ± 0.07
Dy	3.3 ± 0.4	4.8 ± 0.5	3.8 ± 0.3
Ho	0.73 ± 0.15	-	-
Er	2.0 ± 0.2	-	-
Tm	0.30 ± 0.06	-	0.37 ± 0.04
Yb	2.1 ± 0.3	2.7 ± 0.3	2.3 ± 0.2
Lu	0.31 ± 0.07	0.37 ± 0.03	0.37 ± 0.4
Sc	-	9.7 ± 0.3	-
Y	22 ± 4	-	24 ± 3

Lancaster et al. [114] made investigations on the use of N_2O as a reaction gas for the determination of 73 elements including REEs. However, the authors did not conduct any application studies on geological materials. The Na_2O_2 fusion/ICP-MS/MS method was found to be useful for the rapid screening of samples from quartz-rich geological areas for REE content during exploration studies. The tandem ICP-MS technique is very powerful

and even competes with the detection limits obtainable by HR-ICP-MS (Table 5). Zhu [79] accurately determined REE concentrations in seawater by ICP-MS/MS after adopting the coprecipitation with magnesium hydroxide separation and preconcentration method. Mass-shift mode was used for their measurement by permitting each isotope to pass through the first quadrupole and make it react with oxygen to form a monoxide of the metal, which was permitted to pass through and then be measured by the detector. The Gakara REE deposit, Burundi in Africa is one of the world's highest grades REE deposits, and the formation of this deposit is linked to a carbonatitic magmatic–hydrothermal activity. The U-Th-Pb geochronology of monazite and bastnaesite grains from the Gakara deposit was studied by in situ LA-ICP-MS/MS using an ESI NWR193UC Excimer laser directly in thin sections. The ages obtained for bastnaesite and monazite were 602 ± 7 Ma and 589 ± 8 Ma, respectively, demonstrating that bastnaesite crystallization was rapidly followed by monazite alteration, and reinforcing Ref. [115]. This work demonstrates the usefulness of ICP-MS/MS with LA sampling even for in situ dating studies.

2.9.3. ICP-TOF-MS

The development of ICP time-of-flight MS (ICP-TOF-MS) brought yet another dimension to the REE determinations in geological materials [116–118]. The principle of ICP-TOF-MS is that after the ions are extracted from the ICP source, the ion optics guide them into a repeller region where all ions are electrostatically accelerated to a uniform KE into a field-free flight tube and reflected back at the end of the flight to a drift region, where they reach the detector after traveling an equal distance in the reverse direction. This leads to velocity focusing and an increase in overall flight path, which help in significantly increasing the resolution. Since all ions are accelerated to a uniform KE, ions of different masses (m/z) will have different velocity (v) in the flight tube, obeying the equation:

$$\mathrm{KE} = 1/2\ \mathrm{mv}^2 \quad (1)$$

The mass is linearly related to the time ($\sqrt{t}$) taken to reach the ion detector. The time taken by an ion to reach the detector is then converted to m/z value. ICP-TOF-MS offers extremely high data acquisition speeds (~30,000 scans/s), high ion transmission, and quasi-simultaneous measurement of all masses in a packet extracted from the ion source, leading to better detection limits than those offered by quadrupole ICP-MS (Table 5). Dick et al. [119] determined REEs in Antarctic ice using ICP-TOF-MS with recovery rates of ~103%, and precisions of ~3.4% RSD. This study demonstrated that the ICP-TOF-MS technique meets the demands of restricted sample mass, and the results are in very good agreement with those obtained by ICP-MS as well as HR-ICP-MS. LA-ICP-TOF-MS was used for the determination of REEs in zircon crystals collected from Himalayan orogen. The technique was also used to determine U-Pb ages at sampling depths in the range of 0.59–0.66 µm [120]. Peng et al. [121] used high-resolution mapping by LA-ICP-TOF-MS for the visualization of critical metals including REEs in manganese nodules in deep oceans for understanding redox conditions with the help of Ce concentrations during their growth process, with advantages, such as time-saving as a result of high-speed stage movement and high lateral resolution at the micro-scale. The seemingly simultaneous detection capability of LA-TOF-MS allows rapid multi-element (including REE) analysis of very fast transient signals (i.e., laser ablation imaging in low dispersion laser ablation cells) and is also ideally suited to 2D and 3D imaging of geological materials, and will likely replace LA-ICP-MS for such applications in future [122].

2.9.4. Magnetic Sector or High-Resolution ICP-MS (HR-ICP-MS)

The magnetic sector field or high-resolution inductively coupled plasma–mass spectrometer (HR-ICP-MS) combines an ICP source with a double-focusing magnetic analyzer to perform trace/ultra-trace metal analysis and/or isotope ratio measurements [123,124]. HR-ICP-MS uses a combination of electrical and magnetic sector fields for separating trace analytes from interferences. The ions are sampled from the plasma in a conventional

manner and then accelerated in the ion optic region to a few kilovolts before they enter the mass analyzer. The magnetic field, which is dispersive with respect to ion energy and mass, focuses all of the ions with diverging angles of motion from the entrance slit. The electrostatic analyzer (ESA), which is only dispersive with respect to ion energy, then focuses the ions onto the exit slit, where the detector is positioned. More details are provided by Thomas [125]. The high mass-resolution capability (up to 10,000 R) of HR-ICP-MS allows for the identification of almost any targeted analyte ion from interfering molecular and/or atomic isobars. The other advantages include the higher transmission combined with very low background levels over conventional quadrupole ICP-MS. As a result, the detection limits are much superior not only to those obtainable by quadrupole ICP-MS but also to other popular analytical techniques (Table 4). Several common oxide and hydroxide interferences can be eliminated. The instrument is normally operated in three resolution settings: low (300 R), medium (3000 R), and high (10,000 R) for the elimination of different types of interferences.

Since this is a very highly sensitive technique, the laboratory environment has to be extremely clean for obtaining optimum performance. In fact, this technique has gained confidence among the geological community due to its capability to clearly resolve several spectroscopic interferences and offer extremely high sensitivity. Charles et al. [126] noticed very little use of the high resolving power of the technique during the determination of REEs in manganese nodule-certified reference materials (Table 7). Balaram et al. [127] designed and developed a procedure for the determination of REEs and Y in seawater samples by HR-ICP-MS after preconcentration using bis-2-ehtyl hexyl phosphoric acid (HDEHP) complexing agent. Gao et al. [128] used HR-ICP-MS for the determination of REE contents in the coals (∑REE 15.17 μg/g) and silty mudstones (∑REE 210.57 μg/g) of the Ordos Basin, North China, and found that REEs are mainly derived from felsic and intermediate rocks in a continental island arc setting. Table 8 presents REE data (ng/mL) determined by HR-ICP-MS in different water samples drawn from a drill hole, a spring, a couple of lakes, and some rivers, from the Ladakh region in India. An analytical procedure was devised to determine REE impurities in praseodymium oxide (Pr_6O_{11}) after the REE impurities were separated by using HPLC and determined by HR-ICP-MS, with recoveries ranging from 85% to 100% and with measurement precisions varying between 3 and 5% RSD [129]. Analysis of REEs in seawater is difficult even when a highly sensitive technique like HR-ICP-MS is used, because of their extremely low concentration levels and high total dissolved salts (TDS).

Table 7. REE concentrations in manganese nodule CRMs determined by HR-ICP-MS in low- and high-resolution settings in comparison with those obtained by a quadrupole-ICP-MS.

REE	Nod A-1 (μg/g)			Nod P1 (μg/g)		
	ICP-MS Value [130]	HR-ICP-MS Value [126]		ICP-MS Value Nath et al., 1992 [130]	HR-ICP-MS Value [126]	
		LR	HR		LR	HR
La	115	111.2	110.0	105	106.4	107.1
Ce	656	745	740	318	319	321
Pr	21.7	23.85	23.79	27.5	23.85	23.79
Nd	94	99.55	99.45	114	132.2	134.5
Sm	20.4	21.79	21.73	27.2	31.87	32.41
Eu	6.10	5.28	5.41	7.44	7.68	7.97
Gd	23.6	24.28	24.75	33.8	30.28	30.85
Tb	4.20	3.84	3.90	4.53	4.71	4.74
Dy	25.80	23.06	22.92	25.99	26.29	27.03

Table 7. *Cont.*

REE	Nod A-1 (µg/g)			Nod P1 (µg/g)		
	ICP-MS Value [130]	HR-ICP-MS Value [126]		ICP-MS Value Nath et al., 1992 [130]	HR-ICP-MS Value [126]	
		LR	HR		LR	HR
Ho	5.09	4.96	5.02	4.73	5.00	5.16
Er	15.6	14.31	14.52	13.3	13.42	12.70
Tm	2.19	-	-	1.72	-	-
Yb	15.40	13.48	13.69	13.26	12.70	13.08
Lu	2.21	2.08	2.14	1.75	1.82	1.93
%RSD	<5.0	<2.9	<5.37	<5.0	<1.4	<5.73

HR/LRs range from 0.989 to 1.029 for NOD-A-1 and HR/LRs range from 1.006 to 1.058 for NOD-P-1, proving that high-resolution acquisition mode is unnecessary to achieve high quality data for REEs in Fe–Mn oxides.

Table 8. REE data (ng/mL) determined by HR-ICP-MS in different water samples drawn from the Ladakh region, India.

Analyte	1A	2A	3A	4A	5A	6A	7A	8A	9A	10A	11A	12A	13A
Location	Puga Drill Hole	Puga River	Chumathang	Chumathang	Chumathang	Kiagor-Tso Lake	Tso-Morari	Yan River Side	Kalra Nala	Ribil	Sundo Confluence	Indus River	Indus River
Type	Spring Water	River Water	Spring Water	River Water	River Water	Lake Water	Lake Water	River Water	River Water	River Water	River Water	River Water	River Water
Sc	23.1	5.6	19.7	5.3	3.5	1.5	4.7	1.1	1.4	4.7	2.6	5.6	4.7
Y	53.8	153.8	21.2	626.3	393.6	91.6	90.6	77.5	23.3	433.9	222.3	128.6	49.0
La	46.2	303.4	27.7	1441.9	847.1	149.5	177.5	196.4	31.6	1176.3	443.1	176.4	67.3
Ce	74.5	482.0	40.2	2273.0	1321.6	254.7	287.3	278.8	48.9	1879.7	695.8	274.3	99.8
Pr	5.9	35.7	4.1	147.9	86.4	16.5	20.2	22.0	5.0	116.0	46.7	21.2	8.6
Nd	19.7	71.8	18.0	277.4	169.9	36.9	44.1	50.0	21.7	227.6	100.8	50.9	31.2
Sm	6.1	19.7	4.9	73.1	43.1	11.3	11.6	13.2	4.4	54.0	25.1	13.1	6.4
Eu	0.6	0.9	0.6	3.9	2.5	0.6	0.7	0.6	0.3	3.5	1.8	0.7	0.4
Gd	3.2	8.0	2.2	27.5	16.2	4.9	5.2	4.6	1.9	21.2	10.2	5.6	2.4
Tb	1.0	2.2	0.5	6.8	4.3	1.3	1.4	1.2	0.5	4.8	2.4	1.4	0.7
Dy	3.6	8.8	1.9	29.7	19.5	5.7	5.3	5.1	2.2	21.1	10.9	7.1	3.3
Ho	1.8	1.6	0.8	4.8	3.2	0.9	1.0	0.8	0.5	3.7	1.9	1.3	0.7
Er	7.4	5.2	3.2	14.3	8.5	2.5	2.4	2.4	1.3	11.3	5.6	4.1	2.5
Tm	0.5	3.4	0.4	1.5	1.1	0.5	0.5	0.4	0.3	1.4	0.8	0.5	0.4
Yb	1.7	2.4	1.4	6.1	4.1	1.8	1.7	1.3	1.1	5.6	3.2	2.0	1.3
Lu	0.6	0.9	0.4	2.8	2.0	0.7	0.7	0.5	0.4	2.6	1.3	0.8	0.4

Data acquired at 300 R. International CRMs NASS-5 and SLEW-3 from NRC, Canada, were used to calibrate and check the accuracy of the analysis. The precision was checked by repeated analysis of CRMs and was found to be <3% RSD.

Soto-Jiménez et al. [131] used a four-step method consisting of (i) filtration and acidification (pH < 2) of the sample, (ii) matrix separation by a separation and preconcentration system (seaFAST-SP3™ system), (iii) offline injection of the eluted sample, and (4) analysis by HR-ICP-MS. Estuarine water CRM, SLEW-3, was used for validation of the results. Table 9 presents the analytical results of REEs in water CRM, SLRS-4, obtained by different well-established ICP-MS-based analytical techniques including HR-ICP-MS and ID-HR-ICP-MS from different laboratories, in comparison with certified values.

Table 9. The analytical results of REEs in water reference material, with SLRS-4 obtained by different well-established ICP-MS based analytical techniques in comparison with certified values.

REE	Concentration (pg/mL)					
	ICP-MS/MS [132]	ICP-MS [133]	HR-ICP-MS [134]	ID-HR-ICP-MS [135]	Compiled Values [132]	Compiled Value [136]
La	294.5 ± 3.2	302.2 ± 7.3	279 ± 12	290.3 ± 6.4	291 ± 9	287 ± 8
Ce	357.5 ± 3.2	378.4 ± 8.2	369 ± 15	364.1 ± 3.5	363 ± 9	360 ± 12
Pr	70.9 ± 0.4	73.6 ± 1.5	75.4 ± 8.0	70.6 ± 2.3	71 ± 2.4	69.3 ± 1.8
Nd	274.2 ± 3.2	277.4 ± 5.7	261 ± 9	270.3 ± 2.8	271 ± 6	269 ± 14
Sm	58.5 ± 1.9	59.3 ± 1.4	54.3 ± 5.0	57.2 ± 0.3	57.6 ± 1.8	57.4 ± 2.8
Eu	8.06 ± 0.41	8.09 ± 0.61	8.4 ± 0.8	8.00 ± 0.7	8.44 ± 0.57	8.0 ± 0.6
Gd	33.86 ± 1.46	35.13 ± 1.01	38.3 ± 6.0	33.80 ± 0.36	34.2 ± 1.8	34.2 ± 2.0
Tb	4.27 ± 0.20	4.50 ± 0.23	4.1 ± 0.5	4.30 ± 0.12	4.32 ± 0.14	4.3 ± 0.4
Dy	22.82 ± 0.75	23.91 ± 0.66	21.7 ± 3.0	23.60 ± 0.16	23.6 ± 1.0	24.2 ± 1.6
Ho	4.39 ± 0.19	4.86 ± 0.11	4.2 ± 0.5	4.60 ± 0.18	4.66 ± 0.27	4.7 ± 0.3
Er	13.21 ± 0.46	13.53 ± 0.70	11.4 ± 3.0	13.10 ± 0.06	13.2 ± 0.8	13.4 ± 0.6
Tm	1.75 ± 0.11	1.91 ± 0.04	1.8 ± 0.2	1.80 ± 0.02	1.82 ± 0.08	1.7 ± 0.2
Yb	11.73 ± 0.36	12.03 ± 0.51	10.6 ± 2.0	12.30 ± 0.07	12.2 ± 0.7	12.0 ± 0.4
Lu	1.76 ± 0.09	1.86 ± 0.11	1.7 ± 0.4	1.95 ± 0.02	1.91 ± 0.10	1.9 ± 0.10

2.9.5. MH-ICP-MS

This is a different type of ICP-MS instrument that fits into a compact Mattauch–Herzog geometry (MH-ICP-MS) with a permanent magnet and a semiconductor ion detector. In Mattauch–Herzog geometry, ions of all masses focus along a line that coincides with the second magnetic field boundary. The resolved ion beams can be recorded on a large spatially resolving semiconductor ion detector which has the capability to detect a number of elements/isotopes simultaneously (https://www.britannica.com/science/mass-spectrometry/Electrostatic-field-analysis, accessed on 27 July 2023). An MH-ICP-MS instrument will have a single 4800-pixel element detector permitting the simultaneous detection of isotopes over the full relevant inorganic mass spectrum from ^{6}Li to ^{238}U, including REEs in aqueous samples using only sample amounts as small as 1–4 mL [81,137]. REE composition in 66 freshwater samples determined by MH-ICP-MS, from various rivers and lakes in Upolu Island, Samoa, in the South Pacific Ocean, are presented in Table 10. The detection limits obtainable by MH-ICP-MS for REE are presented in Table 5. It can be seen that the detection limits offered by different ICP-MS techniques varied significantly, and they are also element- and technique-dependent. Obviously, HR-ICP-MS and ICP-MS/MS techniques offer the lowest detection limits.

Table 10. Average REE compositions in 66 freshwater samples determined by MH-ICP-MS, from various rivers and lakes in Upolu Island, Samoa, the South Pacific Ocean [138].

REE	Mean Concentrations (ng/mL)
La	0.075
Ce	0.17
Pr	0.021
Nd	0.064
Sm	0.053

Table 10. *Cont.*

REE	Mean Concentrations (ng/mL)
Eu	0.012
Gd	0.026
Tb	0.0083
Dy	0.017
Ho	0.012
Er	0.014
Tm	0.0025
Yb	0.025
Lu	0.0025
Sc	-
Y	0.094

3. Isotopic Studies

The study of isotopic abundances (radiogenic as well as stable) and their distribution provides clues for understanding various geological processes that these elements/isotopes underwent during the crustal evolution. Particularly, radiogenic isotope signatures are used to understand the long-term evolution and the origin of sources of volcanic rocks and the evolution of the Earth. Stable isotopes have a lot of applications in exploration, water and soil management, and in tracer studies. On the other hand, radiogenic isotope pairs, like ^{147}Sm-^{143}Nd, and ^{176}Lu-^{176}Hf, are used for dating applications to determine the ages of rocks and minerals, and also to evaluate the nature and evolution of their source regions. REE isotopes in geological materials are applied very extensively in geological sciences to obtain new insights into several natural processes, ranging from crustal formation to chemical weathering and ocean circulation. Different mass spectrometric techniques, such as TIMS, MC-ICP-MS, SIMS, and SHRIMP, are used for the precise determination of isotopic abundances and isotopic ratios both in liquid and solid materials. The following sections discuss each of these techniques for different REE isotopic applications.

3.1. Multi-Collector ICP-MS (MC-ICP-MS)

A basic MC-ICP-MS instrument contains an ICP source, an energy filter, a double-focusing mass spectrometer of Neir–Johnson geometry consisting of two analyzers, namely a traditional electromagnet and an electrostatic analyzer (ESA), and an array of detectors, typically Faraday cups for the simultaneous detection of a number of isotopes of interest When the sample, in the form of a solution or direct solid sample using a laser ablation sampling, is introduced into the high-temperature ICP, the sample aerosol is evaporated, dissociated, atomized, and ionized to generate positively charged ions of different elements. The positively charged ions are then extracted from the argon plasma into the high vacuum of the mass spectrometer. The ions are accelerated and focused into an electrostatic analyzer (ESA). The ions emerging from the ESA enter a magnetic field region, which acts to disperse the ions according to their mass-to-charge ratios. Careful alignment of the detectors to the individual isotope beam needs to be carried out when analyzing different elements [139,140]. Among REEs, Nd, for example, is highly incompatible and refractory and has seven isotopes. The variations in Nd isotopes can be caused by both mass-dependent and mass-independent effects which are used to understand a number of geological processes [141]. However, their precise determination is very challenging when utilizing some instruments, like TIMS, because of severe interference effects. But the advent of MC-ICP-MS, together with advanced sample preparation methods and separation methods, such as the use of a two-column ion-exchange separation procedure, has allowed the high precision determination of isotope ratios of various REEs [142]. In

addition to the precise isotope ratios, MC-ICP-MS is also used for the determination of elemental concentrations.

Lee and Ko [143] determined REE concentrations in a natural river water CRM, SLRS-6, very accurately and precisely after group separation by 2-hydroxyisobutyric acid (HIBA). As isotope dilution methods are highly accurate and robust, Kent et al. [144] used isotope dilution-MC-ICP-MS (ID-MC-ICP-MS) to accurately determine eleven REE abundances in several international geological CRMs (USGS, NIST, GSJ) using rock powders and glass discs made of these rock powders. The authors also made a comparative study of the determination of REE concentrations by both ID-MC-ICP-MS and ID-TIMS. Unfortunately, ID methods cannot be used for monoisotopic elements, like Tb, as the method requires a minimum of two isotopes. Replicate analysis of both rock powder and glass materials agreed very well with analytical uncertainty, which is typically about 1%. Pourmand et al. [145] devised a novel extraction chromatography method after reducing the REE impurities in the fusion flux and used the MC-ICP-MS technique for rapid analysis of REE, Sc, and Y in primitive chondrites using a desolvating nebulizer and standard-sample bracketing technique. Baker et al. [146] developed a method for a high-precision analysis of REE by ID-MC-ICP-MS which is superior in terms of the analytical reproducibility or rapidity of analysis, on smaller sample amounts compared with ID-ICP-MS or with ID-TIMS. Bastnäsite is one of the important REE minerals and is the end member of a large group of carbonate–fluoride minerals which represents the major economic LREE deposits related to carbonatite and alkaline intrusions. Yang et al. [147] used LA-MC-ICP-MS for the determination of age by the U-Th-Pb geochronology method and Sr-Nd isotopic composition. Monazite and bastnasite are two principal REE ore minerals in the most famous Bayan Obo REE deposit in China. An Sm-Nd chronometer and LA-MC-ICP-MS were used to understand the primary crystallization timing of the REE deposit at 1293 ± 48 Ma [148].

3.2. Thermal Ionization Mass Spectrometry (TIMS)

In TIMS, ions are produced by the interaction of analyte species with a heated surface, which is usually a metal, like tungsten. Mostly singly charged ions are extracted, accelerated, and focused into a mass spectrometer where these ions can be separated based on their mass/charge ratios and detected using a Faraday cup detector. A multi-collector-TIMS uses a number of detectors for the simultaneous detection of multiple isotopes. For isotope dilution analysis by TIMS, chemical separations of REEs are usually made into two or more factions to separate LREEs and HREEs in order to reduce the inter-elemental interferences during the analysis. It requires a minimum of two isotopes for isotope dilution and it is not possible to analyze monoisotopic elements, like Pr, Ho, and Tm. TIMS is used mostly for dating applications in addition to elemental and isotope determinations. The new ages of 296.9 ± 1.65 Ma and 296 ± 4.2 Ma were obtained by U–Pb zircon dating by TIMS from tonstein layers interbedded with coal seams from the Candiota coalfield in the southern Paraná Basin, Brazil [149]. The Pope's Hill REE deposit in Labrador, Canada, was studied by LA-ICP-MS and ID-TIMS U-Pb geochronology and in situ Sm-Nd isotopes using LA-MC-ICP-MS in monazite from the ore and host rock to understand the timing of the deposit formation and to determine the source of the REEs [150]. Ramesh et al. [151] determined REEs and heavy elements in surficial sediments of the Himalayan River system by TIMS to understand the behavior of REEs during weathering and transport in a secondary sedimentary environment. In addition, the decay systems of the radioactive REE isotopes ^{138}La, ^{147}Sm, and ^{176}Lu were used to establish the ages of a range of geological events, starting from the first steps of planetary formation to some of the younger events, like Deccan volcanism, and the TIMS technique was proved to be very valuable in such studies. Uranium isotope (^{234}U/^{238}U, ^{235}U/^{238}U) ratio data generated by TIMS was used to understand the occurrence and provenance of Kanyakumari Beach placer deposits of REEs in India [152].

3.3. Sensitive High-Resolution Ion Micro Probe (SHRIMP)

SHRIMP is a high-resolution and highly sensitive instrument developed by William Compston at the Australian National University, primarily used for geological applications, especially in situ U–Pb dating of the mineral apatite, as well as zircon [153]. SHRIMP is basically a mass spectrometer that works on the principle of secondary ion mass spectrometry (SIMS). The ion beam made up of negatively-charged O_2 at mass 32 is found to be the most effective primary species for bombarding the sample surface, producing a larger second ionization yield. The collisions between the primary ions and the surface physically erode, or 'sputter', the sample, ejecting particles from the surface. The secondary ions, released in all directions, are then focused and steered towards a magnetic analyzer. Different ions (isotopes) of interest are simultaneously detected by a multi-collector (detector) assembly [32]. SHRIMP dating methods have been extensively applied for the dating of a number of REE deposits the world over. REE deposits, such as carbonatite deposits, can be dated very precisely using the decay systems of the radioactive REE isotopes ^{138}La, ^{147}Sm, and ^{176}Lu not only for understanding the age of REE deposits but also a range of events, starting from the first steps of planetary formation to younger steps of geodynamic development [154]. Thus, the abundance of all REEs occurring in a large range of concentrations as well as precise isotope ratios must be analyzed in different geomaterials for such studies. Campbell et al. [155] dated zircon from the Bayan Obo Fe–Nb–REE deposit to understand carbonatite-related magmatism and REE mineralization events. These SHRIMP dating studies indicated that Bayan Obo zircon cores represent part of a magmatic, intrusive, carbonatitic protolith suite that crystallized at 1325 ± 60 Ma. Bhunia et al. [156] used SHRIMP to date the carbonatite-hosted REE deposit of Kamthai, northwest India. This is one of the well-studied carbonatite REE deposits in India which gave an age of 68.4 ± 1.8 Ma which is linked to the carbonatite emplacement of the Deccan Large Igneous Province that triggered the mass extinctions near the K–Pg boundary. SHRIMP is capable of producing high transmission at high-resolution data of REE abundances in some minerals, like zircon and apatite [157]. SHRIMP-RG was used to determine REEs to understand their distribution in coal, as the knowledge of the REE distribution is essential to design cost-effective REE extraction procedures from coal and its by-products (Kolker et al. [158]. Carbonatite–alkaline complexes in northwest Pakistan were dated using the SHRIMP U-Pb dating technique of zircons, namely Koga syenites, which are spatially associated with the carbonatite deposit and which gave mean ages of 283.6 ± 1.7(1σ) providing a useful timing for alkaline magmatism in that area [159]. Such in-depth studies on well-proven REE deposits in general shed light on the full origin of these world-class mineral deposits.

4. Mineralogical Studies and In Situ Analytical Techniques

The mineralogical characteristics of different REE ores and resources are extremely important, as the leaching process depends on their mineralogical composition and the morphological distribution of different elements. Such studies help in the determination of the best leaching/extracting process during the extraction of REE from different ores. Mineral characterization techniques, such as XRD, scanning electron microscopy–energy dispersive spectrometry (SEM-EDS), and laser ablation-ICP-MS (LA-ICP-MS) are popular for the qualitative and quantitative identification of different REE minerals. During exploration studies, pXRD and Raman spectrometry are used to understand the mineralogy of a geological formation in the field itself for planning future courses of action. Some of the important analytical tools for understanding mineralogy are discussed below.

4.1. X-ray Diffractometry (XRD)

Identification of different indicator minerals and their concentrations in rocks, ores, and soils is extremely important in mineral exploration studies. XRD is one of the most powerful methods used to identify and quantify minerals in different earth materials [160]. The interaction of the incident monochromatic X-ray beam with the sample produces constructive interference (and a diffracted ray) when conditions satisfy Bragg's law

($n\lambda = 2d \sin \theta$). This law relates the wavelength of electromagnetic radiation to the diffraction angle and the lattice spacing in a crystalline sample. These diffracted X-rays are then detected, processed, and counted. By scanning the sample through a range of 2θ angles, all possible diffraction directions of the lattice should be attained due to the random orientation of the powdered material. Conversion of the diffraction peaks to d-spacings allows the identification of a mineral because each mineral has a set of unique d-spacings. Typically, this is achieved by comparison of d-spacings with standard reference patterns. XRD was effectively used in the identification of different minerals in the clay fractions of REE-enriched weathered anorthosite complex in Hadong district, South Korea [161]. In order to understand the differences between the mineralogy and mineral chemistry of REEs in phosphate and carbonates in the Bahoruco karsr bauxites in the Dominican Republic, Villanova-de-Benavent et al. [162] utilized XRD, SEM-EDS, and EPMA. This study revealed that phosphates are mostly enriched in Y and HREE (Gd, Dy); on the other hand, carbonates display a wide range of compositions in terms of LREE (La, Ce, Nd, SM) and HREE (Gd). The lignite deposits of Barmer Basin, Rajasthan, India, were characterized using a host of analytical techniques including XRF, XRD, and ICP-MS to understand mineralogical and elemental distribution. XRD analysis revealed the presence of minerals, such as hematite (Fe_2O_3), nepheline, anhydrite, magnesite, andalusite, spinel, and anatase. Other minor minerals included albite, siderite, periclase, calcite, mayenite, hauyne, pyrite, cristobalite, quartz, nosean, and kaolinite. Major and minor elements were determined by XRF, and REEs and several other trace elements were determined by ICP-MS. These investigations revealed the predominant mineral concentration, elemental makeup, trace elements, and REEs associated with lignite reserves in the Barmer Basin [163].

4.2. Electron Probe Micro Analyzer (EPMA)

EPMA operates under the principle that when a solid material is bombarded by an accelerated and focused electron beam, electron–sample interactions mainly liberate heat, electrons, and X-rays due to inelastic collisions of the incident electrons with electrons in the inner shells of atoms in the sample. Different kinds of detectors are arranged around the sample chamber that is used to collect X-rays and electrons emitted from the sample. A light microscope allows for direct optical observation of the sample. X-rays are used to determine the chemical composition of the sample using an ED-XRF unit. EPMA can be used for the detection and determination of high concentrations of REEs in rocks and also to understand the REE distribution patterns in different minerals [164]. It is a non-destructive technique and uses EDS to accurately determine the chemical composition of small amounts of solid materials by comparing it with the standards of similar and known compositions. EPMA and other analytical techniques, such as ICP-MS and scanning electron microscopy (SEM), were used to study the occurrence and distribution of REEs in a fly ash sample from the Qianxi coal-fired power plant in Guizhou province in China. Discrete REE mineral particles distributed throughout were seen directly by SEM and EPMA, and these studies revealed that the ∑REE concentration in coal fly ash was 630.51 μg/g and wet-grinding followed by acid-leaching was found to liberate more REEs during the extraction process [165]. Many times, such multi-disciplinary approaches would help in devising economically viable and eco-friendly extraction procedures for REEs from coal fly ash which has been found to be a promising alternative source for REEs [166]. Sano et al. [167] determined all REEs in oceanic basalt glasses by EPMA. The concentrations measured by EPMA compared favorably with those obtained by ICP-MS. The same authors also developed a method to determine REEs in glass samples by SHRIMP with a detection limit of ~6 ng/g.

4.3. Ion Microprobe (SIMS)

Secondary ion mass spectrometry (SIMS) or ion microprobe is one of the best techniques for the in situ analysis of REEs in geological materials [168]. The principle of SIMS analysis involves the use of a primary ion beam (consisting of O^- or Cs^+) to strike the sample surface of a polished rock or a thin section, and the sputtering process produces

secondary ions which are extracted into a mass spectrometer and analyzed. This technique provides a unique combination of extremely high sensitivity for all elements from hydrogen to uranium, including all REEs, with a detection limit down to both the ng/g level with extremely high spatial resolution. High-resolution SIMS (HR-SIMS) with large-diameter and double-focusing SIMS offer >5000 R and can measure the isotopic and elemental abundances in minerals at a 10 to 30 µm-diameter scale, and with a depth resolution of 1–5 µm. This instrument can also be used as an ion microscope for providing elemental distribution imaging maps. Zinner and Crozaz [169] used an ion microprobe for the quantitative measurement of REEs in phosphates. REE working curves were found to be linear over a wide range. The detection limits were found to be >50 ng/g for LREEs and ~200 ng/g for HREEs. It is possible to determine REE concentrations in individual mineral grains, such as zircon and monazite, using the SIMS technique.

Shi et al. [170] developed a method to analyze all REEs in silicate glasses and zircon minerals using a high lateral resolution SIMS (nano SIMS) with a high mass-resolving power of 9400 R. Table 11 presents REE concentrations in AS3 zircon together with reference values. Ling et al. [171] used high-resolution SIMS (HR-SIMS) to date bastnaesites to understand the mineralization time of the Himalayan Mianning–Dechang REE deposits in China. Bastnaesite is a major economic REE mineral which is normally considered to be a promising geochronological tool for determining mineralization time by the U–Pb dating method. For example, the SIMS bastnaesite Th–Pb dating of the Dalucao deposit yielded ages of 11.9 ± 0.2 Ma and 11.8 ± 0.2 Ma. Sahijpal et al. [172] devised analytical procedures for the measurement of REEs in two primitive carbonaceous chondrite samples using an ion probe with uncertainties of ~10 to 15%. In these studies, REE abundances provided insights to understand even the microscopic details of the early Solar System.

Table 11. REE concentrations determined by nano SIMS in AS3 zircon together with reference values [170].

REE	AS3 Zircon (µg/g)	
	Nano SIMS Value	**Certified Value**
La	0.250 ± 0.147	0.096 ± 0.063
Ce	11.56 ± 0.362	7.69 ± 1.07
Pr	0.544 ± 0.295	0.578 ± 0.173
Nd	7.34 ± 3.07	7.60 ± 2.09
Sm	12.77 ± 4.45	9.21 ± 2.24
Eu	0.399 ± 0.159	0.331 ± 0.073
Gd	42.7 ± 11.4	40.9 ± 8.5
Tb	15.63 ± 3.65	14.94 ± 3.18
Dy	165.6 ± 34.5	168.5 ± 30.0
Ho	53.2 ± 9.9	63.3 ± 10.7
Er	222.5 ± 45.8	261.0 ± 41.7
Tm	40.5 ± 6.7	54.2 ± 8.2
Yb	332.5 ± 50.8	408.6 ± 57.3
Lu	62.7 ± 10.3	89.6 ± 12.2

4.4. Scanning Electron Microprobe (SEM-EDS)

A SEM is essentially a high magnification microscope, which uses a focused scanned electron beam to produce images of the sample, usually on thin sections of the samples. The X-rays emitted are characteristic of the elements in the top few µm of the sample and are measured by the EDX detector. Thus, SEM-EDS combines the capabilities of a scanning electron microscope and an ED-XRF for material characterization and has proved

to be very useful for mineral characterization [173]. In a study related to the leaching recovery of REEs from coal fly ash, Pan et al. [174] used SEM-EDS and XRD techniques to prove that monazite, apatite, scheelite, and aluminosilicate were the major phases that were REE carriers. Such studies help in devising cost-effective procedures for the leaching and recovery of REEs from different ores. Palozzi, et al. [104] used SEM-EDS and integrated mineral analysis (TIMA) to study fine <5 μm monazite grains in the coal fly ash which were typically bound to Al/Si-rich phases. These studies helped to devise more efficient extraction procedures using aqua regia. In a study to find out the potential of the carbonatite tailings and to identify the major mineral phases for the REE recovery, by using XRD and SEM-EDS, Sarker et al. [28] found that monazite and florencite were the main REE-bearing minerals. The SEM-EDS-based liberation analysis indicated that REE-minerals were found to be primarily associated with goethite and were locked within the larger particle sizes over 100 μm, but, when the particle size was reduced to 50 μm, most REE mineral grains were liberated. These findings suggested that grinding the ore material to 63 μm would potentially liberate the most REE minerals for the subsequent separation processes, such as gravity, magnetic, and floatation methods [28]. Li et al. [175] detected anomalously high concentrations of REEs in acid mine drainage of a coal mine in northern Guizhou, China. SEM-EDS analysis revealed two types of REE-bearing minerals. Bastnaesite and monazite were detected in the claystone samples, and they were found to be adsorbed by a large amount of clay minerals, mainly kaolinite. Careful documentation of mineralogical and geochemical variations in REE deposits is extremely important for a clear understanding of difficulties in mineral processing and to arrive at an optimal process for mineralogical beneficiation. SEM-EDS and XRD were effectively utilized to understand the mineralogy of the Bear Lodge REE deposit (Wyoming, US) and to classify it into four types: (i) fluor-carbonates (bastnaesite, parisite, synchysite), (ii) phosphates (monazite, xenotime, florencite, rhabdophane, churchite), (iii) cerianite, and (iv) ancylite, and the distribution of REE was found to be very heterogeneous throughout the deposit [176].

5. Laser Ablation ICP-MS (LA-ICP-MS)

The determination of elemental concentrations and isotope ratios directly in solid samples has been an attractive frontier in the applications of these in situ techniques in earth science studies. Gray [177] was the first to demonstrate the feasibility of analyzing direct solids by ICP-MS using laser ablation sampling (LA-ICP-MS). A solid sample with a polished surface or a fused sample with a flux (just like fused pellets of XRF analysis) is ablated with a pulsed laser in a closed chamber, and the ablated material is forwarded into the ICP and analyzed in the usual way, as in the case of ICP-MS. Compared with solution nebulization-ICP-MS for the bulk analysis of geological samples, LA-ICP-MS analysis has several advantages, such as very low background interference, lower oxide and hydroxide interference levels, a simpler sample preparation procedure, faster analyses, and cost-effectiveness for the determination of REE concentrations and isotope compositions. However, they are affected by interferences caused by polyatomic, oxide, and hydroxide ion species formed in the plasma. In addition, the fractionation effects leading to non-stoichiometric behavior also affect isotope ratio measurements. LA-ICP-MS is one of the most powerful microbeam techniques for the direct analysis of minerals, and for mineral inclusions generally using a spot size of 20–50 μm for the determination of major, minor, and trace elements. Recently, LA-ICP-MS was utilized for the direct analysis of different elements including REEs in micrometer-scale ilmenite lamellae in titanomagnetite with high precision (>10% RSD) and accuracy [178]. Guo et al. [179] determined REE concentrations in scheelite minerals from scheelite quartz veins in the Honghuaerji scheelite deposit, Inner Mongolia, Northeast China, using LA-ICP-MS, which showed that the scheelite samples contain elevated REE concentrations with ΣREE + Y contents in the range of 3339 to 6321 μg/g. This information was useful in understanding how these minerals became crystallized from relatively reduced hydrothermal fluids during their formation. The application of femtosecond lasers instead of the more common nanosecond

lasers in LA-ICP-MS systems reduces laser-induced fractionation and matrix effects [140]. Mohanty et al. [180] analyzed detrital zircon grains from the riverbanks and beach placers of coastal Odisha, India, using LA-ICP-MS, and found that Hf (mean = 11,270 μg/g) and Y (mean = 1064 μg/g) were the two most abundant trace elements found within zircon grains as compared to other trace elements. Such studies are useful for understanding the resource potential and delineating the resource regions. Jiu et al. [181] determined REEs, Li, Ga, and Nb in coal from the Jungar coalfield, Ordos Basin, China, by using in situ LA-ICP-MS, in order to understand the distribution and modes of occurrences of these elements in coal. The determination of these elements in the strong organic material makes this technique very challenging but, nevertheless, it is possible. The majority of the La and Ce are found to be concentrated in La- and Ce-enriched minerals, including monazite, bastnaesite, and lanthanite in the coal. Major, minor, and trace elemental analysis including determining REEs by LA-ICP-MS was used to map the barren sandstone distal to mineralized areas, for obtaining the signature of hydrothermal REE mineralization in the Proterozoic Athabasca Basin, Canada. Quantitative evaluation of the element correlations, together with SEM-EDS studies, suggested that most of the elevated U and REEs are hosted in aluminum phosphate sulfate minerals [182]. LA-ICP-MS is especially valuable for the direct analysis of materials like barite, tourmaline, and corundum minerals for chemical analysis, which are difficult to dissolve completely. Oostingh [183] determined REEs in barites by LA-ICP-MS. The author also developed a method of fusion of barite with Na_2CO_3 in the ratio of 1:10 and dissolving the resultant fused material in 6N HCl. Most of the Ba ions (99%) were removed from the solution by an ion-exchange chromatography procedure using 2(ethylhexyl)-orthophosphoric acid as a binding fluid. However, both solutions and LA sampling methods suffered from problems, such as PrO interference on Gd, and Ce contamination in the fusion flux. In this context, LA-ICP-MS/MS is probably the best method to effectively eliminate all these interferences. Liu et al. [184] summarized the applications of LA-ICP-MS for micro-geochemistry and for the bulk analysis of whole-rock and soil samples. Various related issues, such as sample preparation, matrix interferences, sensitivity drift correction, calibration, and the use of matrix-matched CRMs were discussed in depth. Maruyama et al. [185] developed the LA-ICP-MS method of measuring 58 major, minor, and trace elements including all REEs in volcanic glass shards using a femtosecond laser and demonstrated that this technique is a viable alternative to techniques, such as SIMS and EPMA, for chemical characterization of rhyolitic and basaltic glasses.

5.1. LA-ICP-MS/MS

Interestingly LA-ICP-MS/MS was successfully applied to in situ Lu–Hf dating of Paleozoic–Precambrian xenotime, apatite, and garnet. NH_3–He was used as a reaction gas mixture and matrix-matched reference materials were utilized during the study. Lu was detected by mass-shift mode. The accuracy of the single-spot ages is generally better than 1.5%, and for xenotime was comparable to those obtained by in situ U-Pb analysis [186]. Ham-Meert et al. [187] demonstrated that by using a CH_3F/He mixture as the reaction gas, the spectral overlaps can be overcome in a mass-shift approach for Sr isotopic analysis of medieval stained glass with elevated Rb and REE concentrations using LA-ICP-MS/MS, and this can provide a viable alternative when a non-destructive analysis is required.

5.2. Laser Ablation Split Stream (LASS) Technique

The laser ablation split stream (LASS) technique is an innovative idea that was first described by Yuan et al. [188], where the ablated aerosol (a common sampling event) is split and shared by two spectrometers (MC-ICP-MS and any other ICP-MS system). This combination makes simultaneous elemental as well as isotope ratio determinations possible from a single sampling event [140]. Using this technique, Qian and Zhang [189] simultaneously analyzed REEs on the HR-ICP-MS and Nd isotopic composition on the MC-ICP-MS in apatite standards. Kylander-Clark et al. [190] gave an account of how the laser ablation split-stream technology works using dual MC-ICP-MS and HR-ICP-

MS simultaneously for high-speed, high spatial-resolution, simultaneous isotopic and elemental analysis which enables petro-chronology at a new level. These authors also gave a few important examples of how this novel technique is helpful in understanding the evolution of rocks and even more complex geological events.

6. Portable Miniatured Analytical Techniques

Portable devices in general offer fast, accurate, and cost-effective analysis of geological samples with little to no sample preparation, especially in the field during exploration studies and also in the actual mines while the excavation and transportation of the ore material is in progress. One of the most useful features of portable analytical techniques is the possibility to perform on-site measurements with or without minimal sample preparation. Modern geologists have a line-up of portable digital tools at their disposal, such as portable XRF, portable LIBS, GPS, and laptop computers providing access to imagery, maps, and on-site real-time geochemistry.

6.1. Portable XRF (pXRF or µXRF)

Portable XRF technology can be used in a wide range of geological, mineralogical, exploration, mining, and extraction applications. pXRF is extremely useful to locate REE deposits containing <∑REE 300, especially La, Ce, Pr, and Nd in the field during exploration studies. ∑REE 300 µg/g is the industry cut-off grade for several types of REE deposits, and earlier general observations revealed that the Y concentration typically must be present in the order of 25–30 µg/g to indicate an ∑REE concentration ~300 µg/g. Rock samples can be directly analyzed in the field, or, using the sample preparation accessories, representative sample units can be powdered and made into a pressed pellet. In the case of rock samples, since a rock sample is a heterogeneous unit, it is necessary to take analytical measurements at multiple points for obtaining a representative result. Phosphate deposits are one of the major sources of REEs [166]. Simandl et al. [191] used pXRF to determine major, minor, and trace element concentrations including REEs (La, Ce, Pr, Nd, Y) in phosphate rocks from the Fernie Formation, British Columbia, Canada with acceptable precision and accuracy. With suitable sample preparation and by following proper calibration procedures, pXRF can be used to identify zones of REE-enriched phosphate rocks in the field for large-scale exploration projects. For improving the detection of REEs at lower concentrations by pXRF, an advanced 55 kV X-ray tube is available commercially which can effectively analyze all of the light REEs including La, Ce, Pr, Nd, and Sm, and also a couple of heavy REEs, namely Eu and Gd. Regular commercial instruments which use the industry-typical 50 kV are being used currently for the determination of Y. Yang et al. [147] presented a case study from anthracite-associated clays from north-eastern Pennsylvania, US, by determining only Y contents by a pXRF and proved that Y can serve as an indicator element for the estimation of ∑REE. The use of pXRF is a cost-effective way to carry out REEs exploration studies. Fajber and Simandl [192], during studies related to the evaluation of REE-enriched sedimentary phosphate deposits in south-eastern British Columbia, Canada, obtained acceptable quantitative and semi-quantitative results for Nd, Pr, Ce, La, and Y using the handheld XRF instrument. As pXRF allows the screening of hundreds of samples quickly and reliably during exploration studies, a few samples can be selected and taken to the laboratory for cross-checking the results using more reliable analytical techniques, like ICP-MS. Sukadana et al. [193] used µXRF to identify REE minerals like monazite, zircon, and several other minerals in Adang Volcanic Complexes, Mamuju Area, West Sulawesi, Indonesia, in order to understand the role of carbonatite magma during the hydrothermal process of mineralization.

6.2. pLIBS

For pLIBS analysis, pressed pellets of samples are usually made using a hydraulic press so that they remain consolidated during the ablation process. Gibaga et al. [194] determined selected REEs in ion absorption clays using both pLIBS and ICP-MS and found that there is

a very good agreement between the results obtained by both techniques (Table 12), which proves that pLIBS can be an alternative technique to ICP-MS for a rapid determination of REEs in real-time. In fact, pLIBS can be used directly for field applications which is even more useful for a cost-effective analysis in the field. Bellie et al. [195] developed a new low-cost portable LIBS, with a gross weight of 3 kg, for instant element identification with a provision for mobile access of emission spectra and online system monitoring using the cloud for use by the mining industry.

Table 12. Comparison of selected REE concentrations in ion adsorption clay determined using handheld LIBS and ICP-MS analyses [194].

Selected REE	Average Concentration (μg/g)	
	pLIBS	ICP-MS
La	54.3	53.99
Ce	99.5	94.77
Pr	13.1	13.72
Nd	36.4	52.62
Sm	15.6	11.38
Gd	7.5	10.40
Dy	6.4	9.58
Yb	8.7	4.56

SD < 10.3 for LIBS & <30.02 for ICP-MS.

6.3. pXRD

Hydrometallurgical processes are used for better extraction yield and variable recovery rates particularly when REE ores are being processed. However, there is a limited understanding of the microscale phenomena controlling the extraction of REEs, for example, from fly ash. In order to better understand these processes, fly ash sample phases present at various stages of the processes were characterized by pXRD. This study revealed that the morphology and the elemental makeup of the ash matrix play a critical role in the accessibility of REEs [196]. Although pXRD devices are larger and heavier than handheld pXRF devices, they can still be operated in the field. The ability of pXRD to identify minerals in situ is useful for more accurate geological logging and can provide valuable insights into geological systems.

6.4. Portable Raman Spectrometer

Laser light interacts with molecular vibrations, phonons, or other excitations in the system (sample surface), resulting in the energy of the laser photons being shifted up or down. The shift in energy gives information about the chemical compositions of the sample in the form of a spectrum. Thus, Raman spectroscopy provides information on molecular forms in which the compounds are found. This ability of the laser Raman spectroscopy to optically identify mineralogy in situ makes it an ideal instrument not only for terrestrial field applications but also for extreme environments that prevail in certain places, such as other planets and the deep ocean. The DORISS instrument [197] is the first step in using Raman spectroscopy in the deep ocean. Moroz et al. [198] used a micro-Raman spectrometer to detect carbonate and phosphate minerals with REE associations. These observations confirmed the presence of biogenic presence of the cyanobacteria mat and its impact on the formation of the unique Nb-REE Tomtor deposit in Russia.

6.5. Fourier Transform Infrared (FTIR) Spectrometry

Infrared spectroscopy yields similar information to that of Raman spectroscopy, but it is complementary. The FTIR spectrometer continuously scans the surface in the NIR range and analyses the absorption and intensity. The analysis from the scans is averaged over

one-minute intervals and the result is returned to the control software. This technique is very popular as an online analyzer for following various industrial processes in different industries, such as in bauxite/alumina, coal, and phosphate industries, with several benefits, such as installation entirely above the conveyor belt and because sampling is not necessary. Ye and Bai [199] used microscopy, FTIR spectroscopy, Raman microprobe spectroscopy, and UV–Vis spectroscopy to study the spectral characteristics, mineral structure, mineral composition, and fluid inclusion and REE geochemistry to understand the metallogenic mechanism of the Nanlishu fluorite deposit in Nanlishu, Jilin Province in China. In addition, FTIR is used occasionally to verify and confirm the data obtained by single crystal X-ray diffraction analysis [200].

7. Hyperspectral Remote Sensing Techniques (Handheld, Drone, and Satellite-Based)

Hyperspectral remote sensing techniques have the potential to identify the REE minerals based on their sharp and distinctive absorption features in the visible near-infrared (VNIR) and shortwave infrared (SWIR) electromagnetic spectral profiles [160,201,202]. This is especially valuable with high spatial resolutions where the spectral response is dominated by mineralogy rather than lithology. Here, the intensity and wavelength position of some specific REE^{3+}-related absorption bands are sensitive to different crystal structures and not solely related to varying contents of specific REEs. Nd is one of the most abundant LREEs which can provide distinctive absorption features in the VNIR region of the electromagnetic spectrum even at a concentration of ~1000 μg/g in the Sillai Patti carbonatite complex, Pakistan [202]. Figure 8 presents a hyperspectral remote sensing imaging spectrometer system based on acousto-optic tunable (AOTF) technology [201], and an example of the absorption feature of Nd at wavelength 810.25 nm in a carbonatite sample. In addition to satellite mounting, such systems can also be mounted on a drone in addition to their use as handheld spectrometers on the ground. This modern remote sensing technique has become a novel tool for detecting and quantifying REEs (Nd) in geological materials and can offer an efficient, non-destructive, and relatively less expensive tool. Boesche et al. [203] used multitemporal hyperspectral images consisting of two sensors, with one operating in the visible and near-infrared (350 nm–1000 nm) and the other operating in the shortwave infrared (1000 nm–2500 nm) to detect Nd-enriched surface materials for hyperspectral REE mapping of outcrops in Norway recognized for their REE-bearing igneous carbonate rocks. The European Space Agency (ESA) launched Sentinel-2, which contains a multispectral instrument (MSI) that can target the REE (Nd^{3+})-bearing minerals and demonstrate the capability of MSI data. The remote sensing data generated in the visible to shortwave infrared (VNIR-SWIR) region showed the most prominent absorption features of Nd, which was a key pathfinder for REEs when examining the REE-rich Esfordi phosphate deposit, Iran [204]. Booysen et al. [205] utilized data acquired by hyperspectral sensors onboard drones (lightweight unmanned aerial vehicles—UAVs) to detect REEs (Nd) with low detection limits (<200 μg/g for Nd) in carbonatite complexes of Marinkas Quellen, Namibia, and Siilinjärvi, Finland, and introduced a rapid technology for the exploration of REE deposits. This kind of study promotes the use of the cheaper technology of deploying drones for hyperspectral imaging in exploration studies. The advantage is these techniques are that they can cover larger areas in a limited time and the accuracy of results can be verified by laboratory-based techniques, like XRD and ICP-MS. Brazil has some of the largest uranium–phosphate deposits in which very high concentrations of U and REEs have been reported near to phosphorous, which allows for the co-mining of these three ores. In these areas, near-infrared (NIR) spectroscopy was used to investigate REEs in the soil of the uranium–phosphate deposit of Itataia, Brazil. The concentrations of REEs were later verified using ICP-OES. These results show the promise of NIR spectroscopy as a tool for mapping the concentrations of REEx in topsoil [206]. Wang et al. [207] investigated the potential of Vis–NIR reflectance spectroscopy as a simple and rapid method of determining REEs (La, Ce, Pr, Nd, Sm, and Eu) in soil (Figure 9). Turner et al. [208] studied REE-bearing silicate minerals using reflectance spectroscopy in the VSWIR regions (500 to 2500 nm).

Some specific REE-related absorptions, such as an Er^{3+} and Yb^{3+} related absorption near 978 nm and Nd^{3+}-related absorptions near 746, 803, and 875 nm, were used to identify different REEs. Later on, these results were verified by SEM and EPMA techniques.

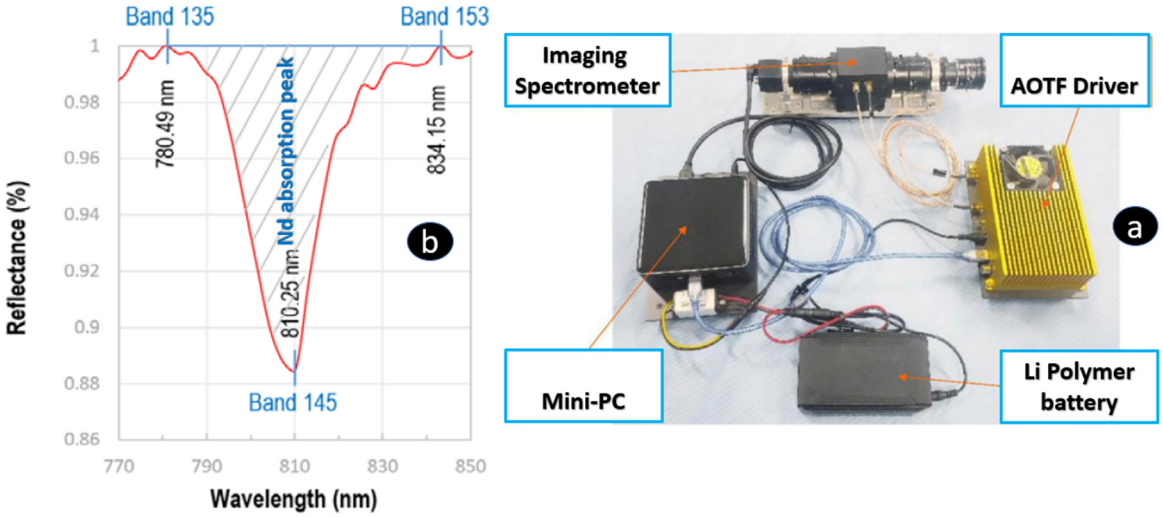

Figure 8. (**a**) The acousto-optic tunable (AOTF) technology imaging system consisting of AOTF imaging spectrometer, a AOTF driver, a MINI-PC, and an Li-polymer battery; (**b**) the absorption feature at wavelength 810.25 nm corresponds to the Nd concentration in carbonatite samples (modified from [201,202]).

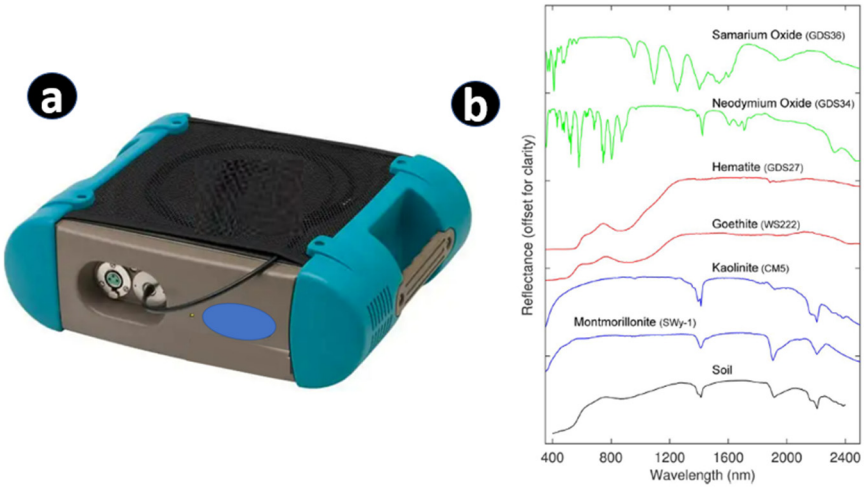

Figure 9. (**a**) Commercial field portable SWIR (400–2500 nm) spectrometer for geological studies; (**b**) reflectance spectra (offset for clarity) of clay minerals (blue lines, montmorillonite and kaolinite), iron oxides (red lines, goethite and hematite), rare earth oxides (green lines, neodymium oxide and samarium oxide), and soil (black line), modified from [207].

8. Electrochemical Methods and Biosensors for the Detection of REEs

A biosensor is an analytical device that works on the principle that the interaction between the biomolecule (bioreceptor) and the target analyte results in a chemical reaction that produces a signal, such as an electrical current or potential, which is directly proportional to the specific metal in solution [209]. Biosensors are generally easily miniaturized, contributing to the development of in situ and automated procedures. A terbium-specific biosensor was used to quantify 3 ng/mL of Tb directly from acid mine drainage at pH 3.2 in the presence of a 100-fold excess of other REEs and a 100,000-fold excess of other metals. The presence of Tb in acid mine drainage would indicate higher concentrations of other important and expensive REEs, like Sm and Dy. Successful application of this kind of

biosensor leads to the development of rapid and inexpensive tools for selective sensing of individual REEs [210]. A gold electrode modified with 2-pyridinol-1-oxide was used as a novel electrochemical sensor for the rapid detection of Eu in different environmental samples including river water [211]. This method requires no sample pre-treatment.

9. Miscellaneous Analytical Techniques

Fluorite (CaF_2) is one of the most common hydrothermal minerals in many deposits and has a relatively high REE content. Shehu and Bagudo [212] used XRF, FTIR, and UV–Vis spectrometry to obtain mineralogical information on fluorite samples. The REEs in the fluorite samples were found to be responsible for its color. Hirose et al. [83] determined La, Pr, Nd, Gd, and Tb in metallic REE matrices by glow discharge mass spectrometry (GD-MS) with ng/g detection limits and with precisions < 5%. Xiong et al. [213] analyzed REEs in an aqueous solution using a new analytical technique called a microwave plasma torch coupled with linear ion trap mass spectrometry (MPT-MS) with detection limits ranging from 0.04 to 0.574 ng/mL for different REEs. Subsequently, Yuan et al. [214] termed this technique microwave plasma torch mass spectrometry (MPT-MS) which can offer higher sensitivity with detection limits at the sub-ng/mL level and was used to determine several trace elements including REE in the water samples in the local Poyang Lake, China. The authors are of the opinion that the separation of individual REEs is necessary for more accurate analysis. Fayyaz et al. [215] utilized a new analytical technique called laser ablation time-of-flight mass spectrometry (LA-TOF-MS) for the elemental analysis of geological ore samples containing REEs. LA-TOF-MS showed very good agreement for La, Ce, and Nd when data comparison was made with those obtained by LIBS and ED-XRF. Near-infrared spectroscopy is a valuable technique for the qualitative identification of some REEs, like Sc, Y, Pr, and Sm, in soils and sediments. However, to confirm their presence and determine exact concentrations, standard analytical techniques, like ICP-OES and ICP-MS, have to be utilized. Therefore, near-infrared spectroscopy is a viable tool for rapid monitoring of REEs and other trace elements in soil and bed sediments in a river basin [216].

A rapid determination of major REE minerals, such as bastnäsite, monazite, and xenotime, enables the efficient exploration of REE mines. In this context, Imashuku [217] used cathodoluminescence (CL) imaging to qualitatively identify bastnäsite in mineral ores and determine a rough estimate of bastnäsite content rapidly for subsequent verification by more precise quantitative analysis by another technique, like an electron-probe micro analyzer (EPMA). The isolation of individual REEs has always been a challenging task because of their similar physical and chemical properties. Zeolites, such as ferrierite, faujasite, and the Linde type L, are well-known for their ion-exchange capabilities that would be potentially applicable for the REE separation. Duplouy [218] characterized them by XRD, ED-XRF, and attenuated total reflectance FTIR (ATR-FTIR). It was noticed that the uptake sequence followed La > Nd > Dy, which indicated the decrease in capacity with increased atomic number. Almost all of the REEs could be leached off from the REE-loaded zeolites at a pH of 1.51 with a nitric acid solution. These studies help in understanding their ion-exchange behavior and devising a suitable separation process. Borst et al. [219] used synchrotron X-ray absorption spectroscopy for understanding the distribution and local bonding environment, with Y and Nd as proxies for heavy and light REEs in the regolith-hosted ion absorption clay deposits, respectively. Such knowledge is important to devise the best extraction methods for REEs from ores. Obhodaš et al. [220] proposed a couple of nuclear techniques for the in situ measurement of ^{176}Lu radioactivity, and a device that utilizes the neutron sensor for the measurement of Gd by thermal neutron capture. From Lu and Gd concentrations by both techniques, the ∑REE can be calculated, as both Lu and Gd show a strong correlation to the ∑REE. These techniques in a remotely operated vessel (ROV) can be used for the in situ measurement of these elements from a ship on the ocean floor during deep ocean exploration for REE deposits [221]. In order to understand REE binding environments and the association with various mineral phases in coal and coal-by products, it is necessary to have the speciation information of REEs in coal and coal-by

products. Stuckman et al. [222] used synchrotron microscopy and spectroscopy to obtain such information on coal and coal by-products. The REE results from all three techniques were found to be in good agreement. Jochum et al. [223] utilized isotope dilution spark source mass spectrometry (ID-SSMS) for the quantitative determination of 35 elements including REEs in geological materials with detection limits ranging from 0.001 to 0.05 μg/g and with precisions and accuracies ranging < 5%. This technique is valuable when many elements are needed on a very small amount of sample.

10. Analysis of La, and a Continuous Stream of Data Collection by In Situ Gamma Spectrometry during an Industrial Extraction Process

During an industrial extraction or a metallurgical process, quick or continuous feedback on the concentration(s) of a certain element(s) is important to have appropriate control of the processes and also for the successful completion of the required industrial process. However, offline analytical techniques, such as XRF, ICP-OES, and ICP-MS may struggle to achieve real-time feedback. In order to meet such demands for direct analysis of La during the lanthanum extraction process, Zhao et al. [224] successfully designed a device that is capable of detecting changes in the composition of a sample traveling through a pipe, as illustrated in Figure 10a, based on in situ and high-sensitivity detection of La by monitoring the peak at 1435.8 keV through online germanium gamma spectrometry with minimum detectable concentration ranging from 4.66 to 4.99 μg/g. Because ^{138}La is an isotope with stable abundance (0.089%), emitting characteristic gamma-ray 1435.8 keV (65.5%) during the decay process, it is practicable to determine lanthanum via detecting the characteristic gamma-ray.

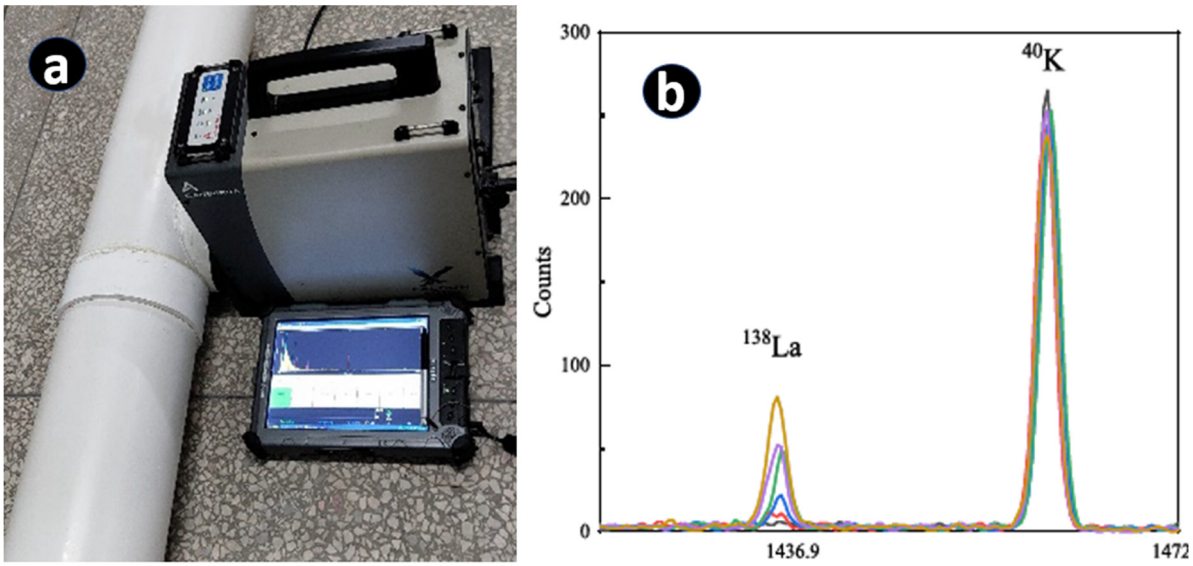

Figure 10. (**a**) Online experimental flatform of gamma-ray spectrometry, (**b**) for monitoring the ^{138}La characteristic peak during an industrial process. As the process progresses the concentration of La is seen increasing while K concentration remained constant. The La peak is positively correlated with the concentration of lanthanum in the extraction liquid, modified from [224].

11. Comparison of Different Analytical Techniques for REE Analysis

The isotope dilution method is the most accurate method for the determination of metals using mass spectrometry methods. Shen et al. [225] determined all REE in BCR-2 (USGS basalt CRM) to be within 2% of expected values (4% for Gd) by isotope dilution MC-ICP-MS without separation of individual elements demonstrating the ability to produce high-quality REE patterns of comparable quality to traditional methods which require labor- and time-intensive REE separation, although some, like Lee and Ko [143], preferred the separation of REEs as a group from the rock matrix for obtaining more accurate data.

Adeti et al. [27] compared the performances of ICP-MS, INAA, tube-based XRF, and ^{241}Am excitation-based XRF, for the detection of Sc, La, Ce, Nd, Sm, Eu, Tb, and Lu in volcanic rock specimens from Ghana. Folkedahl et al. [226] conducted a round robin interlaboratory study involving 13 laboratories on REEs in geological materials to understand lab-to-lab and method-to-method variability in analyzing REEs in geological materials, like coal, fly ash, shale, and mine waste. Different dissolution/sample preparation procedures and instrumental techniques, such as INAA, ICP-OES, and ICP-MS, were utilized. Although variability was relatively higher, exceeding 13% RSD (relative standard deviation), three of the five labs reported excellent performance in terms of repeatability, and reproducibility in the whole exercise [226]. Ardini et al. [227] compared the performance of ICP-MS, HR-ICP-MS, and ICP-AES for the determination of REEs in geological materials. The authors obtained a significant decrease (about 50%) in the oxide ions formation by use of a cooled spray chamber, thereby minimizing the polyatomic interference effects using a quadrupole ICP-MS. Comparable or better limits of detection for different REEs were obtained using HR-ICP-MS. Accurate results were obtained for the majority of REEs by ICP-AES equipped with a pneumatic or ultrasonic nebulization system, which was also utilized after a careful selection of the emission lines and compensation for non-spectral interferences by internal standardization. On the other hand, Pr, Tb, Ho, Tm, and Lu could not be measured by ICP-AES, due to strong spectral interferences and/or insufficient sensitivity. Zuma et al. [228] used acid digestion, heat digestion, or extraction prior to REE determination in rock, ore, mineral, crude oil, and coal samples by ICP-MS and ICP-OES. The authors indicated the necessity for the development of more efficient, simple, and environmentally friendly methods, and favored ICP-MS for the determination of REEs in geological samples, as ICP-MS has multi-elemental analysis capabilities, fewer interference effects, faster analysis, and lower detection limits.

12. Sample Preparation Methods for REE Studies (Acid, Fusion, and Microwave)

In general, REEs occur in low concentrations in most rocks and, hence, it is essential to employ suitable sample preparation methods and choose measurement techniques that allow for reliable quantification. For example, to obtain the best results by ICP-MS techniques, effective sample preparation involving complete digestion of the sample including refractory phases and minerals, such as zircon, garnet, chromite, and tourmalines is necessary [229]. Use of high-pure acids and other reagents to ensure low blank values, separation of interfering element(s) before analysis, and elimination of molecular interferences (e.g., oxides and hydroxides) by the use of tandem ICP-MS, if possible, ensures reliable REE data.

12.1. Acid Dissolution Methods

Since most analytical techniques offer very low detection limits even for REEs, the sample volumes/weights taken for chemical analysis have been reduced considerably compared to earlier times. Hence, acid dissolution methods are more popular and are reasonably effective for decomposing a large variety of geological materials [229]. Complete dissolution of refractory mineral phases can be assured by using sample preparation involving HF-HCl-HNO_3-$HClO_4$ acid mixtures and either a microwave digestion system or a high-pressure asher and a fusion procedure [98]. Fusion procedures using fluxing agents, like the use of lithium borate, normally produce homogeneous synthetic glasses which can be used in both XRF and LA-ICP-MS. Proper dilution of the sample solution, the use of proper internal standards, the application of matrix matching rock and mineral-certified reference materials (CRMs), and a clean laboratory environment are prerequisites for accurate and precise REE concentration and isotope ratio determination in geological and industrial materials [96,154]. Red mud is a potential REE resource that has very high concentrations of many matrix elements, such as Al and Fe, which cause interferences to the determination of REEs by ICP-OES. For dissolution, the red mud sample [230] was melted with NaOH, and the contents were extracted with hot water. Al and Fe were

removed by extraction with a triethanolamine solution. After complexing Ca and Mg, and other elements by EDTA disodium solution, REE hydroxide precipitate was dissolved with hydrochloric acid and determined by ICP-OES with recovery rates between 85% and 105%. The accuracy of the REE results in bauxite obtained by ICP-OES was verified by those obtained by ICP-MS and found to be in good agreement [230].

12.2. Fusion Dissolution Methods

Acid digestion very often results in low recoveries of REEs for certain types of rocks and minerals. In order to overcome this problem, Leitzke et al. [82] used alkali fluxes, like lithium borate to produce homogeneous synthetic glass disks for both XRF and LA-ICP-MS analysis of several elements including REEs. Schramm [231] used a ratio of 1:1 for rock to lithium tetraborate flux in a platinum crucible. The beads obtained after fusing at 1000 °C in a muffle furnace were utilized for XRF analysis. The precisions obtained for an Sm, Gd, Eu, Y and Th range of 0.005%–1% RSD, while, for the rest of REEs, the range is 0.02%–25% RSD. Lett and Paterson [232] made a comparative study of different sample preparations and an instrumental analytical method for the accurate determination of REEs in geological materials. He used lithium metaborate–tetraborate pressed pellets (sample and flux in 1:5 ratio), with 0.2 g sample and 0.8 g of sodium peroxide for 1 h at 480 °C sintering in a closed nickel crucible, and fusion of 0.2 g sample with lithium metaborate–lithium tetraborate flux at 980 °C in a graphite crucible, followed by the dissolution of the fused bead with weak hydrofluoric and hydrochloric acids, and a 0.5 g sample in Teflon test tubes with HF–$HClO_4$–HNO_3–HCl acids, for ICP-MS analysis. The authors found that sodium peroxide sinter-ICP-MS, lithium metaborate fusion-ICP-MS, INAA, and XRF are preferred methods for geochemical research because they produce the most accurate and precise data for REE. Dissolution of REE ores is difficult and often only partially completed with low recoveries because REE oxides and accessory minerals, like zircon, are refractory and resistant to most of the common sample dissolution procedures. Zircon, for example, is a recurrent accessory mineral in many rocks that frequently incorporates P, Hf, REE, Th, and U into its crystal lattice [233]. Over the last three decades, many investigations used four acid dissolution procedures for the digestion of REE ores over fusion procedures, as fusion procedures increase TDS, which some instrumental analytical techniques cannot tolerate [229]. Tupaz et al. [78] developed a modified digestion procedure and accurately determined REEs in mafic and ultramafic rock powders and validated the results using CRMs. The precisions achieved were generally below 5% RSD with minor modifications in the digestion procedure, including changes in the concentrations of different acids and drying temperatures. Udayakumar et al. [234] used a microwave digestion procedure for the dissolution of a Malaysian monazite sample by using both acid dissolution in a mixture of H_2SO_4, HNO_3, and HF, and a fusion procedure by lithium tetraborate, and metaborate flux followed by acid attack. Both procedures gave REE values that are in close agreement and also exhibited consistency with the XRF data. He et al. [235] dissolved uranium ore samples with NH_4F; REEs were separated using an ion-exchange procedure and their concentrations were determined by ICP-MS.

12.3. Microwave, Ultrasound-Assisted, High-Pressure Digestion, and Infrared Heating Methods

Kasar et al. [236] digested geological reference materials and soils by microwave and Savillex digestion procedures to evaluate the best quality control for the analysis of the REEs. Savillex digestion vessels are made of PFA Teflon and can withstand high pressures and help in the rapid dissolution of geological materials. They can be used along with microwave digestion systems or, alternatively, the sealed vessels with flat bottoms can directly be used for hotplate heating and digestion [237]. Microwave digestion was found to be more effective and faster. At present, most hotplate digestions are replaced by microwave digestions and infrared heating, as the former gives low recoveries many times. Hotplate digestions are often not effective in the complete dissolution of geological materials especially when they contain resistance minerals, like chromite, zircon, barite, monazite, and rutile,

and complete recoveries are not obtained [229]. Microwave digestions provide complete dissolution of REE ore and mineral samples and are also faster [238]. Most advanced microwave digestion systems currently have the capability to digest as many as 40 samples at a time, thereby contributing to the high productivity of the laboratory. Helmeczi et al. [68] used focused infrared radiation to expedite the acid digestion of geological materials and achieved efficient digestion in a shorter time. Zuma et al. [239] used microwave-assisted ashing and ultrasound-assisted extraction methods for the determination of REEs in South African coal by ICP-OES with precisions < 5%.

13. Quality Assurance and Quality Control during Analysis

Since REEs have become very important currently, many studies are going on worldwide for the production of concentration anomaly maps, finding new deposits, mining, extraction of REEs from different ores using different methods, and, finally, for the production of pure metals or metal oxides for industrial use. During all these studies, the generation of precise and accurate REE data is important [240]. The use of very dilute sample solutions, internal standardization, and matrix matching calibrations in addition to other quality control protocols, such as offline data reduction algorithms ensure data quality. On several occasions, the accuracy of the REE determination by instrumental techniques, such as LA-ICP-MS is hampered by the lack of matrix-matched reference materials. Zhang et al. [241] synthesized an REE-doped $NaY(WO_4)_2$ single crystal and employed it as a candidate reference material as well as using ^{89}Y as the internal standard for the quantitative determination of the REE in certain geological materials. During the determination of REEs (Ce, La, Nd, Pr, and Sm) by LIBS, due to significant overlapping of REE emission lines, a high pairwise correlation between REE contents in certified reference materials (CRMs) of natural origin, decreasing the multivariate model prediction capacity, is used [242]. Verplanck et al. [243] developed two water CRMs, with elevated REE levels (0.45 to 161 ng/mL) collected from a mine site. The 'round robin' analysis program was participated in by seventeen international laboratories and contributed data for all REEs, Y, and Sc. The most probable values were determined using robust statistical procedures. Even after one year, no change in concentration has been observed.

14. Conclusions

Analytical techniques play an important role in all aspects of REE research and production activities, such as exploration, mining, extraction, and metallurgy. At every stage of these activities, different types of materials, such as ores, concentrates, and finished products have to be analyzed for elemental, isotopic, and mineralogical concentrations using different analytical techniques. In general, for elemental analysis, different ICP-MS techniques are more popular than other analytical techniques because of their excellent performance characteristics, such as speed, high sensitivity (requires lower quantities of samples), fewer interference effects, multi-element/isotopic capability, and high accuracy and precision. Out of these techniques, ICP-MS/MS with solution nebulization or laser ablation sampling is the best and most cost-effective laboratory analytical technique currently available, particularly when compared to the more sophisticated HR-ICP-MS and MC-ICP-MS. Even the detection limits for different elements including REEs by ICP-MS/MS approach are comparable to the detection limits obtainable by the more expensive HR-ICP-MS. However, the less sensitive XRF is still popular for samples with high REE concentrations because of its ease of operation. Since pXRF offers reasonable sensitivity for Y and because of the direct correlation of Y concentration to the ∑REE, portable or handheld XRF instruments are valuable, especially during exploration studies. In general, currently, a number of field portable analytical techniques, such as pXRF and pLIBS, are available. These portable instruments are making REE exploration and other related activities easier, faster, and more cost-effective. Hyperspectral remote sensing techniques including handheld-, drone-, and satellite-based techniques have become very popular in REE exploration studies worldwide because of their ability to cover larger areas in a

limited time, thus, becoming very cost-effective. Microanalytical devices/sensors mounted in remotely operated vehicles (ROV) are being successfully utilized for detecting REE-rich deposits in the deep oceans. Finally, a nuclear technique, in situ gamma spectrometry, is also utilized to monitor and collect a continuous stream of data online for detecting changes in the composition of a sample traveling through a pipe during extraction processes in the REE industry.

SHRIMP, TIMS, SIMS, and MC-ICP-MS techniques are valuable for the precise dating of REE ore bodies and to understand the primary crystallization timing of different REE deposits the world over. Such studies are valuable during large-scale exploration studies in addition to basic fundamental studies. Mineralogical techniques, such as XRD, EPMA, SEM-EDS, and Raman spectrometry, are highly valuable for understanding the mineralogical characteristics of different REE ores and other resources. These studies are important as the leaching processes of different ores depend on their mineralogical composition and morphological distribution of REEs to determine the best leaching/extracting process during the extraction of REEs from different ores.

Funding: This research received no external funding.

Data Availability Statement: There is no other additional data available.

Acknowledgments: The author would like to acknowledge the support of Prakash Kumar, CSIR-National Geophysical Research Institute, Hyderabad, India.

Conflicts of Interest: The author declares no conflict of interest.

References

1. Rogelj, J.; Geden, O.; Cowie, A.; Reisinger, A. Net-zero emissions targets are vague: Three ways to fix. *Nature* **2021**, *591*, 365–368. [CrossRef] [PubMed]
2. Balaram, V. Combating Climate Change and Global Warming for a Sustainable Living in Harmony with Nature. *J. Geogr. Res.* **2023**, *6*, 1–17. [CrossRef]
3. Balaram, V. Recent trends in the instrumental analysis of rare earth elements in geological and industrial materials. *Trends Anal. Chem.* **1996**, *15*, 475–486. [CrossRef]
4. Bandyopadhyay, D.K.; Ghosh, S.; Mondal, A.; Das, D.K. Role of rare earth elements as provenance indicator in coal seams: A case study from IB-River Coalfield, Orissa. *Indian Miner.* **2006**, *60*, 171–180.
5. Drobniak, A.; Mastalerz, M. Rare Earth Elements—A brief overview: Indiana Geological and Water Survey. *Indiana J. Earth Sci.* **2022**, *4*. [CrossRef]
6. U.S. Geological Survey. *Mineral Commodity Summaries 2018*; U.S. Geological Survey: Reston, VA, USA, 2018; pp. 132–133. [CrossRef]
7. European Commission. *Critical Materials for Strategic Technologies and Sectors in the EU—A Foresight Study*; European Commission: Brussels, Belgium, 2020; p. 100.
8. Fedele, L.; Plant, J.A.; De Vivo, B.; Lima, A. The rare earth element distribution over Europe: Geogenic and anthropogenic sources. *Geochem. Explor. Environ. Anal.* **2008**, *8*, 3–18. [CrossRef]
9. Balaram, V. Rare earth elements: A review of applications, occurrence, exploration, analysis, recycling, and environmental impact. *Geosci. Front.* **2019**, *10*, 1285–1303. [CrossRef]
10. Borsato, N.W.; Hoeijmakers, H.J.; Prinoth, B.; Thorsbro, B.; Forsberg, R.; Kitzmann, D.; Jones, K.; Heng, K. The Mantis Network III: Expanding the limits of chemical searches within ultra-hot Jupiters-New detections of Ca, V, Ti, Cr, Ni, Sr, Ba, and Tb in KELT-9 b. *Astron. Astrophys.* **2023**, *673*, A158. [CrossRef]
11. Dai, S.; Finkelman, R.B.; French, D.; Hower, J.C.; Graham, I.T.; Zhao, F. Modes of occurrence of elements in coal: A critical evaluation. *Earth-Sci. Rev.* **2021**, *222*, 103815. [CrossRef]
12. Wagh, A.S.; Pinnock, W.R. Occurrence of scandium and rare earth elements in Jamaican bauxite waste. *Econ. Geol.* **1987**, *82*, 757–761. [CrossRef]
13. Cocker, M.D. Lateritic supergene rare earth element (REE) deposits. In *Arizona Geological Survey, Special Paper 9*; Chapter # 4, 1–20; Arizona Geological Survey: Phoenix, AZ, USA, 2012.
14. Lister, T.E.; Diaz, L.A.; Clark, G.G.; Keller, P. Process Development for the Recovery of Critical Materials from Electronic Waste. United States 2016. Available online: https://www.osti.gov/biblio/1358185 (accessed on 27 July 2023).
15. Robert, Z.; Andrew, F.; Mark, R.; Jim, P. *Maximizing REE Recovery in Geothermal Systems*; University of California: Davis, CA, USA; University of Oregon: Eugene, OR, USA, 2018. [CrossRef]
16. Hartzler, D.; Bhatt, C.; Jain, J.; McIntyre, D.L. Evaluating laser induced breakdown spectroscopy sensor technology for rapid source characterization of rare earth elements. *J. Energy Resour. Technol.* **2019**, *141*, 070704. [CrossRef]

17. Balaram, V. Rare Earth Element Deposits-Sources, and Exploration Strategies. *J. Geol. Soc. India* **2022**, *98*, 1210–1216. [CrossRef]
18. Valetich, M.; Zivak, D.; Spandler, C.; Degeling, H.; Grigorescu, M. REE enrichment of phosphorites: An example of the Cambrian Georgina Basin of Australia. *Chem. Geol.* **2022**, *588*, 120654. [CrossRef]
19. Cheatham, M.M.; Sangrey, W.F.; White, W.M. Sources of error in external calibration ICP-MS analysis of geological samples and an improved non-linear drift correction procedure. *Spectrochim. Acta* **1993**, *48B*, E467–E506. [CrossRef]
20. Pu, Q.; Liu, P.; Hu, Z.; Su, Z. Spectrophotometric determination of the sum of rare earth elements by flow-injection on-line preconcentration with a novel aminophosphonic–carboxylic acid resin. *Anal. Lett.* **2002**, *35*, 1401–1414. [CrossRef]
21. Saputra, H.A.; Anggraeni, A.; Mutalib, A.; Bahti, H.H. Development of a Fast Simultaneous Analysis Method for Determination of Middle Rare-Earth Elements in Monazite Samples. *J. Kim. Sains Dan Apl.* **2021**, *24*, 177–184. [CrossRef]
22. Potts, P.J. X-ray fluorescence analysis. In *Geochemistry. Encyclopedia of Earth Science*; Springer: Dordrecht, The Netherlands, 1998. [CrossRef]
23. De Vito, I.E.; Olsina, R.A.; Masi, A.N. Enrichment method for trace amounts of rare earth elements using chemofiltration and XRF determination. *Fresenius' J. Anal. Chem.* **2000**, *368*, 392–396. [CrossRef]
24. Juras, S.J.; Hickson, C.J.; Horsky, S.J.; Godwin, C.I.; Mathews, W.H. A practical method for the analysis of rare-earth elements in geological samples by graphite furnace atomic absorption and X-ray fluorescence. *Chem. Geol.* **1987**, *64*, 143–148. [CrossRef]
25. Wu, W.; Xu, T.; Hao, Q.; Wang, Q.; Zhang, S.; Zhao, C. Applications of X-ray fluorescence analysis of rare earths in China. *J. Rare Earths* **2010**, *28*, 30–36. [CrossRef]
26. De Pauw, E.; Tack, P.; Lindner, M.; Ashauer, A.; Garrevoet, J.; Vekemans, B.; Falkenberg, G.; Brenker, F.E.; Vincze, L. Highly Sensitive Nondestructive Rare Earth Element Detection by Means of Wavelength-Dispersive X-ray Fluorescence Spectroscopy Enabled by an Energy Dispersive pn-Charge-Coupled-Device Detector. *Anal. Chem.* **2020**, *92*, 1106–1113. [CrossRef]
27. Adeti, P.J.; Amoako, G.; Tandoh, J.B.; Gyampo, O.; Ahiamadjie, H.; Amable, A.S.K.; Kansaana, C.; Annan, R.A.T.; Bamford, A. Rare-earth element comparative analysis in chosen geological samples using nuclear-related analytical techniques. *Nucl. Instrum. Methods Phys. Res. Sect. B Beam Interact. Mater. At.* **2023**, *540*, 122–128. [CrossRef]
28. Sarker, S.K.; Bruckard, W.; Haque, N.; Roychand, R.; Bhuiyan, M.; Pramanik, B.K. Characterization of a carbonatite-derived mining tailing for the assessment of rare earth potential. *Process Saf. Environ. Prot.* **2023**, *173*, 154–162. [CrossRef]
29. Yao, M.; Wang, D.; Zhao, M. Element Analysis Based on Energy-Dispersive X-Ray Fluorescence. *Adv. Mater. Sci. Eng.* **2015**, *2015*, 290593. [CrossRef]
30. Kurniawati, S.; Santoso, M.; Lestiani, D.D.; Adventini, N.; Yatu, W.; Syahfitri, N. Analytical Capabilities of EDXRF for Determination of Rare Earth Elements. *Indones. J. Nucl. Sci. Technol.* **2021**, *22*, 1–9. [CrossRef]
31. Taam, I.; Jesus, C.S.; Mantovano, J.L.; Gante, V. Quantitative Analysis or Rare Earths By X-Ray Fluorescence Spectrometry. In Proceedings of the International Nuclear Atlantic Conference-INAC 2013, Recife, Brazil, 24–29 November 2013; Associação Brasileira De Energia Nuclear–ABEN: Recife, PE, Brazil, 2013. ISBN 978-85-1-05-2.
32. Balaram, V. Current and emerging analytical techniques for geochemical and geochronological studies. *Geol. Jour.* **2021**, *56*, 2300–2359. [CrossRef]
33. Rethfeldt, N.; Brinkmann, P.; Riebe, D.; Beitz, T.; Köllner, N.; Altenberger, U.; Löhmannsröben, H.-G. Detection of Rare Earth Elements in Minerals and Soils by Laser-Induced Breakdown Spectroscopy (LIBS) Using Interval PLS. *Minerals* **2021**, *11*, 1379. [CrossRef]
34. Harikrishnan, S.; Ananthachar, A.; Choudhari, K.S.; George, S.D.; Chidangil, S.; Unnikrishnan, V.K. Laser-Induced Breakdown Spectroscopy (LIBS) for the Detection of Rare Earth Elements (REEs) in Meteorites. *Minerals* **2023**, *13*, 182. [CrossRef]
35. Korotkova, N.A.; Baranovskaya, V.B.; Petrova, K.V. Microwave Digestion and ICP-MS Determination of Major and Trace Elements in Waste Sm-Co Magnets. *Metals* **2022**, *12*, 1308. [CrossRef]
36. Nakayama, K.; Nakamura, T. X-ray Fluorescence Analysis of Rare Earth Elements in Rocks Using Low Dilution Glass Beads. *Anal. Sci.* **2005**, *21*, 815–822. [CrossRef]
37. Ndjama, J.; Mafany, G.; Ndondo, R.G.N.; Belmond, B.E.; Bessa, A.Z.E. Rare earth elements in surface waters and sediments of the Mgoua watershed, south western Cameroon. *Arab. J. Geosci.* **2022**, *15*, 1001. [CrossRef]
38. Tanaka, T.; Lee, S.-G.; Kim, T.; Han, S.; Lee, H.M.; Lee, J.I. Precise determination of 14 REEs in GSJ/AIST geochemical reference materials JCp-1 (coral) and JCt-1 (giant clam) using isotope dilution ICP-quadrupole mass spectrometry. *Geochem. J.* **2017**, *51*, 75–79. [CrossRef]
39. Oliveira, S.M.B.; Larizzatti, F.E.; Fávaro, D.I.T.; Moreira, S.R.D.; Mazzilli, B.P.; Piovano, E.L. Rare earth element patterns in lake sediments as studied by neutron activation analysis. *J. Radioanal. Nucl. Chem.* **2003**, *258*, 531–535. [CrossRef]
40. Awad, H.; Zakaly, H.M.H.; El-Taher, A.; Sebak, M. Determination of lanthanides in phosphate rocks by instrumental neutron activation analysis. In *June 2022 AIP Conference Proceedings*; AIP Publishing: New York, NY, USA, 2022; Volume 2466, p. 050002. [CrossRef]
41. Figuelredo, A.M.G.; Marques, L.S. Determination of rare earths and other trace elements in the Brazilian geological standards, BB-1 and GB-1 by neutron activation analysis. *Geochim. Bras.* **1989**, *3*, 1–8.
42. Bounouira, H.; Choukri, A.; Elmoursli, R.C.; Hakam, O.; Chakiri, S. Distribution of the rare earth elements in the sediments of the Bouregreg river (Morocco) using the instrumental neutron activation analysis (INAA). *J. Appl. Sci. Environ. Manag.* **2007**, *11*, 57–60. [CrossRef]

43. Sitko, R.; Zawisza, B.; Czaja, M. Fundamental parameters method for determination of rare earth elements in apatites by wavelength-dispersive X-ray fluorescence spectrometry. *J. Anal. At. Spectrom.* **2005**, *20*, 741. [CrossRef]
44. Manard, B.T.; Wylie, E.M.; Willson, S.P. Analysis of Rare Earth Elements in Uranium Using Handheld Laser-Induced Breakdown Spectroscopy (HH LIBS). *Appl. Spectrosc.* **2018**, *72*, 1653–1660. [CrossRef]
45. Alamoudi, Z.; El-Taher, A. Application of Nuclear Analytical Techniques in Elemental Characterization of Wadi El-Nakhil Alabaster, Central Eastern Desert, Egypt. *Sci. Technol. Nucl. Install.* **2016**, *2016*, 2892863. [CrossRef]
46. Klinkhammer, G.; German, C.R.; Elderfield, H.; Greaves, M.J.; Mitra, A. Rare earth elements in hydrothermal fluids and plume particulates by inductively coupled plasma mass spectrometry. *Mar. Chem.* **1994**, *45*, 179–186. [CrossRef]
47. Wu, C.C. Advanced and Applied Studies on Ultra-Trace Rare Earth Elements (REEs) in Carbonates Using SN-ICPMS and LA-ICPMS. Ph.D. Thesis, National Taiwan University, Taipei, Taiwan, 2021; pp. 1–74.
48. Vukotić, P. Determination of rare earth elements in bauxites by instrumental neutron activation analysis. *J. Radioanal. Chem.* **1983**, *78*, 105–115. [CrossRef]
49. Baidya, T.K.; Mondal, S.K.; Balaram, V.; Parthasarathi, R.; Verma, R.; Mathur, P.K. PGE-Ag-Au mineralisations in a Cu-Fe-Ni sulphide-rich breccia zone of the Precambrian Nuasahi ultramafic-mafic complex, Orissa, India. *J. Geol. Soc. India* **1999**, *54*, e473–e482.
50. Silachyov, I. Zircon concentrate analysis for sixteen rare earth elements by the complex of nuclear analytical methods. *J. Radioanal. Nucl. Chem.* **2023**, *332*, 2017–2026. [CrossRef]
51. Ravisankar, R.; Manikandan, E.; Dheenathayalu, M.; Rao, B.; Seshadreesan, N.P.; Nair, K.G.M. Determination and distribution of rare earth elements in beach rock samples using instrumental neutron activation analysis (INAA). *Nucl. Instrum. Methods Phys. Res. B* **2006**, *251*, 496–500. [CrossRef]
52. Krishnan, K.; Saion, E. Distributions of Rare Earth Element (REE) in Mangrove Surface Sediment by Nuclear Technique. *Int. J.* **2022**, *2022*, 1–7.
53. Ahmed, M.E.; Bounouira, H.; Abbo, M.A.; Amsil, H.; Didi, A.; Aarab, I. Utilizing the k0-IAEA program to determine rare earth elements in soil samples from gold-mining areas in Sudan. *J. Radioanal. Nucl. Chem.* **2023**, *332*, 9. [CrossRef]
54. Kin, F.D.; Prudêncio, M.I.; Gouveia, M.Â.; Magnusson, E. Determination of Rare Earth Elements in Geological Reference Materials: A Comparative Study by INAA and ICP-MS. *Geostand. Geoanalytical Res.* **1999**, *23*, 47–58. [CrossRef]
55. Heinz-Günter, S. Neutron Activation Analysis of the Rare Earth Elements (REE)—With Emphasis on Geological Materials. *Phys. Sci. Rev.* **2016**, *1*, 20160062. [CrossRef]
56. El-Taher, A. Nuclear Analytical Techniques for Detection of Rare Earth Elements. *J. Rad. Nucl. Appl.* **2018**, *3*, 53–64. [CrossRef]
57. Ghannadpour, S.S.; Hezarkhani, A. Prospecting rare earth elements (REEs) using radiation measurement: Case study of Baghak mine, Central Sangan iron ore mine, NE of Iran. *Env. Earth Sci.* **2022**, *81*, 363. [CrossRef]
58. Huang, Y.; Wen, W.; Liu, J.; Liang, X.; Yuan, W.; Ouyang, Q.; Liu, S.; Gok, C.; Wang, J.; Song, G. Preliminary Screening of Soils Natural Radioactivity and Metal(loid) Content in a Decommissioned Rare Earth Elements Processing Plant, Guangdong, China. *Int. J. Environ. Res. Public Health* **2022**, *19*, 14566. [CrossRef]
59. Mohanty, S.; Khan, R.; Tamim, U.; Adak, S.; Bhunia, G.S.; Sengupta, D. Geochemical and Radionuclide studies of sediments as tracers for enrichment of beach and alluvial placers along the eastern coast of India. *Reg. Stud. Mar. Sci.* **2023**, *63*, 103003. [CrossRef]
60. Walsh, A. The application of atomic absorption spectra to chemical analysis. *Spectrochim. Acta* **1955**, *7*, 108–117. [CrossRef]
61. L'vov, B.V. A continuum source vs. line source on the way toward absolute graphite furnace atomic absorption spectrometry, Spectrochimica. *Acta Part B At. Spectrosc.* **1999**, *54*, 1637–1646. [CrossRef]
62. Balaram, V.; Sunder Raju, P.V.; Ramesh, S.L.; Anjaiah, K.V.; Dasaram, B.; Manikyamba, C.; Ram Mohan, M.; Sarma, D.S. Rapid partial dissolution method in combination with atomic absorption spectroscopy techniques for use in geochemical exploration. *At. Spectrosc.* **1999**, *20*, 155–160.
63. Hammer, M.R. A magnetically excited microwave plasma source for atomic emission spectroscopy with performance approaching that of the inductively coupled plasma. *Spectrochim. Acta Part B At. Spectrosc.* **2008**, *63*, 456–464. [CrossRef]
64. Balaram, V. Microwave plasma atomic emission spectrometry (MPAES) and its applications: A critical review. *Microchem. J.* **2020**, *159*, 18. [CrossRef]
65. Balaram, V.; Dharmendra, V.; Roy, P.; Taylor, C.; Kar, P.; Raju, A.K.; Krishnaiah, A. Determination of Precious Metals in Rocks and Ores by Microwave Plasma-Atomic Emission Spectrometry (MP-AES) for Geochemical Prospecting. *Curr. Sci.* **2013**, *104*, 1207–1215.
66. Balaram, V.; Dharmendra, V.; Roy, P.; Taylor, C.; Kamala, C.T.; Satyanarayanan, M.; Kar, P.; Subramanyam, K.S.V.; Raju, A.K.; Krishnaiah, A. Analysis of Geochemical Samples by Microwave Plasma-AES. *At. Spectrosc.* **2014**, *35*, 65–78.
67. Kamala, C.T.; Balaram, V.; Dharmendra, V.; Roy, P.; Satyanarayanan, M.; Subramanyam, K.S.V. Application of Microwave Plasma Atomic Emission Spectrometry (MP-AES) for Environmental Monitoring of Industrially Contaminated sites in Hyderabad City. *Environ. Monit. Assess.* **2014**, *186*, 7097–7113. [CrossRef]
68. Helmeczi, E.; Wang, Y.; Brindle, I.D. A novel methodology for rapid digestion of rare earth element ores and determination by microwave plasma-atomic emission spectrometry and dynamic reaction cell-inductively coupled plasma-mass spectrometry. *Talanta* **2016**, *160*, 521–527. [CrossRef]

69. Varbanova, E.; Stefanova, V. A comparative study of inductively coupled plasma optical emission spectrometry and microwave plasma atomic emission spectrometry for the direct determination of lanthanides in water and environmental samples. *Ecol. Saf.* **2015**, *9*, 362–374.
70. Greenfield, S.; Jones, I.L.I.; Berry, C.T. High pressure plasmas as spectroscopic emission sources. *Analyst* **1964**, *89*, 713–720. [CrossRef]
71. Wendt, R.H.; Fassel, V. Inductively-coupled plasma spectrometric excitation source. *Anal. Chem.* **1965**, *37*, 920–922.
72. Balaram, V.; Anjaiah, K.V.; Reddy, M.R.P. A comparative study o the trace and rare earth element analysis o an Indian Polymetallic Nodule Reference Sample by Inductively Coupled Plasma Atomic Emission Spectrometry and Inductively Coupled Plasma Mass Spectrometry. *Analyst* **1995**, *120*, 1401–1406. [CrossRef]
73. Kumar, N.S.; Dharmendra, V.; Sreenivasulu, V.; Asif, M.; Balaram, V. Separation and Preconcentration of Pb and Cd in Water Samples using 3-(2-hydroxyphenyl)-1H-1,2,4-triazole-5(4H)-thione (HTT) and their Determination by Inductively Coupled Plasma Atomic Emission Spectrometry (ICP-AES). *Metals* **2017**, *7*, 240. [CrossRef]
74. Makombe, M.; van der Horst, C.; Silwana, B.; Iwuoha, E.; Somerset, V. *Optimization of Parameters for Spectroscopic Analysis of Rare Earth Elements in Sediment Samples*; Chapter 3; INTECH, Open Science: London, UK, 2017. [CrossRef]
75. Gorbatenko, A.A.; Revina, E.I. A review of instrumental methods for determination of rare earth elements. *Inorg. Mater.* **2015**, *51*, 1375–1388. [CrossRef]
76. Pradhan, S.R.; Ambade, B. Extractive separation of rare earth elements and their determination by inductively coupled plasma optical emission spectrometry in geological samples. *J. Anal. At. Spectrom.* **2020**, *35*, 1395–1404. [CrossRef]
77. Nóbrega, J.; Schiavo, D.; Amaral, C.; Barros, J.; Mogueira, A.R.; Virgilio, A.; Machado, R. Determination of rare earth elements in geological and agricultural samples by ICP-OES. *Spectroscopy* **2017**, *32*, 32–36.
78. Tupaz, C.A.J.; Gregorio, C.G.C.; Arcilla, C. Determination of Scandium (Sc), Yttrium (Y), and Rare-Earth Elements (REEs) in Mafic and Ultramafic Rock Powder by a Modified and Validated Digestion Protocol and Inductively Coupled Plasma—Mass Spectrometry (ICP-MS). *Anal. Lett.* **2022**, *56*, 932–943. [CrossRef]
79. Zhu, Y. Determination of rare earth elements in seawater samples by inductively coupled plasma tandem quadrupole mass spectrometry after coprecipitation with magnesium hydroxide. *Talanta* **2020**, *209*, 120536. [CrossRef]
80. Robinson, P.; Townsend, A.T.; Yu, Z.; Münker, C. Determination of Scandium, Yttrium and Rare Earth Elements in Rocks by High Resolution Inductively Coupled Plasma-Mass Spectrometry. *Geostand. Geoanalytical Res.* **1999**, *23*, 31–46. [CrossRef]
81. Bauchle, M.; Ludecke, T.; Rabieh, S.; Calnek, K.; Bromage, T.G. Quantification of 71 detected elements from Li to U for aqueous samples by simultaneous-inductively coupled plasma-mass spectrometry. *RSC Adv.* **2018**, *8*, 37008–37020. [CrossRef] [PubMed]
82. Leitzke, F.P.; Wegner, A.C.; Porcher, C.C.; Vieira, N.I.M.; Berndt, J.; Klemme, J.; Conceição, R.V. Whole-rock trace element analyses via LA-ICP-MS in glasses produced by sodium borate flux fusion. *Braz. J. Geol.* **2021**, *51*, 2. [CrossRef]
83. Hirose, F.; Itoh, S.; Okochi, H. Determination of Rare-earth Elements in Metallic La, Pr, Nd, Gd and Tb by Glow Discharge Mass Spectrometry. *Tetsu—Hagane* **1991**, *77*, 598–604. [CrossRef]
84. Pedarnig, J.D.; Trautner, S.; Grünberger, S.; Giannakaris, N.; Eschlböck-Fuchs, S.; Hofstadler, J. Review of Element Analysis of Industrial Materials by In-Line Laser—Induced Breakdown Spectroscopy (LIBS). *Appl. Sci.* **2021**, *11*, 9274. [CrossRef]
85. Harmon, R.S.; Senesi, G.S. Laser-Induced Breakdown Spectroscopy—A geochemical tool for the 21st century. *Appl. Geochem.* **2021**, *128*, 104929. [CrossRef]
86. Alamelu, D.; Sarkar, A.; Aggarwal, S.K. Laser-induced breakdown spectroscopy for simultaneous determination of Sm, Eu and Gd in aqueous solution. *Talanta* **2008**, *77*, 256–261. [CrossRef]
87. Abedin, K.M.; Haider, A.F.M.Y.; Rony, M.A.; Khan, Z.H. Identification of multiple rare earths and associated elements in raw monazite sands by laser-induced breakdown spectroscopy. *Opt. Laser Technol.* **2011**, *43*, 45–49. [CrossRef]
88. Bhatt, C.R.; Jain, J.C.; Goueguel, C.L.; McIntyre, D.L.; Singh, J.P. Determination of Rare Earth Elements in Geological Samples Using Laser-Induced Breakdown Spectroscopy (LIBS). *Appl. Spectrosc.* **2017**, *72*, 114–121. [CrossRef]
89. Unnikrishnan, V.K.; Nayak, R.; Devangad, P.; Tamboli, M.M.; Santhosh, C.; Kumar, G.A.; Sardar, D.K. Calibration based laser-induced breakdown spectroscopy (LIBS) for quantitative analysis of doped rare earth elements in phosphors. *Mater. Lett.* **2013**, *107*, 322–324. [CrossRef]
90. Long, J.; Song, W.R.; Hou, Z.Y.; Wang, Z. A data selection method for matrix effects and uncertainty reduction for laser-induced breakdown spectroscopy. *Plasma Sci. Technol.* **2023**, *25*, 075501. [CrossRef]
91. Haider, A.F.M.Y.; Khan, Z.H. Identification of multiple rare earths and other associated elements in zircon by laser-induced breakdown spectroscopy. *J. Bangladesh Acad. Sci.* **2020**, *44*, 59–68. [CrossRef]
92. Liu, C.; Jiang, J.; Jiang, J.; Zhou, Z.; Ye, S. Automatic coal-rock recognition by laser-induced breakdown spectroscopy combined with an artificial neutral network. *Spectroscopy* **2023**, *38*, 23–28.
93. Gaft, M.; Raichlin, Y.; Pelascini, F.; Panzer, G.; Motto Ros, V. Imaging rare-earth elements in minerals by laser-induced plasma spectroscopy: Molecular emission and plasma-induced luminescence. *Spectrochim. Acta Part B At. Spectrosc.* **2019**, *151*, 12–19. [CrossRef]
94. Afgan, M.S.; Hou, Z.; Song, W.; Liu, J.; Song, Y.; Gu, W.; Wang, Z. On the Spectral Identification and Wavelength Dependence of Rare-Earth Ore Emission by Laser-Induced Breakdown Spectroscopy. *Chemosensors* **2022**, *10*, 350. [CrossRef]
95. Houk, R.S.; Fassel, V.A.; Flesch, G.D.; Svec, H.J.; Gray, A.L.; Taylor, C.E. Inductively coupled argon plasma as an ion source for mass spectrometric determination of trace elements. *Anal. Chem.* **1980**, *52*, 2283–2289. [CrossRef]

96. Balaram, V. Strategies to overcome interferences in elemental and isotopic geochemical studies by quadrupole ICP-MS: A critical evaluation of the recent developments. *Rapid Commun. Mass Spectrom.* **2021**, *35*, e9065. [CrossRef]
97. Atsunori, N.; Ran, K.; Atsuyuki, O. Multi-element analysis of geological samples using ICP-MS equipped with integrated sample introduction and aerosol dilution systems. *Bull. Geol. Surv. Jpn.* **2023**, *74*, 71–85.
98. Mnculwane, H.T. Rare Earth Elements Determination by Inductively Coupled Plasma Mass Spectrometry after Alkaline Fusion Preparation. *Analytica* **2022**, *3*, 135–143. [CrossRef]
99. Veerasamy, N.; Sahoo, S.K.; Murugan, R.; Kasar, S.; Inoue, K.; Fukushi, M.; Natarajan, T. ICP-MS Measurement of Trace and Rare Earth Elements in Beach Placer-Deposit Soils of Odisha, East Coast of India, to Estimate Natural Enhancement of Elements in the Environment. *Molecules* **2021**, *26*, 7510. [CrossRef]
100. Lin, R.; Bank, T.L.; Roth, E.A.; Granite, E.J.; Soong, Y. Organic and inorganic associations of rare earth elements in central Appalachian coal. *Int. J. Coal Geol.* **2017**, *179*, 295–301. [CrossRef]
101. Nguyen, V.H.; Ramzan, M.; Kifle, D.; Wibetoe, G. A simple separation system for elimination of molecular interferences for purity determination of europium and ytterbium oxides by HPLC-ICP-MS. *J. Anal. At. Spectrom.* **2020**, *35*, 2594–2599. [CrossRef]
102. Liu, W.; An, Y.; Qu, Q.; Li, P.; Zhang, L.; Li, C.; Wei, S.; Zhou, H.; Chen, J. An efficient method for separation of REEs from Ba for accurate determination of REEs contents in Ba-rich samples by ICP-MS. *J. Anal. At. Spectrom.* **2023**, *38*, 449–456. [CrossRef]
103. Wysocka, I. Determination of rare earth elements concentrations in natural waters—A review of ICP-MS measurement approaches. *Talanta* **2021**, *221*, 121636. [CrossRef] [PubMed]
104. Palozzi, J.; Bailey, J.G.; Tran, Q.A.; Stanger, R. A characterization of rare earth elements in coal ash generated during the utilization of Australian coals. *Int. J. Coal Prep. Util.* **2023**, 1–30. [CrossRef]
105. El-Taher, A.; Ashry, A.; Ene, A.; Almeshari, M.; Zakaly, H. Determination of phosphate rock mines signatures using XRF and ICP-MS elemental analysis techniques: Radionuclides, oxides, rare earth and trace elements. *Rom. Rep. Phys.* **2023**, *75*, 701.
106. Krasavtseva, E.; Sandimirov, S.; Elizarova, I.; Makarov, D. Assessment of Trace and Rare Earth Elements Pollution in Water Bodies in the Area of Rare Metal Enterprise Influence: A Case Study—Kola Subarctic. *Water* **2022**, *14*, 3406. [CrossRef]
107. Xin, W.C.; Zhu, Z.G.; Song, X.Y.; Zhu, A.M.; Zhang, D.L. On pretreatment method for the determination of rare earth elements in deep sea REY-rich sediments by inductively coupled plasma-mass spectrometry. *Mar. Geol. Front.* **2022**, *38*, 92–96. [CrossRef]
108. Li, H.; Tong, R.; Guo, W.; Xu, Q.; Tao, D.; Lai, Y.; Jina, L.; Hu, S. Development of a fully automatic separation system coupled with online ICP-MS for measuring rare earth elements in seawater. *RSC Adv.* **2022**, *12*, 24003. [CrossRef]
109. Wysocka, I.A.; Kurzawa, D.K.; Porowski, A. Development and validation of seaFAST-ICP-QMS method for determination of rare earth elements total concentrations in natural mineral waters. *Food Chem.* **2022**, *388*, 133008. [CrossRef]
110. Li, D.; Wang, X.; Huang, K.; Wang, Z. Multielemental Determination of Rare Earth Elements in Seawater by Inductively Coupled Plasma Mass Spectrometry (ICP-MS) After Matrix Separation and Pre-concentration with Crab Shell Particles. *Front. Environ. Sci.* **2021**, *9*, 781–996. [CrossRef]
111. Balaram, V. Inductively Coupled Plasma-Tandem Mass Spectrometry (ICP-MS/MS) and Its Applications. *J. ISAS* **2022**, *1*, 1–26. [CrossRef]
112. Zhu, Y. Determination of Rare Earth Elements by Inductively Coupled Plasma–Tandem Quadrupole Mass Spectrometry with Nitrous Oxide as the Reaction Gas. *Front. Chem.* **2022**, *10*, 912938. [CrossRef] [PubMed]
113. Santoro, A.; Thoss, V.; Ribeiro Guevara, S.; Urgast, D.; Raab, A.; Mastrolitti, S.; Feldmann, J. Assessing rare earth elements in quartz rich geological samples. *Appl. Radiat. Isot.* **2016**, *107*, 323–329. [CrossRef] [PubMed]
114. Lancaster, S.T.; Prohaska, T.; Irrgeher, J. Characterisation of gas cell reactions for 70+ elements using N_2O for ICP tandem mass spectrometry measurements. *J. Anal. At. Spectrom.* **2023**, *38*, 1135–1145. [CrossRef]
115. Ntiharirizwa, S.; Boulvais, P.; Poujol, M.; Branquet, Y.; Morelli, C.; Ntungwanayo, J.; Midende, G. Geology and U-Th-Pb Dating of the Gakara REE Deposit, Burundi. *Minerals* **2018**, *8*, 394. [CrossRef]
116. Myers, P.; Li, G.; Yang, P.; Hieftje, G.M. An inductively coupled plasma-time-of-flight mass spectrometer for elemental analysis. Part I: Optimization and characteristics. *J. Am. Soc. Mass Spectrom.* **1994**, *5*, 1008–1016. [CrossRef]
117. Mahoney, P.P.; Ray, S.J.; Hieftje, G.M.; Li, G. Continuum background reduction in orthogonal-acceleration time-of-flight mass spectrometry with continuous ion source. *J. Am. Soc. Mass Spectrom.* **1997**, *125*, 125–131. [CrossRef]
118. Balaram, V.; Satyanarayanan, M.; Murthy, P.K.; Mohapatra, C.; Prasad, K.L. Quantitative multi-element analysis of cobalt crust from Afanasy-Nikitin seamount in the North Central Indian Ocean by inductively coupled plasma time-of-flight mass spectrometry. *MAPAN-J. Metrol. Soc. India* **2013**, *28*, 63–77.
119. Dick, D.; Wegner, A.; Gabrielli, P.; Ruth, U.; Barbante, C.; Kriews, M. Rare earth elements determined in Antarctic ice by inductively coupled plasma—Time of flight, quadrupole and sector field-mass spectrometry: An inter-comparison study. *Anal. Chim. Acta* **2008**, *621*, 140–147. [CrossRef]
120. Nakazato, M.; Asanuma, H.; Niki, S.; Iwano, H.; Hirata, T. Depth-Profiling Determinations of Rare Earth Element Abundances and U-Pb Ages from Zircon Crystals Using Sensitivity-Enhanced Inductively Coupled Plasma-Time of Flight-Mass Spectrometry. *Geostand. Geoanalytical Res.* **2022**, *46*, 603–620. [CrossRef]
121. Peng, J.; Li, D.; Hollings, P.; Fu, Y.; Sun, X. Visualization of critical metals in marine nodules by rapid and high-resolution LA-ICP-TOF-MS mapping. *Ore Geol. Rev.* **2023**, *154*, 105342. [CrossRef]
122. Chew, D.; Drost, K.; Marsh, H.; Petrus, J.A. LA-ICP-MS imaging in the geosciences and its applications to geochronology. *Chem. Geol.* **2021**, *559*, 119917. [CrossRef]

123. Bradshaw, N.; Hall, E.F.H.; Sanderson, N.E. Inductively coupled plasma as an ion source for high-resolution mass spectrometry. *J. Anal. At. Spectrom.* **1989**, *4*, 801–803. [CrossRef]
124. Satyanarayanan, M.; Balaram, V.; Sawant, S.S.; Subramanyam, K.S.V.; Krishna, V.; Dasaram, B.; Manikyamba, C. Rapid determination of REE, PGE and other trace elements in geological and environmental materials by HR-ICP-MS 2018. *At. Spectrosc.* **2018**, *39*, 1–15. [CrossRef]
125. Thomas, R. A Beginner's Guide to ICP-MS Part VII: Mass Separation Devices—Double-Focusing Magnetic-Sector Technology. *Spectroscopy* **2001**, *16*, 22–27.
126. Charles, C.; Barrat, J.A.; Pelleter, E. Trace element determinations in Fe–Mn oxides by high resolution ICP-MS after Tm addition. *Talanta* **2021**, *233*, 122446. [CrossRef] [PubMed]
127. Balaram, V.; Roy, P.; Subramanyam, K.S.V.; Durai, L.; Mohan, M.R.; Satyanarayanan, M.; Vani, K. REE geochemistry of seawater from Afanasy-Nikitin seamount in the eastern equatorial Indian Ocean by high resolution inductively coupled plasma mass spectrometry. *Indian J. Geo-Mar. Sci.* **2015**, *44*, 339–347.
128. Gao, J.; Lv, D.; van Loon, A.T.; Hower, J.C.; Raji, M.; Yang, Y.; Ren, Z.; Wang, Y.; Zhang, Z. Reconstruction of provenance and tectonic setting of the Middle Jurrasic Yan'an Formation (Ordos Basin, North China) by analysis of major, trace and rare earth elements in the coals. *Ore Geol. Rev.* **2022**, *151*, 105218. [CrossRef]
129. Pedreira, W.R.; Sarkis, J.E.S.; Rodrigues, C.; Queirozb, C.A.D.T.; Abrao, A. Determination of trace amounts of rare earth elements in highly pure praseodymium oxide by double focusing inductively coupled plasma mass spectrometry and high-performance liquid chromatography. *J. Alloys Compd.* **2001**, *323–324*, 49–52. [CrossRef]
130. Nath, B.N.; Balaram, V.; Sudhakar, M.; Pluger, W.L. Rare earth element geochemistry of ferromanganese deposits from the Indian Ocean. *Mar. Chem.* **1992**, *38*, 185–208. [CrossRef]
131. Soto-Jiménez, M.F.; Martinez-Salcido, A.I.; Morton-Bermea, O.; Ochoa-Izaguirre, M.J. Lanthanoid analysis in seawater by seaFAST-SP3™ system in off-line mode and magnetic sector high-resolution inductively coupled plasma source mass spectrometer. *MethodsX* **2022**, *9*, 101625. [CrossRef] [PubMed]
132. Zhu, Y.; Nakano, K.; Shikamori, Y.; Itoh, A. Direct determination of rare earth elements in natural water samples by inductively coupled plasma tandem quadrupole mass spectrometry with oxygen as the reaction gas for separating spectral interferences. *Spectrochim. Acta Part B At. Spectrosc.* **2021**, *179*, 106100. [CrossRef]
133. Lawrence, M.G.; Greig, A.; Collerson, K.D.; Kamber, B.S. Direct quantification of rare earth element concentrations in natural waters by ICP-MS. *Appl. Geochem.* **2006**, *21*, 839–848. [CrossRef]
134. Chung, C.-H.; Brenner, I.; You, C.F. Comparison of micro-concentric and membrane desolvation sample introduction systems for determination of low rare earth element concentrations in surface and subsurface waters using sector field inductively coupled plasma mass spectrometry, Spectrochim. *Acta Part B* **2009**, *64*, 849–856. [CrossRef]
135. Rousseau, T.C.C.; Sonke, J.E.; Chmeleff, F.; Candaudap, J.; Lacan, F.; Boaventura, G.; Seyler, P.; Jeandel, C. Rare earth element analysis in natural waters by multiple isotope dilution–sector field ICP-MS. *J. Anal. At. Spectrom.* **2013**, *28*, 573–584. [CrossRef]
136. Yeghicheyan, D.; Carignan, J.; Valladon, M.; Coz, M.B.; Cornec, F.L.; Castrec-Rouelle, M.; Serrat, E. A Compilation of Silicon and Thirty-one Trace Elements Measured in the Natural River Water Reference Material SLRS-4 (NRC-CNRC). *Geostand. Geoanalytical Res.* **2001**, *25*, 465–474. [CrossRef]
137. Balaram, V.; Copia, L.; Kumar, U.S.; Miller, J.; Chidambaram, S. Pollution of Water Resources, Causes, Application of ICP-MS Techniques in Hydrological Studies, Monitoring, and Management. *Geosyst. Geoenviron.* **2023**, *2*, 100210. [CrossRef]
138. Rabieh, S.; Bayaraa, O.; Romeo, E.; Amosa, P.; Calnek, K.; Idaghdour, Y.; Ochsenkühn, M.A.; Amin, S.A.; Goldstein, G.; Bromage, T.G. MH-ICP-MS Analysis of the Freshwater and Saltwater Environmental Resources of Upolu Island, Samoa. *Molecules* **2020**, *25*, 4871. [CrossRef]
139. Walder, A.J.; Freedman, P.A. Communication. Isotopic ratio measurement using a double focusing magnetic sector mass analyzer with an inductively coupled plasma as an ion source. *J. Anal. At. Spectrom.* **1992**, *7*, 571. [CrossRef]
140. Balaram, V.; Rahaman, W.; Roy, P. Recent Advances in MC-ICPMS Applications in the Earth, Environmental Sciences: Challenges and Solution. *Geosyst. Geoenviron.* **2022**, *1*, 100019. [CrossRef]
141. Bai, J.-H.; Liu, F.; Zhang, Z.-F.; Ma, J.-L.; Zhang, L.; Liu, Y.-F.; Zhong, S.-X.; Wei, G.-J. Simultaneous measurement stable and radiogenic Nd isotopic compositions by MC-ICP-MS with a single-step chromatographic extraction technique. *J. Anal. At. Spectrom.* **2021**, *36*, 2695–2703. [CrossRef]
142. Bai, J.H.; Lin, M.; Zhong, S.X.; Deng, Y.N.; Zhang, L.; Kai, L.; Wu, H.; Ma, J.; Wei, G. High intermediate precision Sm isotope measurements in geological samples by MC-ICP-MS. *Anal. At. Spectrom.* **2023**, *38*, 629–637. [CrossRef]
143. Lee, S.G.; Ko, K.S. Development of an analytical method for accurate and precise determination of rare earth element concentrations in geological. materials using an MC-ICP-MS and group separation. *Front. Chem.* **2023**, *10*, 906160. [CrossRef]
144. Kent, A.J.R.; Jacobsen, B.; Peate, D.W.; Waight, T.E.; Baker, J.A. Isotope Dilution MC-ICP-MS Rare Earth Element Analysis of Geochemical Reference Materials NIST SRM 6 10, NIST SRM 6 12, NIS T SRM 6 14, BHVO-2G, BHVO-2, BCR-2G, JB-2, WS-E, W-2, AGV-1 and AGV-2. *Geostand. Geoanalytical Res.* **2004**, *28*, 417–429. [CrossRef]
145. Pourmand, A.; Dauphas, N.; Ireland, T.J. A novel extraction chromatography and MC-ICP-MS technique for rapid analysis of REE, Sc and Y: Revising CI-chondrite and Post-Archean Australian Shale (PAAS) abundances. *Chem. Geol.* **2012**, *291*, 38–54. [CrossRef]

146. Baker, J.; Waight, T.; Ulfbeck, D. Rapid and highly reproducible analysis of rare earth elements by multiple-collector inductively coupled plasma mass spectrometry. *Geochim. Cosmochim. Acta* **2002**, *66*, 3635–3646. [CrossRef]
147. Yang, X.; Kozar, D.; Gorski, D.; Marchese, A.; Pagnotti, J.; Sutterlin, R.; Rezaee, M.; Klima, M.S.; Pisupati, S.V. Using yttrium as an indicator to estimate total rare earth element concentration: A case study of anthracite-associated clays from northeastern Pennsylvania. *Int. J. Coal. Sci. Technol.* **2020**, *7*, 652–661. [CrossRef]
148. Li, X.C.; Yang, K.F.; Spandler, C.; Fan, H.R.; Zhou, M.F.; Hao, J.L.; Yang, Y.H. The effect of fluid-aided modification on the Sm-Nd and Th-Pb geochronology of monazite and bastnäsite: Implication for resolving complex isotopic age data in REE ore systems. *Geochim. Cosmochim. Acta* **2021**, *300*, 1–24. [CrossRef]
149. Guerra-Sommer, M.; Cazzulo-Klepzig, M.; Menegat, R.; Formoso, M.L.L.; Basei, M.S.; Barboza, E.G.; Simas, M.W. Geochronological data from the Faxinal coal succession, southern Paraná Basin, Brazil: A preliminary approach combining radiometric U-Pb dating and palynostratigraphy. *J. South Am. Earth Sci.* **2008**, *25*, 246–256. [CrossRef]
150. Chafe, A.N.; Hanchar, J.M.; Fisher, C.; Piccoli, P.M.; Crowley, J.L.; Dimmell, P.M. Direct dating and characterization of the Pope's Hill REE Deposit, Labrador. In Proceedings of the American Geophysical Union, Fall Meeting 2012, abstract id. V43C-2845, San Francisco, CA, USA, 3–7 December 2012.
151. Ramesh, R.; Ramanathan, A.; Ramesh, S.; Purvaja, R.; Subramanian, V. Distribution of rare earth elements and heavy metals in the surficial sediments of the Himalayan River system. *Geochem. J.* **2000**, *34*, 295–319. [CrossRef]
152. Natarajan, T.; Inoue, K.; Sahoo, S.K. Rare earth elements geochemistry and $^{234}U/^{238}U$, $^{235}U/^{238}U$ isotope ratios of the Kanyakumari beach placer deposits: Occurrence and provenance. *Minerals* **2023**, *13*, 886. [CrossRef]
153. Compston, W.; Pidgeon, R. Jack Hills, evidence of more very old detrital zircons in Western Australia. *Nature* **1986**, *321*, 766–769. [CrossRef]
154. Sindern, S. Analysis of Rare Earth Elements in Rock and Mineral Samples by ICP-MS and LA-ICP-MS. *Phys. Sci. Rev.* **2017**, *2*, 2. [CrossRef]
155. Campbell, L.S.; Compston, W.; Sircombe, K.N.; Wilkinson, C.C. Zircon from the East Orebody of the Bayan Obo Fe–Nb–REE deposit, China, and SHRIMP ages for carbonatite-related magmatism and REE mineralization events. *Contrib. Miner. Petrol.* **2014**, *168*, 1041. [CrossRef]
156. Bhunia, S.; Rao, N.V.C.; Belyatsky, B.; Talukdar, D.; Pandey, R.; Lehmann, B. U-Pb Zircon SHRIMP dating of the Carbonatite hosted REE deposit (Kamthai), Late Cretaceous polychronous Sarnu Dandali alkaline Complex, NW India: Links to the Plume-related metallogeny and CO_2 outgassing at the K-Pg boundary. *Gondwana Res.* **2022**, *112*, 116–125. [CrossRef]
157. Sano, Y.; Terada, K.; Fukuoka, T. High mass resolution ion microprobe analysis of rare earth elements in silicate glass, apatite and zircon: Lack of matrix dependency. *Chem. Geol.* **2002**, *184*, 217–230. [CrossRef]
158. Kolker, A.; Scott, C.; Hower, J.C.; Vazquez, J.A.; Lopano, C.L.; Dai, S. Distribution of rare earth elements in coal combustion fly ash, determined by SHRIMP-RG ion microprobe. *Int. J. Coal Geol.* **2017**, *184*, 1–10. [CrossRef]
159. Hong, J.; Khan, T.; Li, W.; Khalil, Y.S.; Narejo, A.A.; Rashid, M.U.; Zeb, M.J. SHRIMP U–Pb ages, mineralogy, and geochemistry of carbonatite–alkaline complexes of the Sillai Patti and Koga areas, NW Pakistan: Implications for petrogenesis and REE mineralization. *Ore Geol. Rev.* **2021**, *139*, 104547. [CrossRef]
160. Balaram, V.; Sawant, S.S. Indicator Minerals, Pathfinder Elements, and Portable Analytical Instruments in Mineral Exploration Studies. *Minerals* **2022**, *12*, 394. [CrossRef]
161. Jo, J.; Shin, D. Geochemical characteristics of REE-enriched weathered anorthosite complex in Hadong district, South Korea. *Geochem. J.* **2023**, *57*, 13–27. [CrossRef]
162. Villanova-de-Benavent, C.; Proenza, J.A.; Torró, L.; Aiglsperger, T.; Domènech, C.; Domínguez-Carretero, D.; Llovet, X.; Suñer, P.; Ramírez, A.; Rodríguez, J. REE ultra-rich karst bauxite deposits in the Pedernales Peninsula, Dominican Republic: Mineralogy of REE phosphates and carbonates. *Ore Geol. Rev.* **2023**, *157*, 105422. [CrossRef]
163. Kumar, O.P.; Gopinathan, P.; Naik, A.S.; Subramani, T.; Singh, P.K.; Sharma, A.; Maity, S.; Saha, S. Characterization of lignite deposits of Barmer Basin, Rajasthan: Insights from mineralogical and elemental analysis. *Environ. Geochem. Health* **2023**, 1–23. [CrossRef]
164. Reed, S.J.B.; Buckley, A. Rare-earth element determination in minerals by electron-probe microanalysis: Application of spectrum synthesis. *Mineral. Mag.* **1998**, *62*, 1–8.
165. Wu, L.; Ma, L.; Huang, G.; Li, J.; Xu, H. Distribution and Speciation of Rare Earth Elements in Coal Fly Ash from the Qianxi Power Plant, Guizhou Province, Southwest China. *Minerals* **2022**, *12*, 1089. [CrossRef]
166. Balaram, V. Potential Future Alternative Resources for Rare Earth Elements: Opportunities and Challenges. *Minerals* **2023**, *13*, 425. [CrossRef]
167. Sano, Y.; Terada, K.; Hidaka, H.; Nishio, Y.; Amakawa, H.; Nozaki, Y. Ion-Microprobe Analysis of Rare Earth Elements in Oceanic Basalt Glass. *Anal. Sci.* **1999**, *15*, 743–748. [CrossRef]
168. Bottazzi, P.; Ottolini, L.; Vannucci, R. SIMS analyses of rare earth elements in natural minerals and glasses: An investigation of structural matrix effects on ion yields. *Scanning* **1992**, *14*, 160–168. [CrossRef]
169. Zinner, E.; Crozaz, G. A method for the quantitative measurement of rare earth elements in the ion microprobe. *Int. J. Mass Spectrom. Ion Process.* **1986**, *69*, 17–38. [CrossRef]
170. Shi, L.; Sano, Y.; Takahata, N.; Koike, M.; Morita, T.; Koyama, Y.; Kagoshima, T.; Li, Y.; Xu, S.; Liu, C. NanoSIMS Analysis of Rare Earth Elements in Silicate Glass and Zircon: Implications for Partition Coefficients. *Front. Chem.* **2022**, *10*, 844953. [CrossRef]

171. Ling, X.X.; Li, Q.L.; Liu, Y.; Yang, Y.H.; Tang, G.Q.; Li, X.H. In situ SIMS Th–Pb dating of bastnaesite: Constraint on the mineralization time of the Himalayan Mianning–Dechang rare earth element deposits. *J. Anal. At. Spectrom.* **2016**, *31*, 1680. [CrossRef]
172. Sahijpal, S.; Marhas, K.K.; Goswami, J.N. Analytical procedures devised for measurement of rare earth element (REE) abundances using a secondary ion mass spectrometer (ion microprobe) are described. *Proc. Indian Acad. Sci. (Earth Planet. Sci.)* **2003**, *112*, 485–498.
173. Singh, S.P.; Balaram, V.; Satyanarayanan, M.; Sarma, D.S.; Subramanyam, K.S.V.; Anjaiah, K.V.; Kharia, A. Platinum group minerals from the Madawara ultramafic–mafic complex, Bundelkhand Massif, Central India: A preliminary note. *J. Geol. Soc. India* **2011**, *78*, 281–283.
174. Pan, J.; Zhang, L.; Wen, Z.; Nie, T.; Zhang, T.; Zhou, C. The Mechanism Study on the Integrated Process of NaOH Treatment and Citric Acid Leaching for Rare Earth Elements Recovery from Coal Fly Ash. *J. Environ. Chem. Eng.* **2023**, *11*, 109921. [CrossRef]
175. Li, X.; Qiao, X.; Chen, D.; Wu, P.; Xie, Y.; Chen, X. Anomalous concentrations of rare earth elements in acid mine drainage and implications for rare earth resources from late Permian coal seams in northern Guizhou. *Sci. Total Environ.* **2023**, *879*, 163051. [CrossRef]
176. Van Rythoven, A.D.; Pfaff, K.; Clark, J.G. Use of QEMSCAN® to characterize oxidized REE ore from the Bear Lodge carbonatite, Wyoming, USA. *Ore Energy Resour. Geol.* **2020**, *2–3*, 100005. [CrossRef]
177. Gray, A.L. Solid sample introduction by laser ablation for inductively coupled plasma source mass spectrometry. *Analyst* **1985**, *110*, 551–556. [CrossRef]
178. Liu, S.-Q.; Jiang, S.-Y.; Chen, W.; Wang, C.Y.; Su, H.-M.; Cao, Y.; Zhang, H.-X.; Li, W.-T. Precise determination of major and trace elements in micrometer-scale ilmenite lamellae in titanomagnetite using LA-ICP-MS technique: Application of regression analysis to time-resolved signals. *RSC Adv.* **2023**, *13*, 13303. [CrossRef]
179. Guo, Z.; Li, J.; Xu, X.; Song, Z.; Dong, X.; Tian, J.; Yang, Y.; She, H.; Xiang, A.; Kang, Y. Sm-Nd dating and REE Composition of scheelite for the Honghuaerji scheelite deposit, Inner Mongolia, Northeast China. *Lithos* **2016**, *261*, 307–321. [CrossRef]
180. Mohanty, S.; Papadopoulos, A.; Petreli, M.; Papadopoulou, L.; Sengupta, D. Geochemical Studies of Detrital Zircon Grains from River Bank and Beach Placers of Coastal Odisha, India. *Minerals* **2023**, *13*, 192. [CrossRef]
181. Jiu, B.; Huang, W.; Spiro, B.; Hao, R.; Mu, N.; Wen, L.; Hao, H. Distribution of Li, Ga, Nb, and REEs in coal as determined by LA-ICP-MS imaging: A case study from Jungar coalfield, Ordos Basin, China. *Int. J. Coal Geol.* **2023**, *267*, 104184. [CrossRef]
182. Chi, G.; Potter, E.G.; Petts, D.C.; Jackson, S.; Chu, H. LA-ICP-MS Mapping of Barren Sandstone from the Proterozoic Athabasca Basin (Canada)—Footprint of U- and REE-Rich Basinal Fluids. *Minerals* **2022**, *12*, 733. [CrossRef]
183. Oostingh, K. Analysis of Rare Earth Element Concentrations in Barite ($BaSO_4$). Master's Thesis, Department Earth Sciences, Utrecht University, Utrecht, The Netherlands, 2011; pp. 1–96.
184. Liu, Y.S.; Hu, Z.C.; Li, M.; Gao, S. Applications of LA-ICP-MS in the elemental analyses of geological samples. *Chin. Sci. Bull.* **2013**, *58*, 3863–3878. [CrossRef]
185. Maruyama, S.; Hattori, K.; Hirata, T.; Suzuki, T.; Danhara, T. Simultaneous determination of 58 major and trace elements in volcanic glass shards from the INTAV sample mount using femtosecond laser ablation-inductively coupled plasma-mass spectrometry. *Geochem. J.* **2016**, *50*, 403–422. [CrossRef]
186. Wu, S.T.; Wang, H.; Yang, Y.H.; Niu, J.; Lan, Z.; Zhang, L.L.; Huang, C.; Xie, L.W.; Xu, L.; Yang, J.H.; et al. In situ Lu-Hf geochronology with LA-ICP-MS/MS analysis. *J. Anal. At. Spectrom.* **2023**, *38*, 1285–1300. [CrossRef]
187. Ham-Meert, A.V.; Bolea-Fernandez, E.; Belza, J.; Bevan, D.; Jochum, K.P.; Neuray, B.; Stoll, B.; Vanhaecke, F.; Van Wersch, L. Comparison of Minimally Invasive Inductively Coupled Plasma–Mass Spectrometry Approaches for Strontium Isotopic Analysis of Medieval Stained Glass with Elevated Rubidium and Rare-Earth Element Concentrations. *ACS Omega* **2021**, *6*, 18110–18122. [CrossRef] [PubMed]
188. Yuan, H.L.; Gao, S.; Dai, M.N.; Zong, C.L.; Gunther, D.; Fontaine, G.H.; Diwu, C. Simultaneous determinations of U–Pb age, Hf isotopes and trace element com-positions of zircon by excimer laser ablation quadrupole and multiple-collector ICP-MS. *Chem. Geol.* **2008**, *247*, 100–118. [CrossRef]
189. Qian, S.P.; Zhang, L. Simultaneous in situ determination of rare earth element concentrations and Nd isotope ratio in apatite by laser ablation ICP-MS. *Geochem. J.* **2019**, *53*, 319–328. [CrossRef]
190. Kylander-Clark, A.R.C.; Hacker, B.R.; Cottle, J.M. Laser-ablation split-stream ICP petrochronology. *Chem. Geol.* **2013**, *345*, 99–112. [CrossRef]
191. Simandl, G.J.; Fajber, R.; Paradis, S. Portable X-ray fluorescence in the assessment of rare earth element enriched sedimentary phosphate deposits. *Geochem. Explor. Environ. Anal.* **2014**, *14*, 161–169. [CrossRef]
192. Fajber, R.; Simandl, G.J. Evaluation of Rare Earth Element-enriched Sedimentary Phosphate Deposits Using Portable X-ray Fluorescence (XRF) Instruments. In *Geological Fieldwork 2011*; Geological Survey of Canada: Sidney, BC, Canada, 2012; pp. 199–210.
193. Sukadana, I.G.; Warmada, W.I.; Pratiwi, F.; Harijoko, A.; Adimedha, T.B.; Yogatama, A.W. Elemental Mapping for Characterizing of Thorium and Rare Earth Elements (REE) Bearing Minerals Using μXRF. *At. Indones.* **2022**, *48*, 2. [CrossRef]
194. Gibaga, C.R.L.; Montano, M.O.; Samaniego, J.O.; Tanciongco, A.M.; Quierrez, R.N.M. Comparative Study on Determination of Selected Rare Earth Elements (REEs) in Ion Adsorption Clays Using Handheld LIBS and ICP-MS. *Philipp. J. Sci.* **2022**, *151*, 1599–1604. [CrossRef]

195. Bellie, V.; Gokulraju, R.; Rajasekar, C.; Vinoth, S.; Mohankumar, V.; Gunapriya, B. Laser induced Breakdown Spectroscopy for new product development in mining industry. *Mater. Today Proc.* **2021**, *45*, 8157–8161. [CrossRef]
196. Gerardo, S.; Davletshin, A.R.; Loewy, S.L.; Song, W. From Ashes to Riches: Microscale Phenomena Controlling Rare Earths Recovery from Coal Fly Ash, Environ. *Sci. Technol.* **2022**, *56*, 16200–16208. [CrossRef]
197. Brewer, P.G.; Malby, G.; Pasteris, J.D. Development of a laser Raman spectrometer for deep-ocean science. *Deep. Sea Res. Part I Oceanogr. Res. Pap.* **2004**, *51*, 739–753. [CrossRef]
198. Moroz, T.N.; Edwards, H.G.M.; Zhmodik, S.M. Detection of carbonate, phosphate minerals and cyanobacteria in rock from the Tomtor deposit, Russia, by Raman spectroscopy. *Spectrochim. Acta Part A Mol. Biomol. Spectrosc.* **2021**, *250*, 119372. [CrossRef]
199. Ye, X.; Bai, F. Spectral Characteristics, Rare Earth Elements, and Ore-Forming Fluid Constrains on the Origin of Fluorite Deposit in Nanlishu, Jilin Province, China. *Minerals* **2022**, *12*, 1195. [CrossRef]
200. Davletshina, N.; Ermakova, E.; Dolgova, D.; Davletshin, R.; Ivshin, K.; Fedonin, A.; Stoikov, I.; Cherkasov, R. Structure and FT-IR spectroscopic analyses of complexes phosphorylated betaines with rare earth metal ions. *Inorganica Chim. Acta* **2023**, *545*, 121245. [CrossRef]
201. Liu, H.; Yu, T.; Hu, B.; Hou, X.; Zhang, Z.; Liu, X.; Liu, J.; Wang, X.; Zhong, J.; Tan, Z.; et al. UAV-Borne Hyperspectral Imaging Remote Sensing System Based on Acousto-Optic Tunable Filter for Water Quality Monitoring. *Remote Sens.* **2021**, *13*, 4069. [CrossRef]
202. Qasim, M.; Khan, S.D. Detection and Relative Quantification of Neodymium in Sillai Patti Carbonatite Using Decision Tree Classification of the Hyperspectral Data. *Sensors* **2022**, *22*, 7537. [CrossRef]
203. Boesche, N.K.; Rogass, C.; Lubitz, C.; Brell, M.; Herrmann, S.; Mielke, C.; Tonn, S.; Appelt, O.; Altenberger, U.; Kaufmann, H. Hyperspectral REE (Rare Earth Element) Mapping of Outcrops—Applications for Neodymium Detection. *Remote Sens.* **2015**, *7*, 5160–5186. [CrossRef]
204. Karimzadeh, S.; Tangestani, M.H. Potential of Sentinel-2 MSI data in targeting rare earth element (Nd3+) bearing minerals in Esfordi phosphate deposit, Iran. *Egypt. J. Remote Sens. Space Sci.* **2022**, *25*, 697–710. [CrossRef]
205. Booysen, R.; Jackisch, R.; Lorenz, S.; Zimmermann, R.; Kirsch, M.; Nex, P.A.M.; Gloaguen, R. Detection of REEs with lightweight UAV-based hyperspectral imaging. *Sci. Rep.* **2020**, *10*, 17450. [CrossRef]
206. Maia, A.J.; da Silva, Y.J.A.B.; do Nascimento, C.W.A.; Veras, G.; Escobar, M.; Cunha, C.S.M.; da Silva, Y.J.A.B.; Nascimento, R.C.; de Souza, P.L.H. Near-infrared spectroscopy for the prediction of rare earth elements in soils from the largest uranium-phosphate deposit in Brazil using PLS, iPLS, and iSPA-PLS models. *Env. Monit Assess.* **2020**, *192*, 675. [CrossRef] [PubMed]
207. Wang, C.; Zhang, T.; Pan, X. Potential of visible and near-infrared reflectance spectroscopy for the determination of rare earth elements in soil. *Geoderma* **2017**, *306*, 120–126. [CrossRef]
208. Turner, D.J.; Rivard, B.; Groat, L. Visible and short-wave infrared reflectance spectroscopy of selected REE-bearing silicate minerals. *Am. Mineral.* **2018**, *103*, 927–943. [CrossRef]
209. Rocha, D.L.; Maringolo, V.; Araújo, A.N.; Amorim, C.M.P.G.; Montenegro, M.D.C.B.S.M. An overview of Structured Biosensors for Metal Ions Determination. *Chemosensors* **2021**, *9*, 324. [CrossRef]
210. Featherston, E.R.; Issertell, E.J.; Cotruvo, J.A., Jr. Probing Lanmodulin's Lanthanide Recognition via Sensitized Luminescence Yields a Platform for Quantification of Terbium in Acid Mine Drainage. *J. Am. Chem. Soc.* **2021**, *143*, 14287–14299. [CrossRef]
211. Cruickshank, L.; Officer, S.; Pollard, P.; Prabhu, R.; Stutter, M.; Fernandez, C. Rare elements electrochemistry: The development of a novel electrochemical sensor for the rapid detection of europium in environmental samples using gold electrode modified with 2-pyridinol-1-oxide. *Anal. Sci.* **2015**, *31*, 623–627. [CrossRef]
212. Shehu, G.; Bagudo, I.M. Mineralogical and Structural Analyses of Natural Fluorite from Yantuwaru Mining Site, Nigeria. *UMYU Sci.* **2023**, *2*, 43–51. Available online: https://scientifica.umyu.edu.ng/ (accessed on 5 June 2023).
213. Xiong, X.; Jiang, T.; Qi, W.; Zuo, J.; Yang, M.; Fei, Q.; Xiao, S.; Yu, A.; Zhu, Z.; Chen, H. Some Rare Earth Elements Analysis by Microwave Plasma Torch Coupled with the Linear Ion Trap Mass Spectrometry. *Int. J. Anal. Chem.* **2015**, *2015*, 156509. [CrossRef]
214. Yuan, L.; Zhou, X.; Cao, Y.; Yan, N.; Peng, L.; Lai, X.; Tao, H.; Jiang, T.; Li, L.; Zhu, Z. Microwave Plasma Torch Mass Spectrometry for some Rare Earth Elements. *Arab. J. Chem.* **2022**, *15*, 104379. [CrossRef]
215. Fayyaz, A.; Ali, R.; Waqas, M.; Liaqat, U.; Ahmad, R.; Umar, Z.A.; Baig, M.A. Analysis of Rare Earth Ores Using Laser-Induced Breakdown Spectroscopy and Laser Ablation Time-of-Flight Mass Spectrometry. *Minerals* **2023**, *13*, 787. [CrossRef]
216. Maia, A.J.; Nascimento, R.C.; da Silva, Y.J.A.B.; Nascimento, C.W.A.D.; Mendes, W.D.S.; Neto, J.G.V.; Filho, J.C.D.A.; Tiecher, T. Near-infrared spectroscopy for prediction of potentially toxic elements in soil and sediments from a semiarid and coastal humid tropical transitional river basin. *Microchem. J.* **2022**, *179*, 107544. [CrossRef]
217. Imashuku, S. Rapid determination of the approximate content of bastnäsite in ores using cathodoluminescence imaging. *Spectrochim. Acta Part A Mol. Biomol. Spectrosc.* **2023**, *287*, 122055. [CrossRef]
218. Duplouy, C. Preliminary Investigation of Rare Earth Elements Ion Exchange on Zeolites. Master's Thesis, Department of Chemistry, University of Helsinki, Helsinki, Finland, 2016; pp. 1–57.
219. Borst, A.M.; Smith, M.P.; Finch, A.A.; Estrade, G.; Villanova-de-Benavent, C.; Nason, P.; Marquis, E.; Horsburgh, N.J.; Goodenough, K.M.; Xu, C.; et al. Adsorption of rare earth elements in regolith-hosted clay deposits. *Nat. Commun.* **2020**, *11*, 4386. [CrossRef] [PubMed]
220. Obhodaš, J.; Sudac, D.; Meric, I.; Pettersen, H.E.S.; Uroić, M.; Nađ, K.; Valković, V. In-situ measurements of rare earth elements in deep sea sediments using nuclear methods. *Sci. Rep.* **2018**, *8*, 4925. [CrossRef] [PubMed]

221. Balaram, V. Deep-sea mineral deposits as a source of critical metals for high-and green-technology applications. *Miner. Miner. Mater.* **2023**, *2*, 5. [CrossRef]
222. Stuckman, M.Y.; Lopano, C.L.; Granite, E.J. Distribution and speciation of rare earth elements in coal combustion by-products via synchrotron microscopy and spectroscopy. *Int. J. Coal Geol.* **2018**, *195*, 125–138. [CrossRef]
223. Jochum, K.P.; Seufert, H.M.; Midinet-Best, S.; Rettmann, E.; Schiinberger, K.; Zimmer, M. Multi-element analysis by isotope dilution-spark source mass spectrometry (ID-SSMS). *Fresenius J. Anal Chem.* **1988**, *331*, 104–110. [CrossRef]
224. Zhao, J.; Xing, Y.; Ge, L.; Wang, L.; Li, T.; Zhang, Q.; Wu, H.; Li, W.; Liu, Y. Direct analysis of lanthanum in extraction process by in-situ gamma spectrometry. *J. Radioanal. Nucl. Chem.* **2022**, *331*, 3807–3817. [CrossRef]
225. Shen, S.; Krogstad, E.; Conte, E.; Brown, C. Rapid unseparated rare earth element analyses by isotope dilution multi-collector inductively coupled plasma mass spectrometry (ID-MC-ICP-MS). *Int. J. Mass Spectrom.* **2022**, *471*, 116726. [CrossRef]
226. Folkedahl, B.; Nyberg, C.; Biswas, S.; Zhang, X. Round-Robin Interlaboratory Study on Rare-Earth Elements in 2 U.S.-Based Geologic Materials. *Minerals* **2023**, *13*, 944. [CrossRef]
227. Ardini, F.; Soggia, F.; Rugi, F.; Udisti, R.; Grotti, M. Comparison of inductively coupled plasma spectrometry techniques for the direct determination of rare earth elements in digests from geological samples. *Anal. Chim. Acta* **2010**, *678*, 18–25. [CrossRef] [PubMed]
228. Zuma, M.C.; Lakkakula, J.; Mketo, N. Recent trends in sample preparation methods and plasma-based spectrometric techniques for the determination of rare earth elements in geological and fossil fuel samples. *Appl. Spectrosc. Rev.* **2020**, *57*, 353–377. [CrossRef]
229. Balaram, V.; Subramanyam, K.S.V. Sample Preparation for Geochemical Analysis: Strategies and Significance. *Adv. Sample Prep.* **2022**, *1*, 100010. [CrossRef]
230. Xuan, H.; Zi-hui, C.; Shu-chao, Z.; Lei, S. Matrix Separation-Determination of Rare Earth Oxides in Bauxite by Inductively Coupled Plasma-Atomic Emission Spectrometry. *Spectrosc. Spectr. Anal.* **2022**, *42*, 3130–3134. [CrossRef]
231. Schramm, R. Use of X-ray Fluorescence Analysis for the Determination of Rare Earth Elements. *Phys. Sci. Rev.* **2016**, *1*, 20160061. [CrossRef]
232. Lett, R.E.; Paterson, K. A Comparison of Several Commercially Available Methods for the Geochemical Analysis of Rare Earth, Rare Metal and High Field Strength Elements in Geological Samples. In *Geological Fieldwork 2010*; British Columbia Geological Survey Paper 2011-1; British Columbia Geological Survey: Victoria, BC, Canada, 2011; pp. 181–188.
233. Hanchar, J.M.; Finch, R.J.; Hoskin, P.W.O.; Watson, E.B.; Cherniak, D.J.; Mariano, A.N. Rare earth elements in synthetic zircon: Part 1. Synthesis, and rare earth element and phosphorus doping. *Am. Mineral.* **2001**, *86*, 5. [CrossRef]
234. Udayakumar, S.; Baharun, N.; Rezan, S.A. Microwave-Assisted Acid Digestion of Malaysian Monazite for Determination of REEs Using ICP-MS. *Key Eng. Mater.* **2022**, *908*, 481–486. [CrossRef]
235. He, H.; Zhao, X.; Zhang, Y.; Zhao, L.; Hu, R.; Li, L. Determination of rare earth elements in uranium ores by ICP-MS after total dissolution with NH_4F and matrix separation with TRU resin. *J. Radioanal. Nucl. Chem.* **2023**, *332*, 1909–1916. [CrossRef]
236. Kasar, S.; Murugan, R.; Arae, H.; Aono, T.; Sahoo, S.K. A Microwave Digestion Technique for the Analysis of Rare Earth Elements, Thorium and Uranium in Geochemical Certified Reference Materials and Soils by Inductively Coupled Plasma Mass Spectrometry. *Molecules* **2020**, *25*, 5178. [CrossRef]
237. Roy, P.; Balaram, V.; Kumar, A.; Satyanarayanan, M.; Rao, T.G. New REE and Trace Element Data on Two International Kimberlitic Reference Materials by ICP-MS. *Geostand. Geoanalytical Res.* **2007**, *31*, 261–273. [CrossRef]
238. Balaram, V. Microwave dissolution techniques for the analysis of geological materials by ICP-MS. *Curr. Sci.* **1997**, *73*, 1019–1023.
239. Zuma, M.C.; Nomngongo, P.N.; Mketo, N. Simultaneous Determination of REEs in Coal Samples Using the Combination of Microwave-Assisted Ashing and Ultrasound-Assisted Extraction Methods Followed by ICP-OES Analysis. *Minerals* **2021**, *11*, 1103. [CrossRef]
240. Balaram, V.; Satyanarayanan, M. Data Quality in Geochemical Elemental and Isotopic Analysis. *Minerals* **2022**, *12*, 999. [CrossRef]
241. Zhang, Y.; Sun, Y.; Zhou, J.; Yang, J.; Deng, J.; Shao, J.; Zheng, T.-F.; Ke, Y.; Long, T. Preparation of REE-doped NaY(WO4)2 single crystals for quantitative determination of rare earth elements in REE:NaY(WO4)2 laser crystals by LA-ICP-MS. *Anal. Methods* **2022**, *14*, 4085–4094. [CrossRef] [PubMed]
242. Akhmetzhanova, T.F.; Popov, A.M. Direct determination of lanthanides by LIBS in REE-rich ores: Comparison between univariate and DoE based multivariate calibrations with respect to spectral resolution. *J. Anal. At. Spectrom.* **2022**, *37*, 2330–2339. [CrossRef]
243. Verplanck, P.L.; Antweiler, R.; CNordstrom, D.K.; Taylor, H.E. Standard reference water samples for rare earth element determinations. *Appl. Geochem.* **2001**, *16*, 231–244. [CrossRef]